Lab on a Chip

CRITICAL REVIEW

View Article Online
View Journal | View Issue

Cite this: *Lab Chip*, 2023, **23**, 1300

Acoustofluidics – changing paradigm in tissue engineering, therapeutics development, and biosensing

Reza Rasouli,[a] Karina Martinez Villegas[a] and Maryam Tabrizian *[ab]

For more than 70 years, acoustic waves have been used to screen, diagnose, and treat patients in hundreds of medical devices. The biocompatible nature of acoustic waves, their non-invasive and contactless operation, and their compatibility with wide visualization techniques are just a few of the many features that lead to the clinical success of sound-powered devices. The development of microelectromechanical systems and fabrication technologies in the past two decades reignited the spark of acoustics in the discovery of unique microscale bio applications. Acoustofluidics, the combination of acoustic waves and fluid mechanics in the nano and micro-realm, allowed researchers to access high-resolution and controllable manipulation and sensing tools for particle separation, isolation and enrichment, patterning of cells and bioparticles, fluid handling, and point of care biosensing strategies. This versatility and attractiveness of acoustofluidics have led to the rapid expansion of platforms and methods, making it also challenging for users to select the best acoustic technology. Depending on the setup, acoustic devices can offer a diverse level of biocompatibility, throughput, versatility, and sensitivity, where each of these considerations can become the design priority based on the application. In this paper, we aim to overview the recent advancements of acoustofluidics in the multifaceted fields of regenerative medicine, therapeutic development, and diagnosis and provide researchers with the necessary information needed to choose the best-suited acoustic technology for their application. Moreover, the effect of acoustofluidic systems on phenotypic behavior of living organisms are investigated. The review starts with a brief explanation of acoustofluidic principles, the different working mechanisms, and the advantages or challenges of commonly used platforms based on the state-of-the-art design features of acoustofluidic technologies. Finally, we present an outlook of potential trends, the areas to be explored, and the challenges that need to be overcome in developing acoustofluidic platforms that can echo the clinical success of conventional ultrasound-based devices.

Received 12th May 2022,
Accepted 11th November 2022

DOI: 10.1039/d2lc00439a

rsc.li/loc

1 Introduction

Acoustic waves have a long history in biomedical sciences and engineering with a wide range of applications from diagnostics and imaging techniques to shock wave lithotripsy using high-energy sound waves. The development of microelectromechanical systems (MEMS) and miniaturized technologies enabled the use of acoustics in minuscule, confined, and well-controlled microfluidic domains referred to as acoustofluidics. The miniaturization of acoustic platforms not only allows for the precise manipulation and analysis of cells, particles, and biomolecules from nanometers to millimeters scales, but also introduces numerous phenomena unique to the micro realm.[1,2] The wide range of working frequencies (from kilohertz to gigahertz), efficient delivery of energy, confined and controlled domain, and the various acoustic phenomena that can be independently chosen and tuned, make this technology suitable for a diverse gamut of applications.

In the biomedical field, acoustofluidics has attracted high interest due to its contactless and label-free nature, its capability to easily modify the energy and frequency of waves to preserve high biocompatibility, and its flexible working media in contrast to electrophoresis or optical tweezers.[3–6] Moreover, miniaturized acoustic platforms allow to generate uniform and well-controlled acoustic pressure profiles using gentle and precise acoustic forces on sensitive bio-samples, thus minimizing uninhibited heating and mechanical stresses.[6] Another distinctive feature of acoustic systems is their ability to be employed as both actuators, for particle and fluid manipulation, and as sensors, to detect bioparticles

[a] *Department of Biomedical Engineering, Faculty of Medicine and Health Sciences, McGill University, Montreal, Quebec, Canada. E-mail: maryam.tabrizian@mcgill.ca*
[b] *Faculty of Dental Medicine and Oral Health Sciences, McGill University, Montreal, Quebec, Canada*

and biomolecules. This versatility emerges from the capability of piezoelectrics to convert energy between mechanical vibrations and electric signals in both directions, through direct and inverse piezoelectric effects.[7]

To move and manipulate objects using acoustic energy, known as acoustophoresis, acoustic waves exert energy on the objects mainly in the form of acoustic radiation forces (ARFs), and/or Stokes' drag forces initiated from acoustic streaming. One advantage of acoustic methods for particle manipulation is that every object that shows a mismatch in density and/or compressibility with its surrounding medium is acoustically visible to the system, without labeling. The acoustic contrast, together with the particle size, determines the magnitude of the acoustic force exerted on the particles and it is subsequently used for accurate and sensitive separation, label-free sorting, enrichment, and patterning of cells, bacteria, and nanoparticles. In addition, these precise and controllable acoustic forces on submicron to millimeter-scale particles, combined with their compatibility with complex biofluids such as sputum and blood, make acoustic manipulation a versatile and powerful tool for handling clinical specimens.

The non-invasive nature of acoustic tweezers can be employed to gently move and pattern single or arrays of bioparticles with a micro-scale precision to study cell–cell communications and to assemble complex cell architectures for tissue engineering.[8–27] Furthermore, by introducing hydrogels before patterning cells, tissue constructs can be preserved *in vitro* for long-term culture after the removal of the acoustic field and can be further implanted *in vivo.*[13]

The interaction of acoustic waves with objects reciprocally impacts the characteristics of the waves too, causing detectable shifts in their amplitude, phase, and propagation velocity. These changes in the wave features can be measured and used as a sensing strategy to detect pathogenic species, quantify proteins and DNA, or even divulge information about the change in physical properties of cells such as viscoelasticity or stiffness. Portable and compact acoustic sensors can be instrumental for the detection of pathogens such as Ebola, Influenza A, and HIV with higher accuracy than the standard polymerase chain reaction (PCR) method.[28–31] Another advantage of these acoustic sensors is their ability to be integrated with smartphones since the radiofrequency input and output of SAW-sensing facilitates the electronic readout.[32] These unique features coupled with the fast detection time, establish acoustofluidics as a promising and powerful sensing technology for point of care testing.[33]

Apart from acoustophoresis and biosensing, acoustofluidic platforms have shown enormous potential in both developing therapeutic agents and also as an efficient method of drug delivery, vaccination, and gene transfection.[34–38] Moreover, acoustofluidics can be further exploited to produce functional mechanical trigger to induce biological phenotypes in samples in unique ways: from enhancing wound healing to inducing concussions to worms for brain injury research![39–41]

With the expansion of the acoustofluidic applications, valuable papers gathered and reviewed the advancement in each application such as acoustic separation,[42,43] acoustic tweezers,[5] active actuation,[44] cavitation,[45] sound-based mechanobiology,[46] and technical aspects.[47] Here, we aim to review some of the less discussed, yet emerging applications where acoustofluidics not only has offered superior

Reza Rasouli received his Ph.D. from McGill University in Biological and Biomedical Engineering. His Ph.D. thesis focuses on the application of acoustofluidic platforms for the manipulation of bioparticles and biofluids. In his research, he developed various acoustic platforms based on boundary-driven acoustic systems and surface acoustic waves for precise microstream handling in applications such as nanoparticle synthesis and spheroids formation.

Karina Martinez Villegas is a master's student in the Department of Biological and Biomedical Engineering at McGill University with a background in Biomedical Mechanical engineering. She has been working in the past three years in the field of acoustofluidics, particularly with Surface Acoustic Waves (SAW)-based platforms, for cell patterning and cell characterization for tissue engineering applications.

Maryam Tabrizian is a full Professor at the Biomedical Engineering Department and Canada Research Chair holder in Regenerative Medicine and Nanomedicine. She is fellow of Guggenheim Foundation in Biomedical Science, the Biomaterials Science & Engineering, Royal Society of Canada-Academy of Science, and Academy of Health Science for her contribution to the field of Biomedical Engineering and Biomedical Sciences. She was the founding director of the Centre for Biorecognition and Biosensors from 2003 to 2011 and is currently the Editor-in-Chief of Materials (MDPI ISSN 1996–1944). Maryam Tabrizian is the author of over 250 peer-reviewed papers. Her research program is built on four main pillars: 1. development of biomimetic materials promoting angiogenesis and osteogenesis, 2. nanoplexes with targeting and tracking/imaging abilities for tissue and cell imaging, 3. real-time monitoring of molecular and cellular events at biointerfaces, and 4. Lab-on a-chip devices for bacterial detection, bioparticle synthesis and sorting.

performances but also has introduced features that are unique to acoustic systems. In this paper, we review the recent advancements in acoustofluidic technologies for diagnostic purposes, tissue engineering, drug synthesis and delivery, fundamental biology studies, bioparticle separation, and sorting. We briefly introduce the physics behind the acoustic phenomena to fathom the mechanism of operation and then put the spotlight on the exciting developments of acoustofluidics in recent years with an application-based perspective. The capacities, working conditions, application-specific considerations, and challenges of state-of-the-art acoustic techniques are described and compared to assist researchers in adopting the best-suited acoustofluidic strategy for their application.

2 Physics and acoustic excitation methods

The generation of acoustic waves in on-chip platforms generally starts by introducing an alternating electric current (AC) to a piezoelectric material. The electrical field modifies the polarization of the dielectric material, in a process known as the *converse piezoelectric effect*. The electrical field is transduced into mechanical oscillations, and subsequently, into acoustic waves which carry the mechanical energy and momentum by compression and rarefication through the medium.[48] The path of propagation in the medium within a piezoelectric slab classifies acoustic waves into two general types: surface acoustic waves (SAWs), which as the name suggests, propagate on the surface plane of the material, and bulk acoustic waves (BAWs), which travel throughout the bulk of the material. Although this general classification is based on the wave path, BAWs and SAWs show more fundamental differences including the selection of the piezoelectric material, the fabrication process, the operating conditions, and the nature of waves interacting with objects.

2.1 Bulk acoustic waves

Bulk acoustic waves are a well-developed technology with decades of history in numerous biomedical applications, many of which are currently commercialized, such as the quartz crystal microbalance (QCM) biosensor. BAWs in microfluidic devices are typically produced by thickness or transverse vibrations of the piezoelectric transducers adhered in the vicinity of the fluid channel (Fig. 1). The piezoelectric material in BAWs is usually piezoceramics, such as lead zirconate titanate (PZT). By tailoring the position, configuration, and the number of piezo elements, and their interaction with intermediate layers, one can induce various acoustic phenomena, including standing acoustic waves, traveling acoustic waves, and different types of microstreaming. Generally, the operational frequency of these devices is lower than 10 megahertz (MHz), corresponding to

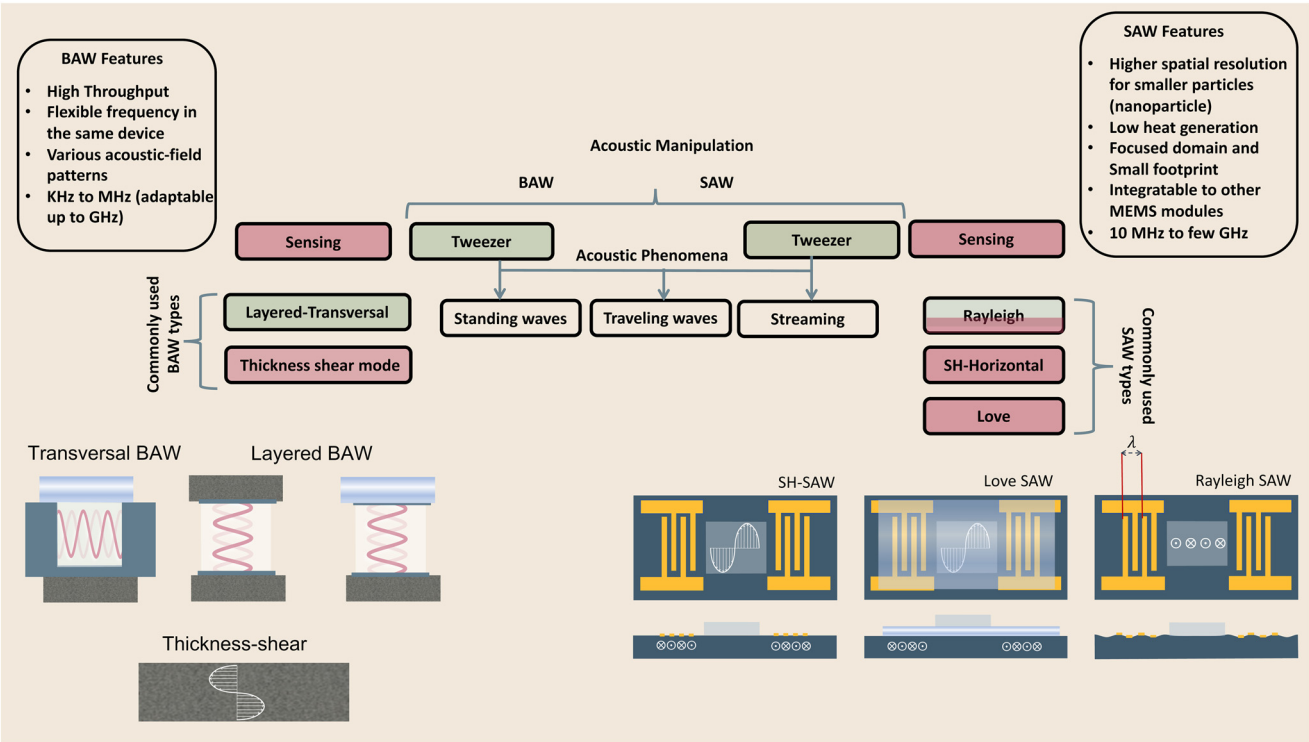

Fig. 1 Schematic and classification of frequently used acoustofluidic technologies for bio-applications. BAWs and SAWs can both be used as tweezers for the manipulation of bio-samples and as biosensors. Transversal and layered BAW settings are commonly used in acoustic tweezers while thickness shear has applications in sensing such as the QCM. Surface acoustic waves' types include Rayleigh waves which are preferred as acoustic tweezers, as well as SH-SAW and Love SAW which are often exploited as sensitive biosensors.

wavelengths ($\lambda > 100$ μm) that are significantly larger than many biological particles, *i.e.* cells, biomolecules, and cellular vesicles. Therefore, the manipulation precision of individual particles can be lower in BAW compared to SAW, however, they can handle bigger clusters of particles and work with high flow rates, making them suitable for scale-up applications.

2.2 Surface acoustic waves

Microfluidic SAW-based devices are fabricated by patterning interdigitated electrodes on highly efficient piezoelectric substrates, for instance, quartz crystals and lithium niobate ($LibNO_3$). Upon activation, each interdigitated transducer (IDT) conducts an electrical signal to generate mechanical oscillations from its fingerprint, which subsequently propagates as surface acoustic waves (Fig. 1).[49] When the wave from one IDT finger reaches the wave from an adjacent finger, it experiences a constructive interference, and the amplitude of the wave increases. In SAW systems, most of the acoustic energy is confined between the surface of the substrate to one wavelength below the surface.[50] This localization of the acoustic energy at the surface leads to confined active regions in SAW devices and minimizes the power consumption compared to that of BAWs.[5,51] SAW devices typically operate in the megahertz (MHz) to lower-end gigahertz (GHz) frequencies which corresponds to micron-order wavelengths. Hence, SAW devices are usually equipped with a high spatial resolution for the manipulation of single cells, and micron-to-nano-sized bioparticles. Since these piezoelectric substrates are biologically inert, the microchannel can be placed in direct contact with the substrate; however, the heat generation should be monitored.[51]

The most explored SAW type is Rayleigh waves, which can efficiently leak into the liquids in contact with the propagation path. Due to this strong liquid coupling, these leaky waves are almost ubiquitously used for the manipulation of biofluids and suspended particles.[33,52] Typically, the standard piezoelectric substrate to create leaky waves is a 127.86° *Y*-rotated, *X*-propagating lithium niobate, although the use of zinc oxide, aluminum nitride, and quartz have been also reported.[49] For sensing applications, shear horizontal surface acoustic waves (SH-SAW) are the gold standard. The horizontal direction of vibration (Fig. 1) in this wave type reduces the leakage of acoustic energy into the media and preserves the signal strength. Hence, SH-SAW offers a higher signal-to-noise ratio compared to Rayleigh waves and is more commonly used for sensing in liquid environments. The most frequently used piezoelectric substrates for SH-SAW include 36° *YX*, 41° *YX*, 64° *YX* $LiNbO_3$, lithium tantalite, and ST-cut quartz.[33,52] Love mode wave is another SAW wave type for biosensing which is similar to SH-SAW with a waveguide layer on the propagation path (Fig. 1). The waveguides, typically SiO_2 layers, have a smaller shear rate compared to that of the substrate and can further inhibit leakage into the media. This leads to the concentration of the acoustic energy at the surface, rendering Love-based devices highly sensitive to physical changes such as mass and viscosity for better sensing in both gas and liquid environments.[33,53]

2.3 Acoustic phenomena

When objects are exposed to acoustic waves, they show distinctive absorption, reflection, and scattering behaviors that lead to various interesting phenomena. In fluids, acoustic forces can create different types of microstreams. On the other hand, for particles, bubbles, and droplets the main acoustic forces are acoustic radiation forces (ARF), Bjerknes forces, and drag forces induced by acoustic streams. These acoustic phenomena are introduced and briefly discussed in the following sections with a focus on the functional concepts and mechanisms. For readers interested in the theory of acoustics, we recommend the insightful articles by Friend's and Bruus' group.[54,55]

2.3.1 Acoustic phenomena in fluids. Acoustic streaming is the formation of steady microvortices by the viscous dissipation of the acoustic energy or vibratory motions within the fluid medium. Two of the most notable acoustic streams in fluids are the Eckart streaming and the boundary-driven streaming.

Eckart streaming. The origin of the Eckart streaming is the viscous attenuation of the acoustic energy during the propagation of the waves in the bulk of a fluid.[56] As the acoustic beam travels away from the source, the energy of the waves dissipates at a rate proportional to the square of their frequency, thus generating an acoustic pressure gradient along the direction of propagation (Fig. 2). In microfluidic channels, this phenomenon usually leads to circulatory streams. For noticeable Eckart streaming to happen, the length of the bulk fluid medium must be in the order of the acoustic attenuation length, which usually occurs in high-frequency SAW devices.[56,57]

Boundary-driven streaming. This streaming, also known as boundary-layer-driven streaming, is the result of the acoustic energy dissipation in a thin boundary layer around oscillatory solid–liquid or gas–liquid interfaces.[58,59] The steep change of velocity from zero (on a no-slip interface) to a free-field value within a thin domain, transforms acoustic energy into a strong streaming flow in the confined boundary layer. The primary stream generates an outer counter-rotating vortex (Fig. 2). This method is commonly employed in microfluidic platforms by embedding oscillatory sharp edges,[60] bubbles,[45] the combination of both,[34] and even channel walls.[61]

2.3.2 Acoustic phenomena in particles, droplets and bubbles. Particles, droplets, and bubbles generally experience three types of forces in an acoustic field: primary acoustic radiation force, secondary acoustic radiation force, and the drag forces induced by acoustic streaming. The first force occurs due to the direct irradiation of acoustic waves, while the two latter are indirectly induced by the acoustic field from wave scattering in other objects.

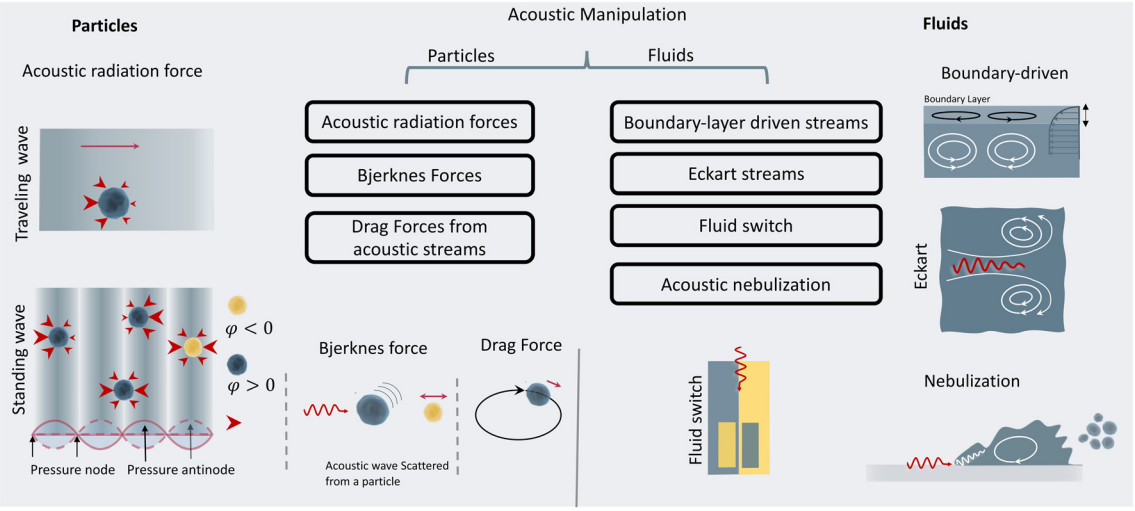

Fig. 2 Acoustic principles for the manipulation of fluids and particles. For particle manipulation, acoustic radiation forces, secnodary Bjerknes force, and drag forces are frequently exploited. For fluid manipulation, boundary-layer streams, Eckart streams, fluid switch and nebulization are the common approaches.

Acoustic streaming-induced drag forces (ASF). ASF is an indirect force of acoustic waves on particles that stems from vortices in their surrounding fluid. The acoustic streaming and their resultant drag forces can manipulate the trajectory of suspended cells or droplets. When a suspended particle with initial velocity ($\boldsymbol{V}_p$) becomes exposed to a streaming velocity field ($\boldsymbol{V}_s$), it experiences a Stokes' drag force, which realigns its direction of motion to the streamline of the vortices. The Stokes' drag forces are calculatable by:

$$\boldsymbol{F}_{drag} = 6\pi\eta R(\boldsymbol{V}_s - \boldsymbol{V}_p) \quad (1)$$

where η is the fluid viscosity and R indicates the radius of the particle. This equation assumes that the particles have a homogenous density.

Primary acoustic radiation force. When acoustic waves face a change in the acoustic properties of their path, such as encountering immersed particles or interfaces of different media, they experience absorption, refraction, and scattering. The change in acoustic momentum creates a net body force on the particles or fluid interface, known as the acoustic radiation force. In general, the acoustic radiation force is comprised of two components: acoustic gradient forces and scattering forces.†[62]

† Baresch *et al.*[280] considered only the monopole and dipole terms in the diffracted field, then derived the analytical ARF based on the generalized Lorenz–Mie theory with the following form:

$$\boldsymbol{F}_{ARF} = \{-\tfrac{1}{2}\{(\mathrm{Re}(\alpha_m)\tfrac{1}{2\rho_0 c_0^2}\nabla|p|^2 - \mathrm{Re}(\alpha_d)\tfrac{1}{2}\rho_0\nabla|\boldsymbol{v}|^2) + (\tfrac{k}{c_0}\mathrm{Im}(\alpha_m) - \tfrac{k^4}{12\pi c_0}\mathrm{Re}(\alpha_m)\mathrm{Re}(\alpha_d))\mathrm{Re}(p\boldsymbol{v}^*) + \rho_0\,\mathrm{Im}(\alpha_d)\,\mathrm{Im}((\boldsymbol{v}\cdot\nabla)\boldsymbol{v}^*)\}$$

($\boldsymbol{F}_{grad}$ and $\boldsymbol{F}_{scat}$)

where: $a_m = \frac{4}{3}\pi R^3\left(1 - \frac{\rho_0 c_0^2}{\rho_p\left(c_l^2 - \frac{4}{3}c_t^2\right)}\right)$ and $a_d = 4\pi R^3\left(\frac{\rho_p - \rho_0}{2\rho_p + \rho_0}\right)$.

$$\underbrace{\propto(kR^3)}_{\boldsymbol{F}_{grad}}\ \underbrace{\propto(kR^6)}_{\boldsymbol{F}_{scat}} \quad (2)$$
$$\boldsymbol{F}_{ARF} = \boldsymbol{F}_{grad} + \boldsymbol{F}_{scat}$$

The gradient forces, as the name suggests, stem from the gradient of the acoustic pressure and it is proportional to R^3, while the scattering component is proportional to R^6. In small particles, the scattering force becomes negligible compared to the gradient pressure force, except when the acoustic field is relatively uniform in space, such as in traveling plane waves.

Standing acoustic waves create a strong ARF on particles by increasing the gradient force factor in eqn (2). This increase in the gradient pressure force is due to standing waves periodically dividing the acoustic domain into regions of low and high pressure that push particles and droplets to either pressure nodes or antinodes (Fig. 1). Standing acoustic waves in BAWs can be constructed through the interference of waves from two facing acoustic sources with the same frequency or through an incident wave from a single source and its reflection by an acoustic reflector. On the other hand, standing surface acoustic waves (SSAW) are usually generated by two or more even pairs of counter-facing IDTs. The acoustic contrast factor of particles, known by:[6]

$$\Phi = \frac{5\rho_p - 2\rho_0}{2\rho_p + \rho_0} - \frac{\beta_p}{\beta_0} \quad (3)$$

where ρ and β are density and compressibility of 'p' particles or '0' surrounding. The acoustic contrast factor determines whether the particles reside in the pressure

nodes (particles with positive contrast) or antinodes (particles with negative contrast) (Fig. 2).

Traveling acoustic waves can be generated in either BAW devices, by using a single piezo ceramic, or SAW devices, by depositing one set of IDTs that propagate waves to the microchannel. By neglecting the gradient component in eqn (2), the ARF reduces to a scattering force with a magnitude that scales with R^6. The scattering forces continuously push particles in the direction of the beam propagation, causing particles to migrate away from the acoustic source.

Secondary acoustic radiation forces. The scattering of primary acoustic waves from particles or bubbles creates a net force on their adjacent particles. This force is also known as the secondary Bjerknes force and can create mutual particle–particle attraction or repulsion depending on the nature of the particles. The intensity of the secondary acoustic radiation force decays by an increase in the distance of particles and is also frequency-dependent, with forces usually peaking when the particle diameter approaches half to one wavelength ($d/\lambda \approx 0.5$–1).[63,64]

3 Acoustic cell patterning for tissue engineering

The interplay of primary and secondary radiation forces, and acoustic streaming forces creates various acoustic phenomena that allow flexible and versatile patterning of cells, while its gentle and non-contact nature preserves cell viability and functionality, rendering it a suitable tool for tissue engineering.[65–67] Reconstructing the physical architecture of the native tissue is one of the key aspects of tissue engineering.[68] Patterning cells is instrumental for analyzing cell–cell interactions and collective cell behavior such as network formations and neurite guidance, angiogenesis, cardiomyocyte beating, and myofibrillogenesis.[13,14,69,70] Acoustic radiation forces are more commonly used to pattern cells into 2D or 3D constructs wherein suspended cells can be actively guided and accurately organized in pressure nodes or antinodes, based on their compressibility and density properties. These reposing sites can be designed to create various spatial patterns, which can remain fixed over time or dynamically reconfigured by changing the frequency or by shifting the phase.[71]

The two main steps in tissue engineering are often divided into the acoustic organization of the cells into the pattern of interest, followed by a step to preserve the cell pattern to establish cell–cell connections and for cell patterns to mature into tissues.[71] The preserving step, *i.e.*, maintaining the patterned architecture over the tissue development period, is highly dependent on the cell type, cell–cell affinity, and cell-environment interactions. Cells with higher affinity rapidly form a strong arrangement dictated by the acoustic pressure node design, while low-affinity cells can easily migrate from their initial position.[23] To overcome this issue, hydrogels are often used to better maintain the cell patterns over time.

3.1 Single pressure node patterning

The linear arrangement of cells is seen in many native tissues and plays a vital role in cell and tissue functionality. For instance, cardiac, endothelial, and fibroblast cells tend to spontaneously organize in linear patterns of elongated cell structures to induce cell–cell interconnections and enhance their capability to withstand contractile and tensile loads in tissues.[72,73] ARFs in SSAW devices have been widely reported to effectively guide cells and particles in parallel lines and nodes within seconds by activating one or two pairs of IDTs

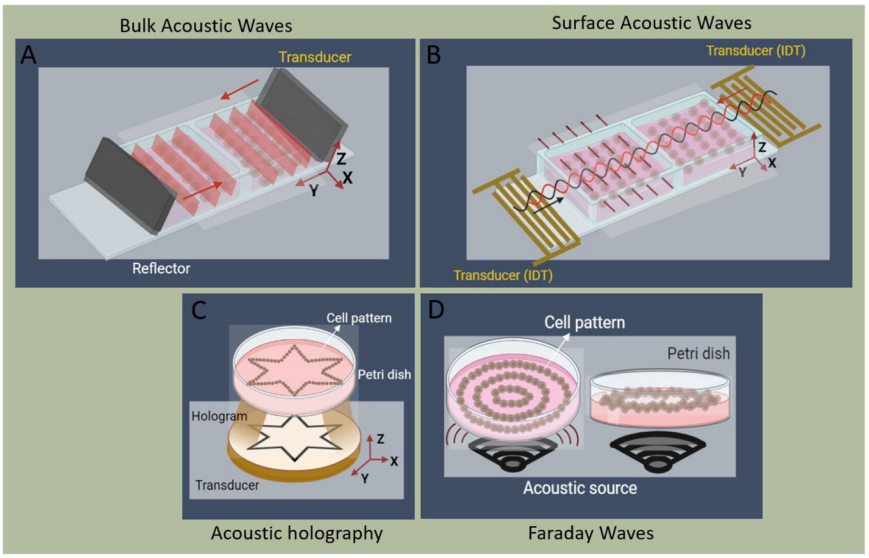

Fig. 3 Schematic of cell patterning modes, including A) bulk acoustic waves, B) surface acoustic waves, C) acoustic holography, and D) Faraday waves.

(Fig. 3B).[74] For instance, SSAWs were used to pattern HEK293T, endothelial (HMVEC), and glioma (U87) cells in pressure nodes and lines to study the gap junctional dye transfer dynamics of homotypic and heterotypic patterns.[75] This method allowed to successfully quantify the average dye transfer rates for all three cell types, showing an increase in intensity signal over time as an indicator of stronger cell–cell interconnection. Taking a step further, epithelial cancer cells (HeLa) and endothelial cells (HMVEC-d) were linearly patterned using SSAWs to study the cell migration of cancer cells with a preserved cell viability after 24 h (>99%). By tuning the phase shift, sequential patterns of heterotypic cell lines were generated to study the cell mobility in monoculture, random co-culture, and acoustic co-culture in real-time to study the events during cancer metastasis.[76]

Despite the rapid acoustic linear cell patterning, one of the main challenges of tissue engineering is the preservation of the cell pattern over time for tissue maturation. One approach for maintaining the cell pattern is to transform the free-moving cells to an adherent state. Under the presence of SSAWs, cells can form linear patterns with a gap above the substrate, avoiding surface contact. Upon the removal of acoustic waves, cells were shown to be gently gravity-deposited on a collagen-treated surface, allowing for the pattern to be maintained.[75] However, this scaffold-free approach to preserving cell patterns can be time-consuming (>1 h) and the patterns can easily be deformed. As a solution, scaffolds have been proposed to maintain the cell pattern over time. The formation of functional collateral cylindroid for ischemia therapy was performed by acoustically patterning endothelial cells (HUVECs) and human adipose-derived stem cells (hASC) in a catechol-conjugated hyaluronic acid hydrogel (Fig. 4B).[13] SSAW patterned structures exhibited higher secretion of angiogenic (VEGF) and anti-inflammatory cytokines (IL-10) factors for up to 7 days prior to transplantation into a mouse model. Another solution to retain acoustically defined patterns is to polymerize the cells and their surrounding hydrogel after SAW exposure. Photocurable polymers, including PEGDA and GelMA, were used to create patterns of HeLa, MC3T3-E1, and P12 Adh cells in capillary tubes using a pair of IDTs,[17] and slanted-finger interdigital transducers (SFITs) for the nodal alignment of cardiomyocytes in GelMA (<10 s).[14] Acoustically patterned cardiac cells demonstrated beating activity after 5–7 days with high cell viability (90%).

Linear patterning *via* BAWs (Fig. 3A) has also been vastly used, for instance, to study angiogenesis. ARFs in the form of standing waves were shown to induce cell banding patterns for HUVECs in 3D collagen-based hydrogels for up to 10 days.[24] Acoustically patterned HUVECs resulted in lumen-containing networks throughout the hydrogel on day 10. Acoustophoresis patterning and high-frequency ultrasound imaging tools have also been integrated to study the vascularization of

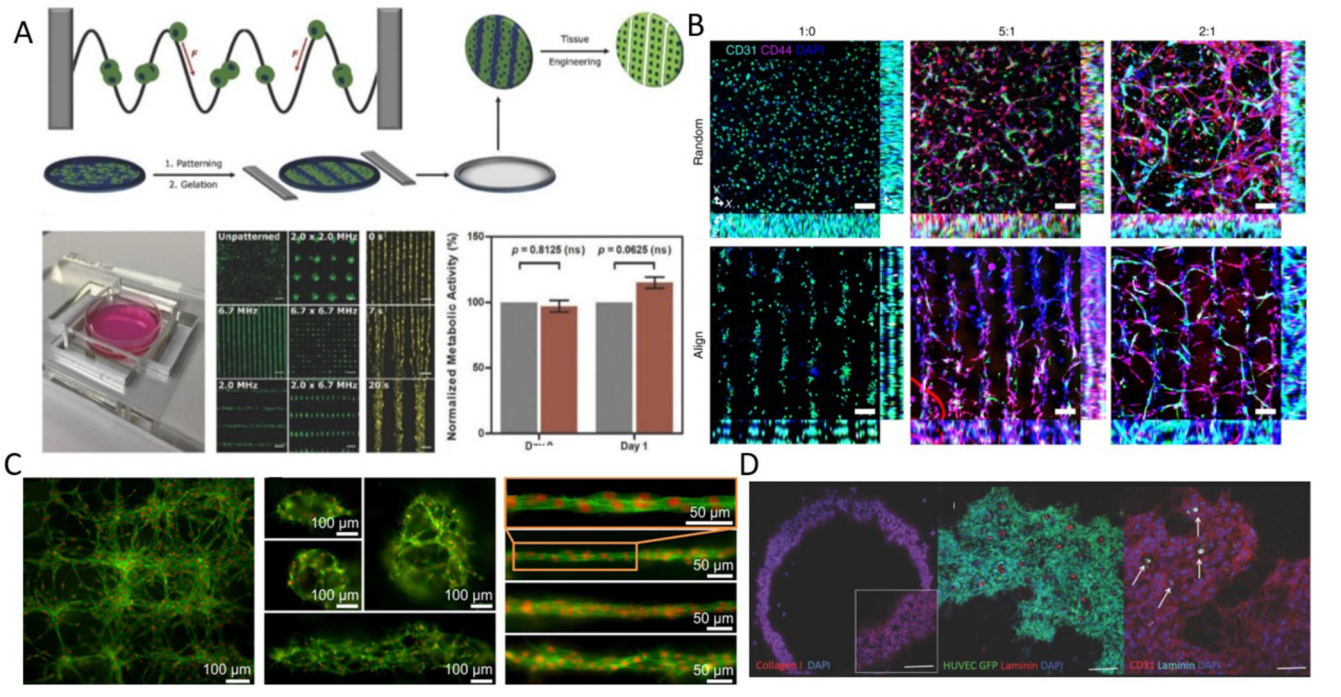

Fig. 4 Acoustic cell patterning for tissue engineering. A) Myoblasts patterning using BAWs with controlled gelation showing pattern preservation over time (scale bar = 200 µm).[70] B) Microvessels in hindlimb muscle *via* SSAW patterning of HUVECs and hADSCs at different HUVEC/hADSC ratios (1 : 0, 5 : 1, 2 : 1) (scale bar = 100 µm).[13] C) SSAW-patterned fibroblasts in fibrin gels with multiple 3D microscale cellular structures forming network (left), cages (center), and unidirectional bundles (right) after 30 hours.[11] D) Fibroblast spheroids patterning in ring shapes using Faraday waves showing vascularization (scale bar = 500 µm).[87] Reprinted with permission.

constructs with defined microvessel size and orientation.[77] One particular prospect of acoustic manipulation of cells is their combination with 3D bioprinting. Acoustic waves were actuated in a bioprinter nozzle to align C2C12 cells and HUVECs in the center of a GelMA fibrin hydrogel, narrowing the cell distribution to 5% of the bioink width and thus enhancing the orientation control and the elongation of the cells in the printing direction.[25] In a similar manner, but using human osteosarcoma cells (MG63) and hASCs, linear cell patterns were successfully produced in an alginate-$CaCl_2$ solution as a bioink for acoustic printing with high cell viability (>80%).[78] Linear patterning has also been reported to recreate muscle fibers and enhance the ability of cells to withstand tensile loads.[70] C2C12 myoblasts cells were suspended and acoustically patterned in GelMA, where cells showed enhanced myofibrillogenesis with aligned bundles of myotubes after 7 days (Fig. 4A).[70]

3.2 Multiple pressure nodes

In addition to linear patterns, complex geometries of cellular arrangements can be attained using acoustofluidics. BAW-based devices have been more often reported for patterning cells and particles into various geometries due to their larger acoustic domain compared to SAWs. For instance, a heptagonal acoustic chamber with 7 transducers could dynamically pattern particles, MDCK cells, and microbubbles in linear and hexagonal geometries by controlling the number, position, and phase-shifting of activated transducers.[8,79] In a similar heptagonal platform, C2C12 and Schwann cells were patterned to form neural network interconnections and study the outgrowth of neurites, which was largely governed by the orientation of the initial pattern.[9,80] ARFs in BAWs also allowed studying the forces for cell adhesion and cell organization, which influence cell functionality. Rat C6 cells were patterned in a hexagonal arrangement, showing an increased concentration of adhesion molecules NCAM and N-cadherin at the cell–cell interfaces after 8 minutes of BAW induction.[22]

As discussed in the previous section, cell patterns can be preserved over time by suspending cells in a hydrogel. As an example, NIH 3T3 fibroblasts were embedded in fibrin gels and were acoustically patterned using SSAW with different nodal configurations. After culturing the samples for 30 hours, different geometries were formed based on their initial patterning, including unidirectional bundles, a network structure, and a cage-like structure due to cell migration and growth (Fig. 4C).[11] Moreover, acoustic radiation forces can levitate cells in multiple parallel horizontal planes to form 3D constructs. Examples have been shown for the development of multilayer brain-like architectures with human embryonic stem cell-derived neuro-progenitors using fibrin hydrogels,[81] and sheet-like assemblies of epithelial and fibroblasts as a polarized epithelial barrier for up to 14 days.[82] Furthermore, Cohen and colleagues applied standing traps for scaled neuronal patterning and demonstrated directed neuronal growth of DRG neurons due to cellular organization, for up to 6 days.[19]

One limitation that should be considered with SAW devices compared to BAWs, is that their operating frequency is usually predetermined by the IDT geometry. As a solution, a dynamic cell mechanism patterning can be performed, using slanted-finger IDT (SFITs).[83] SFITs allow changing the distance between pressure nodal lines, and hence the dynamic adjustment of cell alignments. Circular slanted-finger interdigital transducers (CSFITs) were also reported to dynamically manipulate particles using multi-tone excitation signals.[84] Another approach to create more dynamic geometries is using waveguides, consisting of structures mounted on top of the piezoelectric element. Circular, rectangular, and triangular acoustic waveguides have been studied for guiding particles to the reference waveguide shape.[85] Similarly, but using a Petri dish as the waveguide coupled to a PZT piezo, PC12 cells were successfully patterned in concentric circles.[19]

3.3 Faraday standing waves and acoustic holography

Faraday waves occur at the surface of a fluid that is placed on a vertically vibrating plate and can take various complex shapes to pattern microparticles and cells (Fig. 3D). The patterns of Faraday waves are determined by the nature of vibration (frequency, amplitude, waveform), container geometries (boundary condition), and fluid properties (viscosity, density, surface tension).[86] As an example, a bio-tunable acoustic node assembly using Faraday standing waves was used to form cell spheroids ($>10^4$) within seconds. Both homogenous and heterogeneous tissue constructs were formed using primary rat hepatocytes, fibroblasts, and HUVECs, where the formation of bile canaliculi, hepatic gap junctions, and extracellular matrix was observed (Fig. 4D).[87] Faraday wave manipulation has also been used to induce vascularization, where HUVECs and hMSC spheroids were acoustically formed in fibrin and GelMA hydrogels inside Petri dishes and angiogenesis was recorded after 5 days.[88] The hydrodynamic drag force, generated by Faraday waves was also used to pattern fibroblasts (NIH 3T3) into a ring shape, which was then immobilized by a cross-linkable alginate hydrogel after 72 h.[89] Furthermore, Faraday waves have also been used to pattern pluripotent stem cell cardiomyocytes (hiPSC-CMs) in 3D aggregates *via* fibrin hydrogels, showing high levels of contractile stress, beating frequency, and contraction–relaxation rates.[90] Faraday waves have also been reported to pattern cardiomyocytes as programmable functional biorobots rings. The contraction and relaxation cycles of cardiomyocyte rings can act as self-powered biorobots to induce synchronous locomotion and mechanical actuation.[91]

Another method for creating complex cell patterns is the use of acoustic holography. In order to generate compound patterns by aforementioned methods, multiple acoustic sources must be carefully coordinated to superimpose waves which becomes excessively challenging for the arrangement of a large number of cells into complex topographies, as it requires thousands of transmitters. Static holograms are a smart solution wherein the phase information of the desired structure is encoded in a 3D-printed plate that is mounted on a single transducer and can generate more complex acoustic fields (Fig. 3C).[92] This method was exploited to custom-design acoustic fields for colon cancer cells (HCT-116) in a collagen-based solution.[93] Patterned cells showed high viability rate, where cells exhibited F-actin-based protrusions, indicating good cell growth and cell thriving within the matrix after 1 week. This method can thus add a new dimension to the large-scale patterning of complex shapes. However, as it stands, its resolution and cell–cell connections appear to be inefficient in comparison to SAW and BAW approaches. Using leaky surface acoustic wave holography can overcome the frequency and resolution limits of previous holographic techniques to control three-dimensional acoustic beams at the microscale region.[11]

3.4 Acoustofluidics for spheroids formation

In addition to linear and multiple nodal cell patterning, significant work on 3D spheroid formation *via* acoustophoresis has been conducted. Standing Bulk Acoustic Waves have been effectively used to aggregate cells into spheroids,[23] including embryonic mouse brain cells using photocurable GelMA to model Alzheimer's disease,[26] $HepG_2$ in alginate/$CaCl_2$ showing high viability for up to 10 days,[94] RBCs and $HepG_2$ using different transducer geometries,[95] $HepG_2$ spheroids showing great viability up to 3 weeks,[96] and core-shell ovarian cancer (OVCAR-8) cells for therapeutic studies and tumor interactions.[97]

SAWs have also been exploited to form spheroids by modulating pressure nodes for controlled cellular aggregation. In an SSAW platform, size controllable $HepG_2$ and HEK293 aggregates were formed with a smooth spheroid surface after 24 h and high proliferation and viability for up to 7 days.[98] Similarly, 3D multicellular human mononuclear leukemia spheroids (THP-1) were acoustically formed within

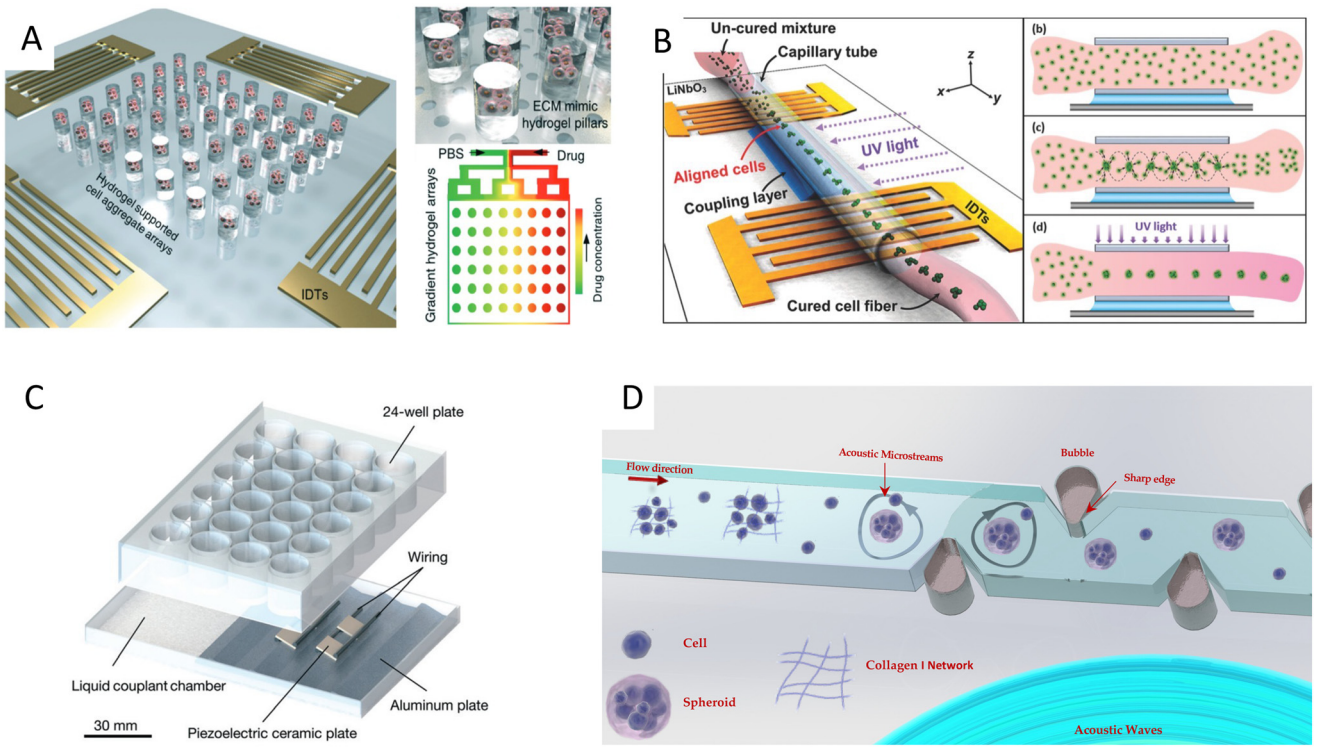

Fig. 5 Cell spheroid formation methods using acoustofluidics. A) Acoustic assembly showing multicellular aggregates encapsulated in the ECM mimic hydrogel pillars (left, top right) and convection–diffusion based gradient drug fluid generating microfluidic system at different drug environments (bottom right).[99] B) SSAW-based spheroid formation platform consisting of a polyethylene tube coupled to a parallel IDT setup with a water-coupling layer (left), where cells seeded in a cross-linkable hydrogel are patterned and UV crosslinked (right).[17] C) Acoustic streaming-based cell agglomeration platform consisting of a fluid coupling layer (left) to transmit acoustic waves to a 24-well plate (right) (scale bar = 30 mm).[102] D) Schematic illustration of acoustic formation platform using boundary-driven acoustic streams, where cells encompassed by collagen fibrils are trapped and reshaped into spheroids.[103] Reprinted with permission.

Table 1 Tissue engineering using acoustofluidics

Acoustic phenomena	Acoustic parameters	Cell/particle	Supporting material; culture time
SSAW	12.65 MHz, 1.5 W cm^{-2}	10 μm beads, HeLa S3, MC3T3-E1, PC12 Adh cells	PEGDA, GelMA[17]
	λ = 300 μm, 24.85 dBm	MCF-7, PS, fluorescent PS microspheres	Collagen type I; 1 day[104]
	3.4, 4.6, 6.4 MHz, −7 to −12 dBm	Neonatal rat ventricular cardiomyocytes	GelMA; 7 days[14]
	1.0, 3.4, 5.4, 7.5 MHz	NIH 3 T3 fibroblast	Fibrin gels; 30 hours[105]
	13.928 MHz	hADSCs, HUVECs, hiPSC-ECSs	HA-CA catechol-conjugated hyaluronic acid; 28 days[13]
BAW	2.46 ± 0.5 MHz (1 kHz step), 15 V_{pp}	HepG2, A498, ACHN, LUTC-2	2% agarose hydrogel; 2 days[23]
	0.5–2.0 MHz, 0–0.2 MPa	HUVEC[24,77] and HMVEC-D[77]	Collagen type I; 10 days[24,77]
	877 kHz;[25] 6.7 MHz, 20 V_{pp}[70]	C2C12 myoblasts[25,70] and HUVECs[25]	GelMA + fibrin; 14 days[25] and type I collagen, GelMa, agarose; 7 days[70]
	0.71–2 MHz, 100 and 200 m V_{pp}	Human adipose derived stem cells	Alginate; 4 days[78]
	340–680 kHz, 5 V	HUES 64 human embryonic stem cells	Fibrin; 30 days[81]
	1.95–2.12 MH, 4 V_{pp}	16HBE14o- epithelial cell and MRC5 fibroblast	Scaffold-free; 14 days[82]
SSAW + SBAW	19.4 MHz, 3–20 V_{pp} (SSAW) and 1.14 MHz, 10 V_{pp} (BAW)	2 μm PS beads, DRG and PC12	Collagen type I; 6 days[19]
Acoustic streaming	16.1 KHz, 10 V_{pp}	MCF-7, MDA-MB231	Collagen type I[103]
Faraday waves	80–157 Hz, 0.5–3 g	TCP particles, GFP-HUVECs and human mesenchymal stem cells	GelMA and fibrin gel; 5 days[88]

pressure nodes using a photocurable GelMA hydrogel. These spheroids showed faithful resemblance to cancer models where the cell aggregate activity was inversely proportional to the drug concentration, with a lower sensitivity to drug toxicity in comparison to monolayers (Fig. 5A),[99] and with high throughputs of 6000 spheroids.[15] Single SSAW fields have also been shown to generate mono-sized spheroids by coupling capillary tubes to the piezoelectric substrate along the wave propagation direction.[17,100,101] In this method, cells are first guided by acoustic pressure nodal arrays and then self-assembled to form spheroids. This mechanism was tested for HeLa cells in polymerized hydrogels (PEGDA and GelMA) to create spheroid embedded fibers ready for transplantation (Fig. 5B).[17]

Although less explored, acoustic streaming can be also used for spheroid formation. The hydrodynamic drag forces induced by acoustic microstreaming *via* a piezo element coupled to a microwell channel can agglomerate cells in the center bottom of the wells, forming spherical and compact spheroids (Fig. 5C).[102] A similar approach, albeit in a SAW setting, used 30 MHz focused surface acoustic waves to create microstreaming for BT-474 cell aggregation in well plates.[16] Furthermore, our group recently reported the rapid formation of cell spheroids in acoustic streams as build blocks for tissue engineering. We used boundary-driven acoustic streams to trap cells, adhere them with collagen, and release them in a continuous flow, all in less than 10 seconds. Using collagen as a natural extracellular matrix (ECM) component allowed to attach multiple cell lines including MDA-MB-231 and MCF-7 spheroids without relying on their ability to secret ECM (Table 1). This approach was compatible with multicellular spheroids as well as cell–particle composite spheroids, and also showed the merging ability of spheroid building blocks to form tissue constructs (Fig. 5D).[103]

4 Acoustofluidics for therapeutic applications

Acoustically formed tissue structures, such as tumoroids, are valuable drug screening models to investigate the response to chemotherapeutics such as Gemcitabine on pancreatic cancer cells (Panc02) and 5-fluorouracil (5-FU) on HepG2 spheroids.[15,98] However, the role of acoustofluidics in drug development is not limited to the model's fabrication. Various phenomena caused by acoustofluidics, such as acoustic streaming and mixing, sonoporation, nebulization, and acoustic forces are shown to be powerful tools for the therapeutic development, from the initial drug synthesis and nanocarrier fabrication to the delivery of active agents to the target tissue using acoustic energy.

4.1 Drug development and nanoparticle synthesis

One of the recent applications of acoustofluidics in drug development is the synthesis of nanoparticles, as drug nanocarriers. Nanoparticles have been increasingly employed for delivering therapeutic agents such as chemotherapeutics and vaccines. These nanocarriers can reduce the toxicity and

immune response by protecting the cargo from opsonization and subsequent sequestration by the phagocyte system. This protective mechanism, combined with targeted delivery and controlled release, can help the nanocarriers to release their cargo more effectively at the target site of interest and reduce their overall toxicity.[106]

Our group developed a boundary-driven acoustic streaming platform for the synthesis of liposomes and PLGA- PEG nanoparticles, two FDA-approved drug carriers. A combination of oscillatory bubbles and sharp-edges induced strong microstreams in the channels to control and accelerate the mixing of precursors and antisolvents. The mixing time generally governs the nucleation rate and the size of the nanoparticles. Therefore, controlling the mixing time allowed us to tune the size of the nanoparticles which is the key physical characteristic for their transportation in the body and the target delivery efficiency. Nanoparticle tracking analysis (NTA) results also showed a surge in the number of the produced nanoparticles using this acoustic streaming method, due to the obviation of aggregates (Fig. 6A).[34] Microstreams raised from the acoustic actuation of sharp edges were also used to synthesize various types of organic and inorganic nanoparticles, such as DNA/lipid complexes, polymeric, and chitosan nanoparticles.[107] The size of nanoparticles was shown to decrease by increasing the number of sharp edges. In another mixing mechanism, a resonating membrane was embedded in a microfluidic platform with multiple edges to induce acoustic microstreams. The microstreams were used to facilitate and accelerate the mixing time for the synthesis of budesonide nanodrugs, a poorly soluble asthma medication.[108] Among various proposed designs, the 8-point star shape system showed the highest throughput of 8 ml min^{-1} with a star shape mixer for the production of Budesonide nanodrugs and DNA nanoparticles (Fig. 6B).[109] A similar star shape acoustic mixer was also used for generating protein nanoparticles CA-P114, in which the size could be tuned by controlling the strength and time of mixing.[110]

In addition to microstreams, SAWs can be exploited for nanoparticle synthesis, albeit through a mechanism known as acoustic nebulization. SAW atomizers, first introduced by Kurosawa,[111] generally consist of a set of IDTs and a nozzle, channel, or paper wicking for the controlled dispensing of liquid at the propagation path of waves. When Rayleigh waves reach the liquid, the waves leak into the medium and deliver the acoustic energy to the fluid (33% approximately). The high-energy leaky SAW can cause destabilizing capillary

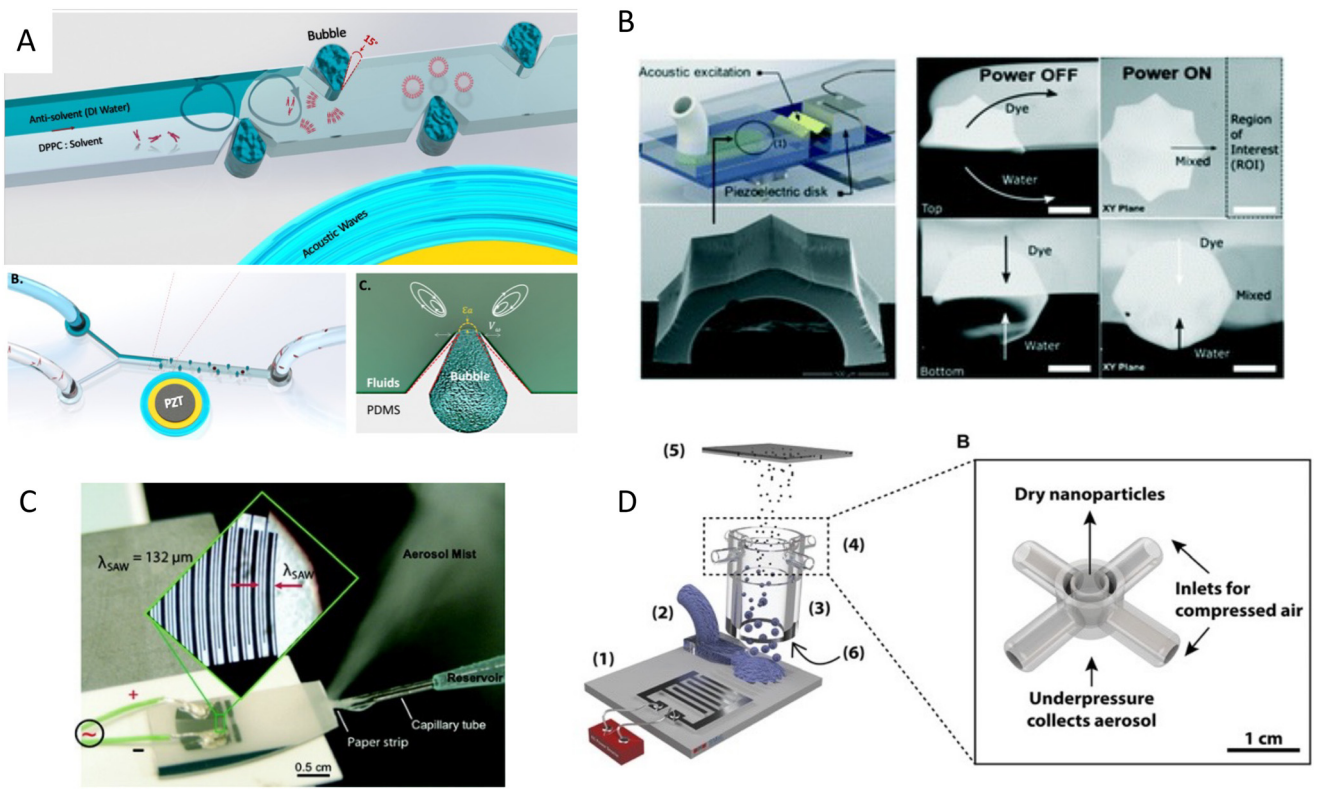

Fig. 6 Mechanism of nanoparticle synthesis using acoustic waves A) strong boundary-driven microstreams are generated by the combination of oscillatory sharp-edges and bubbles to accelerate the mixing for controlled synthesis of PLGA and liposome nanoparticles.[34] B) Acoustic microstreams induced by multiple edges system used for the synthesis of budesonide nanodrugs and DNA nanoparticles.[109] C) SAW nebulization device for the synthesis of multilayer nanocarriers with encapsulated plasmid DNA.[112] D) SAW nebulization device with a gas control unit which introduces reactive gases to atomized airborne drops for the synthesis of amorphous $CaCO_3$ nanoparticles.[119] Reprinted with permission.

waves at the interface of liquid and air, where droplets create fine aerosols (Fig. 6C).[112–114] The size of the aerosols can be tuned within the range of 0.1 and 30 μm by tailoring the acoustic frequency, fluid flow rate, and liquid characteristics, such as the surface tension and viscosity.[114–116]

Furthermore, the lower power requirements and higher operating frequencies in SAW devices lead to higher biocompatibility of these systems, as opposed to the mechanical and cavitation-based aerosolization methods, which tend to cause damage to the structure and functionality of biomolecules during aerosolization. The preserved biocompatibility along with the control on the particle's size, higher delivery percentage,[36] and the miniaturization of the system, render SAW a potential platform for the generation of micro/nano-sized drugs and also as a delivery method, particularly for the pulmonary system.[117,37]

Friend's and Yeo's groups have extensively investigated the use of high-frequency SAWs for nanoparticle generation and drug delivery purposes. They also studied the effects of SAW nebulization on the integrity and functionality of various shear-sensitive bioagents.[118,35] Upon atomization, the solvent content of the aerosols evaporates in flight and leaves behind the polymeric or protein nanoparticles to solidify. Friend *et al.*[113] used this mechanism to synthesize nanoparticles of poly-ε-caprolactone (PCL), a biocompatible and biodegradable polymer used for controlled release drug delivery. They further used this evaporative technique to produce solid protein nanoparticles of BSA and insulin and showed that the size of nanoparticles can be controlled by tuning the initial protein concentration in the solvent.[113] In another work, a SAW atomizer was coupled with a drying unit to control the kinetics of crystallization through the rate of drying, where reactive gases were introduced for chemical modification of drops while in flight. As a proof of concept, CO_2-enriched air was introduced to initiate the reaction with airborne drops of $Ca(OH)_2$ and synthesized amorphous $CaCO_3$ nanoparticles (Fig. 6D).[119]

One unique capacity of this nanoparticle generation method is the fabrication of multilayer polyelectrolyte nanocarriers. Qi *et al.*[112] could successfully synthesize layer-by-layer coated nanoparticles of positively charged chitosan or polyethyleneimine and negatively charged carboxymethyl cellulose. In their method, they collected the condensed nanoparticles of the first layer in an oppositely charged polymer solution to form the second layer. Through the repetition of this atomizing-suspension cycle, nanoparticles with up to 8 alternating layers were produced, with a controlled drug release profile. These nanoparticles were used to encapsulate plasmid DNA and showed the capacity for transfection (gene delivery) of human mesenchymal progenitor cells and COS-7 cells.[112]

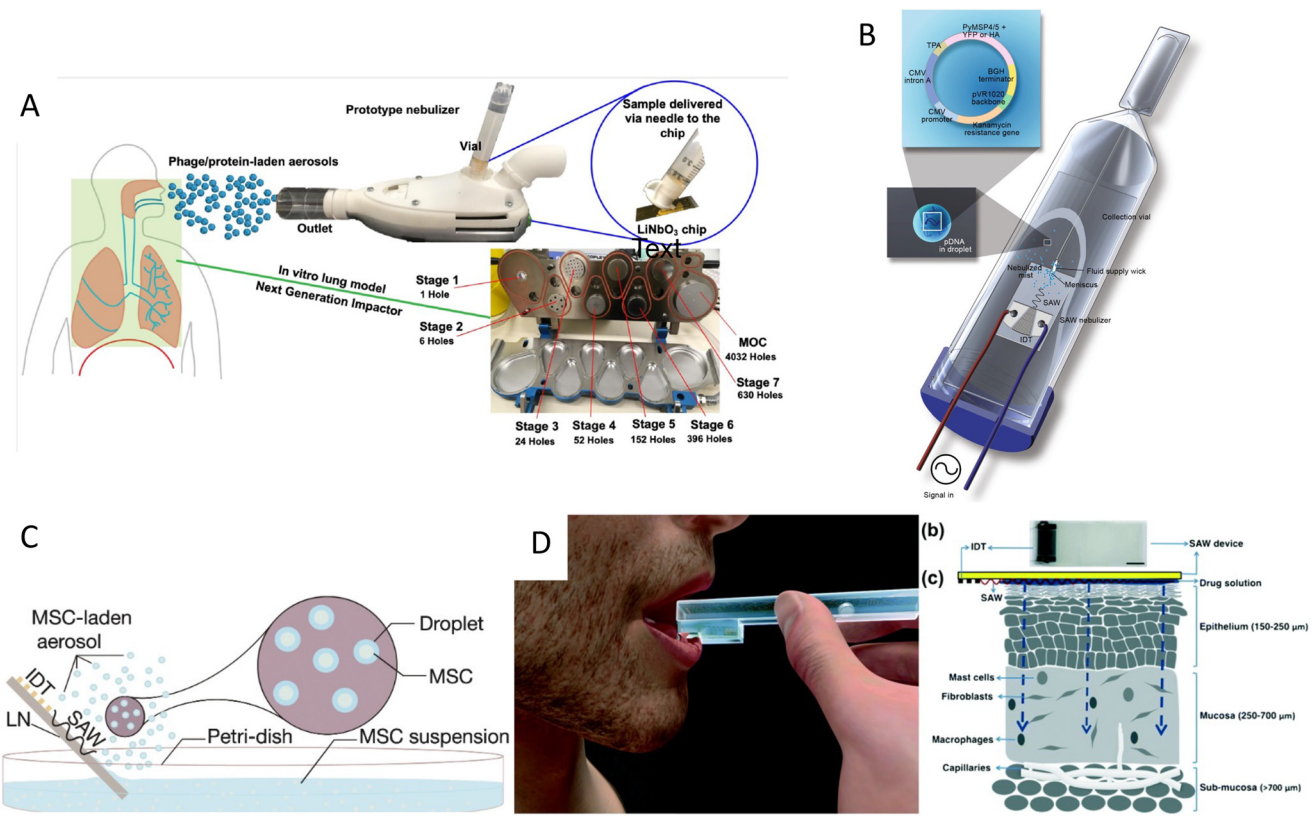

Fig. 7 Acoustic devices for drug delivery. A) Acoustic nebulization for pulmonary drug delivery of aerosols.[123] B) Acoustic nebulization for pulmonary plasmid delivery.[36] C) Stem cell delivery by acoustic nebulization.[124] D) Acoustic waves for permeabilization of tissue and inducing localized immune response.[125] Reprinted with permission.

4.2 Drug delivery

Acoustic nebulization not only could be used for synthesizing therapeutic carriers, but it can act as means to deliver therapeutic cargo, including drugs, RNA, proteins, and even cells. The facile, low-energy, and biocompatible aerosol formation method *via* acoustic atomization has a vast potential for the delivery of drugs to the pulmonary system. In this non-invasive approach, aerosols between 1 and 5 μm diameters can penetrate and deposit in the lower pulmonary tract and alveoli, where the large surface area and network of blood vessels facilitate the drug uptake.[120] Moreover, the high frequency and lower power requirement of SAW atomization methods significantly minimizes the large shear stress and cavitational damages of bigger molecules, thus being ideal for the manipulation of shear-sensitive bioagents, proteins, and DNA.[37,35]

SAW atomization was also shown to be an efficient inhalation therapy method, which can directly deposit 70 to 80% of the short-acting b2 agonist salbutamol (asthmatic steroid) in the lungs, used for the treatment of asthma.[117] In another study,[113] a microdroplet containing bovine serum albumin (BSA) was produced as a proof of concept to show the compatibility of the SAW atomization with proteins. Furthermore, this technique was used to synthesize peptide-laden aerosols of size model anti-mycobacterial peptides for pulmonary peptide delivery.[121] Interestingly, 70% of the aerosols were in a favorable size range for deep lung penetration with a 90% recovery rate, while retaining their integrity and anti-mycobacterial activity.[121] Another antimicrobial application was shown by producing plasma-activated aerosols for surface disinfection. SAW atomized plasma-treated could induce high oxidative stresses on bacteria which led to a 96% reduction in *E. coli* colonies.[122] This method was also used for the pulmonary delivery of antibiotic alternatives, phage K, and lysostaphin, to target Staphylococcus aureus with minimal losses in antimicrobial activity (Fig. 7A).[123] Rajapaksa *et al.*[36] proved the ability of the SAW nebulization method to address some of the challenges in pulmonary gene therapy and vaccination (Fig. 7B). The plasmid DNA encoding virus surface hemagglutinin protein (influenza A, human hemagglutinin H1N1) was delivered through intratracheal instillation to successfully immunize rats and sheep. The results showed that atomization did not harm the integrity of the plasmids nor hindered the vaccine to promote protective antibodies.

A very novel application of biocompatible SAW nebulizers could be in the promising field of stem cell therapy. Cell therapy can be an alternative to chemotherapy for progressive respiratory system diseases. However, the susceptibility of stem cells to stresses during nebulization such as shear, cavitation, and heat, hinders their direct delivery to the lungs. Alhasan and coworkers studied the cell viability and functionality under acoustic nebulization with an optimal 1.5 W driving power with cell viability of up to 86.0%. They showed that the metabolic rate, proliferation, gene expression, and protein expression after SAW nebulization did not show significant differences compared to untreated cells, confirming the feasibility of this approach for pulmonary stem cell therapy (Fig. 7C).[124]

The ability of acoustofluidics as a drug-delivery method is not restricted to nebulization and the pulmonary system. Ramesan *et al.*[125] used SAW to permeabilize the mucosal layer to enhance the delivery of small and large molecular therapeutic agents as an efficient route for vaccine administration. The low penetration depth of SAW waves proved to be useful for inducing a local immune response, allowing to transport the cargo through the mucus lining and epithelial barriers into immunocyte-rich regions. Moreover, this method avoids the cargo passing into the deeper vascularized submucosal regions in which the agent would be taken up by the circulatory system and thus diminishing the immunity (Fig. 7D).[125] Despite this clever use of lower penetration depth in high-frequency acoustic waves, the limited penetration renders this mechanism more applicable for *in vitro* or *ex vivo* applications rather than *in vivo*. One of the growing applications of acoustic waves, especially with high-frequency SAW is to acoustically mediate the transport of biomolecules, siRNA, nanoparticles, DNA, and membrane-impermeable dyes or nanoparticles inside the cell.

The principal mechanism of acoustic-mediated cargo delivery into cells is sonoporation, which is the biophysical disruption of the cells' phospholipid membrane under ultrasound energy. When acoustic pressure waves encounter cells or tissues, they promote both the opening at the cellular junctions, as well as the poration of the cell membrane.[126] Sonoporation has particularly been of interest as a nonviral transfection method to lower the toxicity and immunogenicity of viral transfection.[127]Microbubbles are the focus of many ultrasound sonoporation methods, as the expansion and contraction of microbubbles under acoustic waves are shown to induce cell permeability and facilitate the entry of therapeutics into the cells.[128] If the variation in acoustic pressure is strong enough, it can lead to the collapse of the bubble. This phenomenon is known as inertial cavitation, which creates a shock wave and high shear stresses. Qiu showed that acoustic cavitation could induce pores with diameters from 100 nm to 1.25 μm in cells. The higher acoustic pressure or longer treatment, the larger the pore size, leading to also a higher permeability and better transfection efficiency; nonetheless, at the expense of cell viability.[127,129,130]

Working with the uncontrolled and unpredictable nature of inertial cavitation is challenging as it leads to excessive cell and DNA damage, as well as the production of free radicals and reactive oxygen species and the generation of oxidative stresses.[126,131] Various proven alternatives have been introduced to avoid the micro-jetting forces from inertial cavitation such as stable cavitation. In stable cavitation, the acoustic pressure is controlled to make sure that the expansion and contraction do not lead to the collapse of the bubble. This oscillation can be used directly for infiltrating

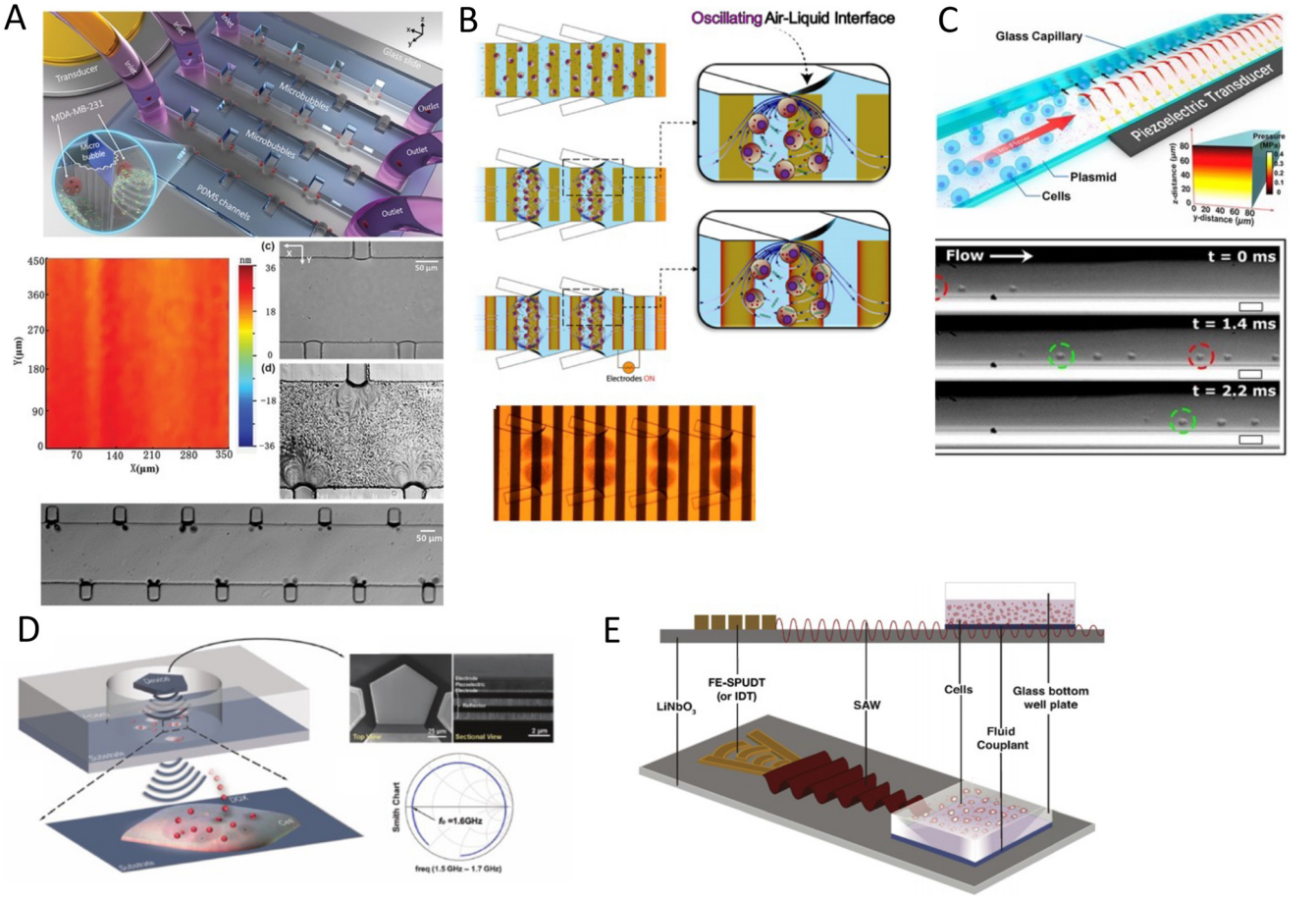

Fig. 8 Acoustic platforms for sonoporation and gene delivery to cells and tissue. A) Sonoporation by acoustic steams from an array of oscillatory bubbles.[134] B) The combination of acoustic microstreams by bubbles and electroporation for gene delivery.[135] C) BAW-based microfluidic device for high-throughput shear stress-sonoporation by the combination of microstreaming and acoustic radiation forces that push cells towards opposite capillary walls.[137] D) High-frequency bulk-based nano-electromechanical device for delivery of eGFP plasmid DNA and doxorubicin through hypersonic membrane poration and acoustic streaming.[139] E) Focused TSAW for delivering siRNA into nonadherent cells.[38] Reprinted with permission.

the cell membrane by pulling and pushing the plasma,[132] or indirectly by generating acoustic microstreams. Although the flow field induced in steadily oscillating bubbles has a generally lower velocity than that of micro-jetting, the continuous shear stress and Stokes' drag force on cells can be sufficient to reduce the micro-viscosity of the lipid bilayer and effectively disrupt the membrane, while remaining controllable and safe for cells.[57,133]

For its part, Meng *et al.*[134] used an array of monosized bubbles, sequestered in the sidewalls of their microfluidic channel to induce sonoporation (Fig. 8A). The microbubbles oscillate stably and created a pair of counter-rotating microstreams. The infused cells were trapped by the drag force from vortices and the secondary acoustic radiation force at the bubble surface, where the shear stress permeabilized MDA-MB-231 cells to allow propidium iodide (PI) to pass through the membrane. It would be of interest to see the performance of this sonoporation system for bigger molecules as well as for the transfection with mRNA or plasmids. Recently, a versatile and high throughput intracellular delivery was proposed by integrating hundreds of oscillating lateral cavities with an interdigitated electrodes array in a platform named acoustic–electric shear orbiting poration (AESOP).[135] In this two-step strategy, cells were initially trapped in the acoustic microstreams where the mechanical shear stress induced nanopores in cell membranes while the electric field from electrodes expanded the nanopores (Fig. 8B). AESOP system showed the delivery of molecules from <1 kDa to 2 MDa into both adherent and suspension cells, with over 90% delivery efficiency, >80% cell viability, and remarkable throughput of 1 million cells per min per chip.

In addition to bubble-based mechanisms, direct interaction of acoustic waves without bubbles can also induce sonoporation, especially using high frequencies.[127,133] For instance, standing waves can be an option to permeabilize the cell membrane in the absence of bubbles. The viability of cells with and without cavitation was compared and the cavitation-free method showed higher viability rates. This platform was further used to enhance the intracellular

delivery of drugs such as doxorubicin, apigenin, and luteolin to cardiac myoblast cells.[136] Belling *et al.*[137] introduced a BAW-based microfluidic device for high throughput sonoporation. Their platform consisted of a square glass microcapillary attached to a piezoelectric operating at 3.3 MHz. Under this acoustic field, cells experienced acoustic microstreaming and acoustic radiation forces that thrust cells towards opposite capillary walls, inducing shear stress-sonoporation (Fig. 8C). The platform showed an efficient gene delivery with a nuclear membrane rupture at a clinically-relevant rate of 200 000 cells min^{-1}, thus promising a non-viral transfection method for gene-modification treatments.[137]

One concurring challenge is that the frequency in these bulk platforms is not high enough to completely obviate the possibility of cavitation. Belling *et al.*[137] mentioned their system may not categorically suppress cavitation. As a solution to avoid the risk of cavitation, Zhang *et al.*[138] used a bulk-based nano-electromechanical device for achieving a hypersound (≈GHz) regimen (Fig. 8D). They proved that both eGFP plasmid DNA and doxorubicin can be delivered through transient nanopores created in the cell membrane by the combination of hypersonic poration and acoustic streaming, with high viability and internalization efficiency.[138] One reason for the high viability of high-frequency molecular delivery devices may lie in the mechanism of cell permeabilization. In high-frequency platforms, unlike with cavitational shock waves, the disruption of the lipid membrane is a temporal and rapidly healing mechanism.[37,139] Hence, high frequencies systems such as SAW platforms can be pertinent technologies for efficient sonoporation.

Table 2 Acoustically mediated therapeutics delivery

Application	Delivery mechanism/acoustic parameters	Nanoparticle and drug agents (target)/cell type (cargo)	Delivery route	Uptake/results advantages/shortcomings
Drug delivery	SAW nebulization (20–30 MHz, 1 W)	pVR1020-PyMSP4/5, pVR1020-YFP; H1N1 (pDNA encoding influenza virus protein) in droplets[36]	Intratracheal instillation (*in vivo*, mice) and pulmonary inhalation (*in vivo*, sheep)	>90% of pDNA integrity preserved, YFP expression after 24 h
	SAW nebulization (20 MHz, 1–1.5 W)	B2 agonist salbutamol–octanol (for asthma) in droplets (2.84 ± 0.14 μm)[117]	*In vitro* pulmonary model (60 L min^{-1} airflow)	70–80% delivery to lung model
	SAW (HYDRA) nebulization (10 MHz, 1.3 mL min^{-1})	Myoviridae (phage K) and a lytic enzyme (lysostaphin) (for staphylococcus aureus) (1–5 μm aerosols)[123]	*In vitro* pulmonary model 'next generation cascade impactor'	>90% recovery rate
	SAW permeabilization (17–55 MHz, 100 mV)	Molecular therapeutic agents (fluorescein, FITC-dextran, FITC-albumin)[125]	Mucosa of a porcine buccal model	>95% penetration rate in mucosal layer
Stem cell therapy	SAW nebulization (30 MHz, 1.5–3 W, 350 μL min^{-1})	MSCs encapsulated in droplets (13.5 ± 0.5 μm)[124]	Lung delivery	86 ± 4.2% cell viability
Transfection & drug delivery	Inertial cavitation (1 MHz, 5–60 s (sonication))	MCF-7 (PEI, DNA complex, pIRES2-eGFP)[129]	Sonoporation	32.0 ± 3.9% DNA transfection efficiency, 80 ± 2.3% cell viability
	Microstreaming and electroporation) (10–30 kHz, 12.5–35 V_{max})	HeLa, K562, Jurkat (plasmid DNA[135] encoding Cas9 protein and sgRNA)		>80% delivery efficiency >20% gene knockout >80% cell viability
	Microstreaming (107 kHz, 30–90 s)	MDA-MB-231 (PI)[134]		96.6 ± 1.74% sonoporation efficiency, 97.9 ± 1.26% cell viability
	BAW (with and without cavitation) (2.27 MHz, 3.2–40 V_{pp})	H9c2 (doxorubicin, apigenin, luteolin)[136]		Cavitation-free showed higher cell viability cytotoxicity >40% (doxorubicin) >50% (apigenin) >90% (luteolin)
	BAW (3.3 MHz, 0.48 ± 0.04 MPa, 40 V_{pp})	Jurkat, PBMCs, CD34 + HSPCs (Cy3-DNA, eGFP-expressing plasmid)[137]		200 000 cells per min delivery throughput >80% cell viability
	TSAW (Rayleigh wave) (10–30 MHz, 10 V_{pp}, 10 min (sonoporation))	Jurkat and HuT78 (siRNA)[38]		2-fold gene knockdown >91% viability
	TSAW (10 MHz, 2 W, 0.5–10 min (sonoporation))	HEK293T and HeLa (Au NP-FITC tagged, dextran, Cy3-labelled siRNA, GAPDH)[140]		>6-fold increase of NP concentration 2-Fold knockdown in gene expression and protein levels >97% cell viability

Under SAWs, the openings in the membrane facilitate intracellular delivery through the cytosol in the absence of endocytosis. This lower power method allows the exogenous biomolecules to be uniformly distributed in the cytosol, escape endosomal recycling, and it also increases their chance of reaching the nuclei while retaining the integrity of both cells and cargo during exposure.[37,140] One of the reasons for the maintained integrity is the nature of exposure, which involves continuous and low-amplitude waves with higher frequencies compared to short and fierce pulses.[38] In this methods, when the transmembrane delivery is achieved and upon the removal of the acoustic excitation, the lipid membrane instantaneously reorganizes into its native structure to keep cells healthy. The high biocompatibility and delivery efficiency can be used for applications such as cell transfection in the emerging field of chimeric antigen receptor (CAR) T-cell therapy.[37,140] The short exposure of cells to SAWs with frequencies above 10 MHz was also shown to facilitate homogenous internalization of gold nanoparticles by two- and six-fold increments after 30 s and 10 min exposure times, respectively. Successful cellular uptake of the fluorescently labeled Dextran and small interfering RNA (siRNA) was reported with cell viability of over 97%. The acoustically-transfected HeLa cells, with GAPDH silencing RNA, showed a two-fold knockdown in the gene expression and protein levels of the target enzyme.[140] In a follow-up study, the same group exploited the use of focused TSAW to deliver siRNA into nonadherent Jurkat and HuT 78 cells which are particularly challenging to transfect (Fig. 8E). The efficiency of this acoustofection technique was comparable to that of the standard nucleofection in achieving a 2-fold gene knockdown, however, with superior cell viability of over 91%, as opposed to 76% in nucleofection (Table 2).[38]

5 Acoustofluidics as a functional force for investigating phenotypes in biological organisms

Acoustic waves can have a complex functional influence on cells and tissues which requires extensive investigation. Sonoporation, as discussed in the previous section, is one of these functional effects of acoustics that leads to the disruption of the cell's membrane and nuclei. However, the interaction of acoustic waves with biological organisms is not

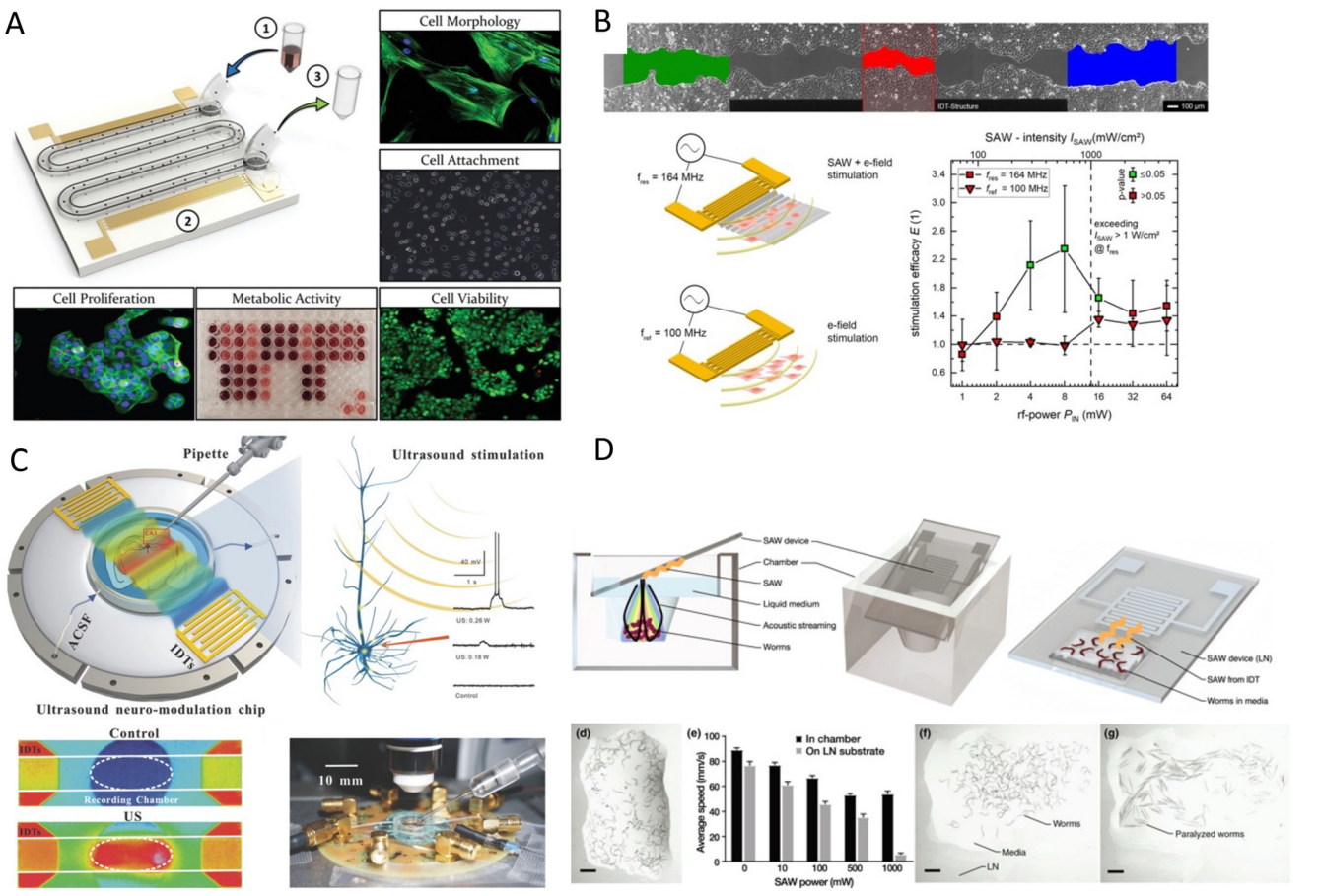

Fig. 9 Acoustic settings to investigate the effect of the wave as functional mechanical stimuli on A) cell's viability, morphology, metabolic activity and proliferation,[143] B) cell migration pattern and wound-healing properties,[147] C) neuromodulation and stimulation of neurons,[155,158] and D) the effect of acoustic waves on sensory neurons of *C. elegans* which induced short-term memory loss and brain injury.[41] Reprinted with permission.

limited to cell membrane rupture. Although many effects have been studied in conventional USW systems, the MEMS-specific wave modes and operating frequencies can also introduce unique and interesting effects on cell behavior, structure, and phenotypes. Moreover, miniaturization allows to focus or amplify the acoustic effects without drawbacks in large-scale systems such as self-heating and cavitation by offering a well-controlled domain.[141]

Martinez Villegas *et al.*[142] demonstrated the enhancement of the osteogenic differentiation and proliferation of adipose-derived stem cells embedded into a photocurable hydrogel *via* acoustic patterning using a frequency of 13.11 MHz (SSAW). Furthermore, Devendran *et al.*[143] scrutinized the phenotypes of four distinct human and mouse cell lines after exposure to 48.5 MHz (SAW). The viability, nuclear morphology, and proliferation rates after exposure remained comparable. However, they noted less cell attachment and spreading for mesenchymal stromal cells and mouse osteosarcoma. More interestingly, SAWs increased the metabolic activity in human keratinocytes and mouse fibroblasts. They hypothesized that the increased metabolic activity might be due to the acoustophoretic forces pushing cells to the side channels, which could protect them from shear stresses by background flow. However, their results confirmed that the acoustic excitation directly increased the cell's metabolic activity (Fig. 9A).[143] As suggested by this study, the SAW effect on cells can be very cell-type dependent. Moreover, since the acoustic radiation forces are often accompanied by other acoustic effects such as acoustic microstreaming, one of these acoustic phenomena might be the dominant effect depending on the experimental conditions. For instance, the change in the proliferation rate that was not observed in the previous study was reported in another study using a similar frequency of 48.8 MHz, but in a streaming-dominant system.[144] The circulation of the culture media by SAW-driven acoustic streaming on a Petri-dish, coupled to a lithium niobate substrate by a layer of PDMS, showed a 36% increase in the rate of cell proliferation.

One other interesting effect was reported by Brugger *et al.*[145] who patterned primary neuron cells in an SSAW platform and investigated the cell growth and cell adhesion direction after acoustic exposure. They observed that the neurite outgrowth was preferentially aligned to the axis of the SSAW pressure nodal lines,[145] which suggests the possibility of the cytoskeleton or the ECM realignment by acoustic waves.[141] The mechanical stimulation of cells by ultrasound waves in low frequency and conventional systems has shown various effects such as the increase in production of IL-8, VEGF, and bFG, with a 112% surge in collagen synthesis and a 35–52% increase in the proliferation rate of fibroblasts and osteoblasts.[146]

Stamp *et al.*[39] scrutinized the mechanical stimulations, along with electrical triggers that might be present in SAW platforms. They used their platform to promote cell growth and to direct the migration of Saos-2 cells in an acoustic path for tissue stimulation, showing a 17% increase in the healing rate of an *in vitro* artificial wound.[39] The same group, in a more in-depth study, explored the effects of different acoustic parameters such as frequency, power, and wave modes on the proliferation rate and ROS levels for various cell types. Cells were exposed to SAWs and electrode-generated electrical fields, activated by similar radiofrequency signals, to distinguish the mechanical effects from the electrical stimulation (Fig. 9B). Cells exposed to piezo mechanical SAWs exhibited a marked increase in growth rate and a 135 ± 85% surge in wound-healing speed, while the electrical-only stimulation did not show a significant effect. By excluding the electrical effects, vibration and its mechanical stimulation on cells were pinpointed as the root cause for enhanced wound-healing and overall proliferation. Moreover, no SAW-induced ROS was observed for power levels $\leq$64 mW.[147] SAW has been also reported as an effective stimulus for wound healing by promoting tissue oxygenation in ischemic feet. Human patients treated with a commercial SAW Patch device (NanoVibronix), experienced an increase in oxygen saturation and an overall reduction in pain.[40]

Additionally, acoustic waves are an interesting topic for studying mechanical cues in stem cell.[126] Low-intensity ultrasound stimulation is associated with enhanced differentiation and production of growth factors in neural stem/progenitor cells,[148] while acoustic biophysical stimuli have been employed to reprogram human dermal fibroblasts into extra multipotent cells.[149] Acoustic waves have been shown to mechanically stimulate human articular chondrocytes aggregates, where tunable biomechanical forces led to the development of engineered human cartilage constructs *in vitro* with mechanical properties comparable to those of native human cartilage.[150]

One recent finding concerning the functional effects of acoustic waves on cells is the enhancement of exosome generation. After 10 min of low-intensity acoustic waves exposure to cancer cell lines, the exosome generation was increased by 1.7-fold.[151] The high exosome production was attributed to increased calcium ion (Ca^{2+}) levels after acoustic exposure, which subsequently triggered a pathway that regulates exosome production.

The change in ion profile by acoustic waves is reported in other studies too. Membrane proteins, including ion channels under acoustic waves, experience mechanical vibrations that can alter the conformation of their active state. Some of these mechanosensitive proteins are calcium, potassium, and sodium ion channel families which can translate mechanical stimuli into biochemical signals, known as mechanotransduction.[152] These ion channels therefore can act as acoustically activated nano-valves which have been particularly a subject of interest in neuromodulation, where an altered ion profile in neurons is the hallmark of neurological disorders.[153] The activation of ion channels and evoking action potentials are fundamental in the study of neuronal circuits and their functionality.[141]

Table 3 Acoustic waves as functional stimuli

Wave mode	Phenotype/phenomena study	Target species	Acoustic parameters	Outcomes
SAW	Enhanced proliferation and osteogenic differentiation	Adipose derived stem cells in methacrylated collagen[142]	13.11 MHz, 10–40 V_{pp}	>85% cell viability, >30% increase in metabolic activity, >80% increase in alkaline phosphatase activity, increase in osteocalcin expression
	Cell adhesion and morphology[143] and cell proliferation[144]	MSCs, MG63, L929 and HaCaT[143] and U-937[144]	48.5–48.8 MHz, 400–800 mV	Increased of metabolic activity in HaCaT and L929, change in morphology in MG63 and MSCs[143] >36% increase in cell proliferation[144]
	Cell growth and direct migration	Saos-2[39]	159 MHz, 4 mW	>15% increased migration
	Cell migration and proliferation rate and ROS production	MDCK-II, SaOs-2, T-Rex-293[147]	164 MHz, 1–16 mW	135 ± 85% wound healing increase
	Wound healing by tissue oxygenation	Ischemic feet patients[40]	96 kHz for 30 min	Increase in oxygen saturation, pain levels dropped
	Ion channel activation[155] and neuromodulation[156]	CA1[155,156] and CA3[155]	27.38–30 MHz, 0.12–0.45 MPa	20% calcein release in I92L-expressing neurons 30% increase of neuronal excitability[155] 13% stimulation of outward potassium currents[156]
	Epilepsy treatment[161]	Human epilepsy brain samples[161]	28 MHz, 0.13 MPa	65% inhibition of epileptiform activities[161]
	Exosome generation	U87-MG, A549[151]	10 MHz, 10 min exposure	1.7 and 10 fold increase of exosome generation and concentration 95% viability
BAW	Cell proliferation, collagen, and NCP synthesis, and cytokine production of interleukin	Gingival fibroblasts, mandibular osteoblasts, monocytes[146]	1–3 MHz (pulsed) and 45 kHz (continuous)	35–52% increase in cell proliferation in fibroblasts and osteoblasts, 112% increase in collagen and NCP synthesis, VEGF production is stimulated by all, IL-8 and bFGF production was enhanced by osteoblasts
	Neurite outgrowth and cell differentiation	NSPCs spheroids[148]	560–1138 kHz, 40 kPa	Attachment and differentiation of NSPCs Increase in calcium ion influx by dual-frequency ultrasound

Ye *et al.*[154] transfected rat hippocampal neurons to express a mechanosensitive channel of large conductance (MscL), and used a 30 MHz SAW system to activate the channel. The MscL in the membrane sensitized the cells to an ultrasound stimulus of 0.25 MPa. While acoustically activated, the open MscL gate allows dyes to pass into the cytoplasm which can be a pathway for drug delivery. Moreover, the MscL-expressing cells showed faithful spike trains in response to acoustic pulses up to 5 Hz with millisecond accuracy. It was also reported that SSAW acoustic neurostimulation can modulate the kinetics of native mechanosensitive ion channels such as sodium and potassium in rat hippocampal slices.[155,156] In doing so, they could control the ion efflux, activate and regulate the shape and rate of spikes, and could study the effects of acoustic waves on neurons' excitability and firing thresholds, as they are the minimum current neurons needed to produce an action potential (Fig. 9C).

The characteristics of acoustic signals such as intensity, duration, continuous or pulsed nature, and frequency of pulses are also influential in promoting or suppressing neuronal activities.[156,157] TSAW was reported to trigger the neuronal behavior of *C. elegans* under a single-shot and short acoustic pulse.[158] It was observed that the mechanical stimulation of USW can reverse the locomotion behavior in *C. elegans*, as 85.29% ± 6.17% of them started to move backward after a 6.4 ms pulse. The analysis of the calcium profile in the worms showed an elevated concentration of Ca^{2+} after acoustic excitation in a type of sensory neuron that is triggered in face of danger or stress.[159,160] This hypothesis suggests that it is possible to directly activate sensory neurons by acoustic waves. In another study, Miansari *et al.*[41] exposed *C. elegans* to SAW for an extended duration of 10 s to induce traumatic brain Injury (Fig. 9D). The continuous exposure, although with less acoustic pressure than that of the pulsed, caused temporary paralysis of the worms and reduced chemotaxis learning and short-term memory loss. The effects of SAW on *C. elegans* in both studies were tightly connected with the mechanical vibrations on the cell membrane by the acoustic waves. This connection is mentioned in many functional acoustic waves studies and suggests that the vibrational stimulus has a dominant effect (Table 3).

6 Acoustic bio-characterization and sensing

The double capacity of acoustic systems as both actuators and sensors renders them unique in offering various characterization and biosensing techniques. In the first part of this section, we discuss the different acoustic actuation methods for the characterization of biosamples, specifically the mechanical properties of cells, such as compressibility and adhesion. In the second part, acoustic biosensors for the characterization of cells, proteins, and other biomolecules are reviewed. Finally, we discuss the combination of the acoustic actuators and biosensors for enhancing the sensing sensitivity through addressing the biofouling issues such as non-specific binding and low mixing.

6.1 Acoustic Mechanotyping

Cell mechanical properties may serve as biomarkers due to their correlation to various diseases, such as malaria, sickle cell anemia, atherosclerosis, cerebral edema, stroke, and cancer.[162–166] Acoustofluidics provides an alternative to conventional atomic force microscopy (AFM) and optical tweezers (OT) for cell analyses with higher throughput (>10 cells per s), contactless nature, and versatility to work in various media.

Xie and colleagues[167] used an acoustic oscillating bubble to deform cells suspended in an acoustic streaming field to quantify cell deformability. This mechanical biomarker was measured in different cells, including HeLa, HEK, and HUVEC in a single experiment. The deformability of each subpopulation in a mixed and heterogeneous cell sample was measured by using both fluorescent markers and mechanical biomarkers. Recently, Läubli *et al.*[168] integrated an acoustic manipulation device with a micro-force sensor to rotate plant species and microorganisms and measure their mechanical properties at different regions of interest. In their model, acoustic radiation forces and acoustic streaming were used to manipulate single L. longiflorum (lily) pollen grains and *C. elegans* and measure the displacement at different regions and depths of the specimen.

Acoustofluidics can be also used to measure cell compressibility based on the acoustic radiation force. A particle/cell exposed to an acoustic field experiences an acoustic radiation force which is dependent on acoustic contrast. By determining all medium and wave properties, ARF can be calculated using cell trajectories in the acoustic fields. Hartono *et al.*[169] recorded cell trajectories in a BAW field and obtained the compressibility of different cell types, which was correlated with a cancer biomarker. For its part, Wang *et al.*[170] investigated the use of BAW-based acoustofluidics for measuring single-cell biophysical properties in cancer cell lines and immortalized cancer cells as biomarkers for cancer staging and prognosis. Cells with similar diameters were successfully classified based on their deflection to the acoustic field, where cells with a higher acoustic contrast factor experienced a higher ARF and hence, bigger deflection. Furthermore, acoustic systems can be also easily integrated to other modules as preparation step, for instance acoustic forces are proposed to align cells in pressure nodes to measure their impedance with the second module of a planar electrode impedance cytometer.[171,172]

The strength of single molecule adhesion has also been characterized with acoustofluidic methods, known as acoustic force spectroscopy (AFS). In this technique, cells and molecules that are in contact with a microfluidic surface are levitated using BAWs. Kamsma and colleagues introduced a single-cell AFS using acoustic waves to exert forces up to 1nN to cells in parallel.[173] AFS has also been used to evaluate the binding and interactions of protein-DNA[174–176] with forces up to 120 pN. ARF has also shown exceptional capacity as a high-throughput force spectroscopy method to quantify intercellular adhesion forces. The controllable and reversible acoustic radiation forces are successfully employed to pair and separate hundreds of cells in repeatable cycles to precisely measure cell affinity. Such platforms can be invaluable tools for the study of cell affinity, particularly for the development of CAR T cell therapies and the detection of the most responsive natural killer cells in the treatment of cancer.[177]

6.2 Acoustic biosensors

Acoustic waves have a long history of application as biosensors, one well-known example is the commercialized quartz crystal microbalance (QCM) and its dissipation version (QCM-D). The QCM-D is a BAW method that can measure mass/density changes, viscosity, and elastic modulus of biological samples inside the liquid medium with a pulsed excitation of 5–20 MHz.[178] In recent years and with the advancements in MEMS manufacturing, the majority of the latest studies have been shifted from QCM-D to SAW

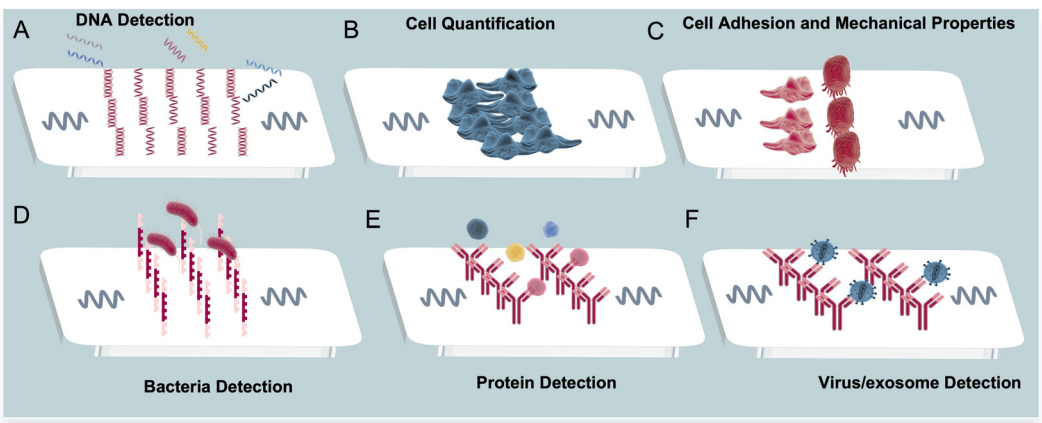

Fig. 10 Acoustic waves as biosensors for A) ssDNA detection, B) cell detection and quantification, C) cell morphology characterization, D) bacteria detection, E) protein detection, and F) virus or exosome detection.

biosensors. The wide range of operating frequencies of SAWs allows for easy customization to detect various biological samples, with higher frequencies yielding better sensitivity for smaller samples, such as biomolecules. Moreover, the confined and well-controlled detection region, low power consumption, and the capability of surface modification are some of the additional advantages of SAWs that render them appealing for biosensing applications.[33] The main sensing mechanism of SAW biosensors is somehow similar to that of QCM, in that the decay in frequency and the amplitude of acoustic waves are quantified for the detection of various biomolecules and biospecies (Fig. 10).[179]

This sensing zone can either be functionalized with probe molecules to bind to the floating target biomolecules and immobilize them for sensing, or it can be directly used for biosensing species, such as cells and tissues. As the acoustic waves, emanated from the input IDT, travel on the surface and reach the sensing region, they interact with the target species adsorbed on the surface, causing a change in the mass loading which is detectable by shifts in the SAW phase, resonant frequency, and amplitude.[33,113,7] When the output acoustic waves are received in the readout IDT, they re-transduce into electric signals for deciphering the measured changes in the acoustic waves into the concentration of target biological species or other sensing targets, such as the viscoelasticity of the species.[118] Alternatively, IDTs can be added to the delay line to act as resonators and minimize the scattering of acoustic waves and improve the signal power and performance.[118] Other strategies such as coating the delay line with waveguides are also commonly used in biosensors to minimize the signal loss while allowing a wide range of operating frequencies. Here, we briefly discuss the potential of acoustics for biosensing cells, biomolecules, and bioparticles.

6.2.1 Acoustic biosensing for cells detection and quantification. The two major applications of acoustic biosensors for cell analysis are the quantification of cells and the characterization of their physical properties, such as viscoelastic properties. For instance, Chang *et al.*[180] devised a leaky SAW sensor for label-free quantification of MCF-7 cells. They coated gold electrodes with aptamers for specific capturing of target MCF-7 to enhance their sensitivity. The sensor showed a linear relationship between phase shift and the logarithmic concentration of MCF-7 cells from 1×10^2 cells per ml to 1×10^7 cells per ml and showed that the detection limit of this method was 32 cells per ml.[180] Wang *et al.*[181] used an SH-SAW sensor to quantify the mass loading of RAW264.7 macrophages and A549 cancer cells, by measuring the frequency shift in both 2D and 3D setups, reporting no significant adverse effects on cell viability. They cultured A549 cells in a nanofiber scaffold to promote tumor formation and were able to monitor the increase in cell density and tumor growth over 8 days. In a similar way, the frequency shift can be monitored to measure the mass of the cells that sit in the delay zone. To increase the sensitivity, a high frequency of 6.4 GHz was used with a confined detection region. The platform showed a high mass detection resolution of 6.7×10^{-16} g cm^{-2} Hz^{-1} and was able to detect EMT6 and 3T3 cells at a single-cell level with a throughput of 10^5 cells.[182]

In addition to cell quantification, acoustic sensors can measure the mechanical properties of cells, such as stiffness and viscoelasticity. An extensive library of papers used QCM-D to measure these important physical properties of cells, which can divulge fundamental information about their physiological behavior and phenotypes.[184] More recently, SAW-based sensors have been reported for measuring the cell mechanical response with higher sensitivity. A Love-mode

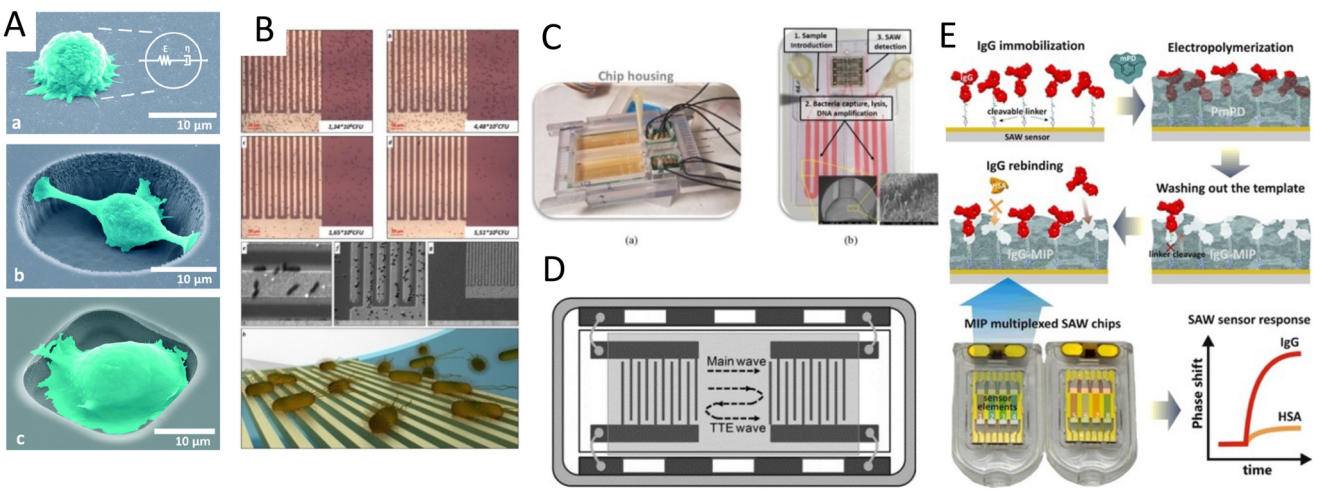

Fig. 11 Acoustic settings for various biosensing strategies: A) embedded microcavities on a SAW platform to characterize the single-cell stiffness,[185] B) a conformable SAW immunosensor for the detection of *E. coli* bacteria,[186] C) integrated LOC device that can capture, lyse, and detect bacteria in separate modules for rapid detection of foodborne pathogens,[189] D) a SAW sensor with three-fold path line for sensitive detection of cardiac disease biomarker,[193] and E) a protein detection platform using imprinted polymers as synthetic probes.[194] Reprinted with permission.

SAW sensor was reported to measure the contractile properties of forces in HL-1 cardiomyocytes.[184] They seeded 10 000 HL-1 cardiomyocytes cells in the detection regions where their contraction forces and stiffness were modulated by treating the cells with *verapamil*, which reduces the contraction forces and stiffness in the cells, and *isoprenaline* which acts reversely. By recording the phase and amplitude shifts, the changes in contractile properties could be correlated to the amplitude shift. Embedded microcavities on the SAW interrogation region could also be used to characterize the single-cell stiffness of MCF7, MDA-MB-231, SKBR3, and JJ012 cell lines.[185] In this method, a single cell was placed in the microcavity, and the phase shift was compared to that of the microcavity filled with only media to calculate the velocity differential, and subsequently, the stiffness modulus of the trapped cell (Fig. 11A).

The high sensitivity of SAW sensors renders them instrumental for the detection of pathogenic cells such as bacteria. Lamanna and colleagues proposed a conformable SAW immunosensor for the detection of *E. coli* bacteria where they grafted *E. coli* binding antibodies on the sensing zone and measured the change in mass loading caused by the bacterial adhesion. Their platform was based on the deposition of a thin film of piezoelectric aluminum nitride (AlN) on a recyclable polyethylene naphthalate substrate. They compared the detection limit of identical IDT designs and piezoelectric (AlN) mounted on flexible PET substrate, to create Lamb wave modes and on a hard silicon wafer to create Rayleigh wave modes. A superior detection limit was attained being 6.54×10^5 CFU (colony-forming units) mL^{-1} on PET substrate compared to 1.04 × 106 CFU mL^{-1} on silicon (Fig. 11B).[186] The above paper is a showcase of direct bacteria detection, however, most studies in this area used the DNA equivalent of bacteria as the model for detection.

6.2.2 DNA detection. The common method for the detection of single-strand DNA (ssDNA), is to immobilize their matching strand as the DNA probe, introduce the sample for binding, and finally measure the changes in the acoustic waves' characteristics. Cai *et al.*[182] immobilized a DNA probe that targeted a specific DNA sequence in the delay area and upon hybridization of the target strand with the immobilized probe strand, a molecular film was formed, changing the wave velocity and the resonance frequency. Their platform showed a high detection sensitivity of 6.7×10^{-16} g cm^{-2} Hz^{-1}, making it capable of detecting a single DNA base.[182]

In addition, a similar mechanism has been specifically used to model bacterial detection, consisting of a shear horizontal surface acoustic wave (SH-SAW) to detect a food pathogenic strain (*E. coli*, O157 : H7).[187] A specific DNA sequence from *E. coli* O157 : H7 was immobilized on the sensing region as the probe of ssDNA, allowing to measure the frequency shift (Δf) upon their hybridization with the complementary DNA with a detection sensitivity of 0.6439×10^{-9} m/0.1 kHz.[187] A Love wave biosensor was also reported for the detection of Salmonella bacteria. The ratio of the amplitude change over phase shift ($\Delta A/\Delta ph$) was monitored during the binding of the target DNA to the Salmonella DNA template that was immobilized in the sensing zone and reported a detection limit of 100 bacteria cell equivalents per sample.[188] In a recent study, an LoC sensing platform that utilized SAW was employed for rapid detection of foodborne pathogens such as Bacillus cereus, Salmonella, *E. coli*, and Listeria (Fig. 11C). This integrated device could capture and lyse bacteria in a separate module with an antibody functionalized surface, amplify the DNA isothermally, and finally introduce the amplified DNA to the SAW module for detection.[189]

SAW biosensors have also been shown to detect DNA mutations in clinical samples. Liu *et al.* conjugated graphene oxide in a SAW-based sensor whereon they immobilized the probe DNA for monitoring DNA mutations. 136 clinical samples were used to measure the DNA hybridization with various targets by recording the phase shift in SAW signals. An identification specificity of 88.6% and a sensitivity of 100% for CC and CT genotype, and 96.2% and 98.0% for diagnosing CT and TT genotype, was recorded respectively.[190] To enhance the detection limit of sequence-specific DNA in blood serum, nanoparticle-DNA complexes can be incorporated to amplify the signal of their SAW biosensor.[191] After the initial hybridization of the DNA target with the DNA probe, the hybridized duplex was exposed to DNA polymerase enzymes that elongated the target protein, creating an extended ssDNA where the Ag^+ specific sequence can hybridize. Finally, the complex was exposed to a reduction agent in which the silver ions nucleated and synthesized the silver nanoparticles, showing that the nanoparticles can significantly increase the mass loading, amplify the signal, and enhance the detection limit by 3 orders of magnitude.

6.2.3 Protein detection and quantification. The mechanism of protein detection, similar to that of DNA detection, generally involves immobilizing the capturing molecules as the corresponding binding antibody on the sensing area. Matatagui *et al.*[192] integrated a love-mode SAW with a PDMS channel to measure the immunoreactions in a continuous flow condition. They immobilized a goat anti-rabbit antibody to capture rabbit immunoglobulins and compared the method with static QCM, reporting superior sensitivity for SAW.[192] Another application of SAW was proposed for detecting cardiac troponin I (cTnI), a standard biomarker for measuring risk stratification of acute myocardial infarction. In this platform, an anti-cTnI antibody on the delay line was anchored to capture the cTnI in human plasma and AuNP conjugated anti-troponin I was used as the detecting antibody. Instead of traveling from input to output, these waves traveled three times due to reflections in IDTs, making their path three-fold longer. This longer path led to higher sensitivity and a better detection limit of 24.3 pg mL^{-1}, compared to 766 pg ml^{-1} for a single path (Fig. 11D).[193]

An alternative to corresponding binding molecules used as probes was proposed by Tretjakov *et al.*,[194] where an imprinted polymer was used to create synthetic receptors. As

Table 4 Biosensing modes using surface acoustic waves

Detection target	Target details	Wave mode (substrate type); frequency/wavelength	Accuracy/detection limit sensitivity
Cells	MCF-7 (human breast cancer cell)[180]	Leaky SAW (36° *YX*-$LiTaO_3$); 100 MHz	32 cells per mL
	A549 (human lung adenocarcinoma tumoroids)[181]	SH-SAW (36° *Y*-cut $LiTaO_3$ with ZnO coating); 14.041 MHz	3000–50 000 in 100 μL
	HL-1 cardiomyocytes[184]	SH-SAW (quartz crystal); λ = 28 μm	10 000 cells per sensor
	E. coli[186]	Lamb wave SAW (polyethylene naphthalate); 500 MHz	LoD 6.54×10^5 CFU mL^{-1}
DNA detection	DNA[182]	SAW (LiNbO3); 6.4GHz	6.7×10^{-16} g cm^{-2} Hz^{-1}
	E. coli O157 : H7 DNA[187]	SH-SAW (64° *Y*-cut $LiNbO_3$); 386 MHz	0.6439 nM/0.1 kHz
	Salmonella enterica, DNA binding[188]	Love wave SAW (*ST*-cut quartz); 267–298 kHz	<100 bacterial cell equivalents
	Typhimurium cells, DNA amplification[189]	Love wave SAW (*ST* quartz); 155 MHz	1–5 cells in 25 mL of milk
	DNA mutation[190]	SAW (graphine oxide)	98.0% sensitivity and 96.2% specificity
Protein detection	Rabbit immunoglobulin (antigen)[192]	Love wave SH-SAW (*ST*-cut quartz); 163 MHz	602 ng cm^{-2} Mass sensitivity of 38 m^2 kg^{-1}
	Cardiac troponin[193]	Triple transit echo TTE SAW (36° *YX*-cut $LiTaO_3$); 200 MHz	Detection limit of 24.3 pg mL^{-1}
	IgA and HAS[194]	Love wave SAW (IgG-MIP ultrathin films); 100–500 MHz	Selectivity factors of 0.3 and 0.09 for IgA and HSA
Exosomes and viruses	Exosomes (HepG2)[195]	SAW (silicon dioxide guiding layer SAW instruments GmbH)	1.1×10^3 particles per mL exosomes
	Ebola virus[28]	SH-SAW (36° *Y*-cut $LiTaO_3$); 80 and 400 MHz	1.9 x 104 PFU mL^{-1}
	Influenza A virus (H1N1)[29]	Love wave SH-SAW (41° *YX* $LiNbO_3$); 120 MHz	Detection limit of 1 ng mL^{-1}
	HIV[30,31]	SH-SAW (quartz crystal 36° *Y*-cut and 90° *X*-propagation); 251.5 MHz	100% sensitivity for anti-gp41. 64.5% sensitivity for anti-p24

Fig. 11E shows, after immobilizing IgG, the polymer was deposited on the substrate to form an ultrathin film *via* electrosynthesis. After washing out the cleavable IgG, its shape remained imprinted on the surface and acted as a template for IgG detection for up to four regeneration cycles. The recognition efficiency of the imprinted surface for IgG was 4 times higher compared to the interfering IgA, and 10 times higher compared to Human serum albumin (HSA).[194]

6.2.4 Exosomes and virus detection. Similar to protein detection, antibodies can be used as probes on the sensor surface to target membrane proteins on nanovesicles. Wang *et al.*[195] coated a SAW sensing zone with antibodies that target CD63 on the exosome surface for probing and interacting with a secondary (EpCAM) antibody, and consequently measured the phase shift for exosome detection. The sensitivity was increased nearly two orders of magnitude by integrating an amplification method for gold nanoparticles, reaching a limit of 1.1×10^3 particles per mL of exosomes.[195]

The capacity of SAW sensors as a rapid and accurate PoC sensor for the detection of the Ebola virus, a relevant interest and necessity due to recent viral outbreaks, has been also demonstrated. By functionalizing the surface with an anti-Ebola virus antibody, inactivated and fragmented Ebola virus could be efficiently captured. A detection limit of 1.9×10^4 PFU (plaque-forming unit) mL^{-1} of the virus before inactivation was reported, being lower than that using standard PCR tests. Moreover, this platform was powered by batteries to make it portable, and also showed a reduction of detection time with a sensing time of 5–10 min.[28] Influenza A virus was also shown to be captured and detected by the immobilization of anti-H1N1 HA antibodies on the SAW platform with a detection limit of 1 ng mL^{-1}.[29]

Furthermore, the potential of SAW sensors as rapid detection chips for clinical applications was effectively proven by Gray *et al.*[30,31] In their design, the authors functionalized detection channels using anti-HIV antibodies (anti-p24 or anti-gp41) through inkjet printing, and they engineered the chip to require only 6 μL of blood plasma. Samples from 31 patients with HIV and 102 healthy volunteers were tested using this device, showing a remarkable 100% for both sensitivity and detection specificity. Moreover, all the positive results were read within 60 s of sample injection, paving the groundwork for their followed smartphone-connected diagnostic platform (Table 4).[30,31]

6.3 Acoustic waves for enhancing sensitivity limitations

One of the main challenges in biosensing assays which are based on the immobilization of the capture probe, such as ELISA and surface plasmon resonance (SPR), is the low signal-to-noise ratio, which weakens the sensing performance. Two of the factors that are key in low signal-to-noise scenarios are the inefficient binding between the probe and target molecules, which causes a low signal, and non-specific adsorption of parasitic molecules, interfering with the target signal.[196] Acoustic waves have been used to address these biofouling issues by improving the target binding kinetics through acoustic mixing, and also by breaking off

the unwanted molecules from the surface through acoustic vibrations and streaming.

Renaudin *et al.*[197] integrated a Rayleigh-mode SAW platform with an SPR sensing system to induce acoustic streaming and enhance the binding kinetics of an avidin-biotin assay (Fig. 12A). The acoustic streams led to effective mixing on the SPR prism and showed a 5-fold acceleration of binding kinetics. Despite these results, they reported interference in signal due to heat generated by the SAW platform.[197] Another SAW-enhanced SPR sensor was proposed to discern the streaming contribution from the heating effect by varying the SAW parameters and monitoring the temperature and streaming velocity (Fig. 12B). By doing so, the saturation time for polyethylene and avidin adsorption was accelerated by 82% and 24%, respectively.[198]

Many studies have also been dedicated to investigating the ability of acoustic waves to break off non-specific bindings. The target biomolecules, especially in clinical samples, are immersed in a cocktail of other biological molecules which can induce noise signals in label-free biosensing applications. Meyer *et al.*[199] used a thickness-shear mode resonator to clean non-target proteins from the patterned protein array, in a non-destructive manner. Upon the penetration of shear waves, the mechanical stress decreased the activation energy for the desorption of nonspecifically bound species, leading to an 85% drop in fluorescent intensity of the non-sensing area and 77% for the sensing area.[199] Another method investigated a high-frequency resonator to create controllable acoustic microstreams and was used to wash off the loosely surface-bound proteins by vortex-induced hydrodynamic forces. A human IgG antibody was immobilized on their platform showing a 58.3% drop in fluorescence intensity of the nonspecific mouse IgG antigen, while the reduction for specific human IgG was only 12.1% after hypersonic treatment (Fig. 12C).[200]

A similar streaming approach for dissociating non-specifically bound (NSB) proteins was reported, albeit with a Rayleigh-mode SAW setting. A section of the delay path was treated with a goat anti-mouse IgG antibody as the sensing zone while the edges were coated with unlabeled BSA as the non-sensing area. The surface was then exposed to a fluorescently labeled IgG antigen for specific binding and also an additional labeled BSA for nonspecific adsorption. Upon exposure to SAW, the fluorescent intensity of BSA and the antigen in non-sensing zones dropped markedly; whereas in the sensing zone, only BSA showed significant desorption, with the specific antigen-receptor interaction remaining exclusively.[201]

Furthermore, a Rayleigh SAW combined with plasmonic silver nanocubes was shown to lower the detection limit for immunofluorescence assays to <1 ng mL^{-1} of the antigen. In this platform BSA and 50 nm silver nanocubes were immobilized on the sensor surface and carcinoembryonic capture antibody was incubated above the nanocubes. After adding a carcinoembryonic antigen, the fluorescently-labeled detection antibody was introduced to complete the sandwich structure. Both effects of acoustic waves improved sensing through enhanced mixing and prevention of nonspecific protein adsorption. The mixing induced by acoustic streaming reduced the antibody/antigen incubation time to 1/6th of the acoustic-absent setup. Moreover, removing the

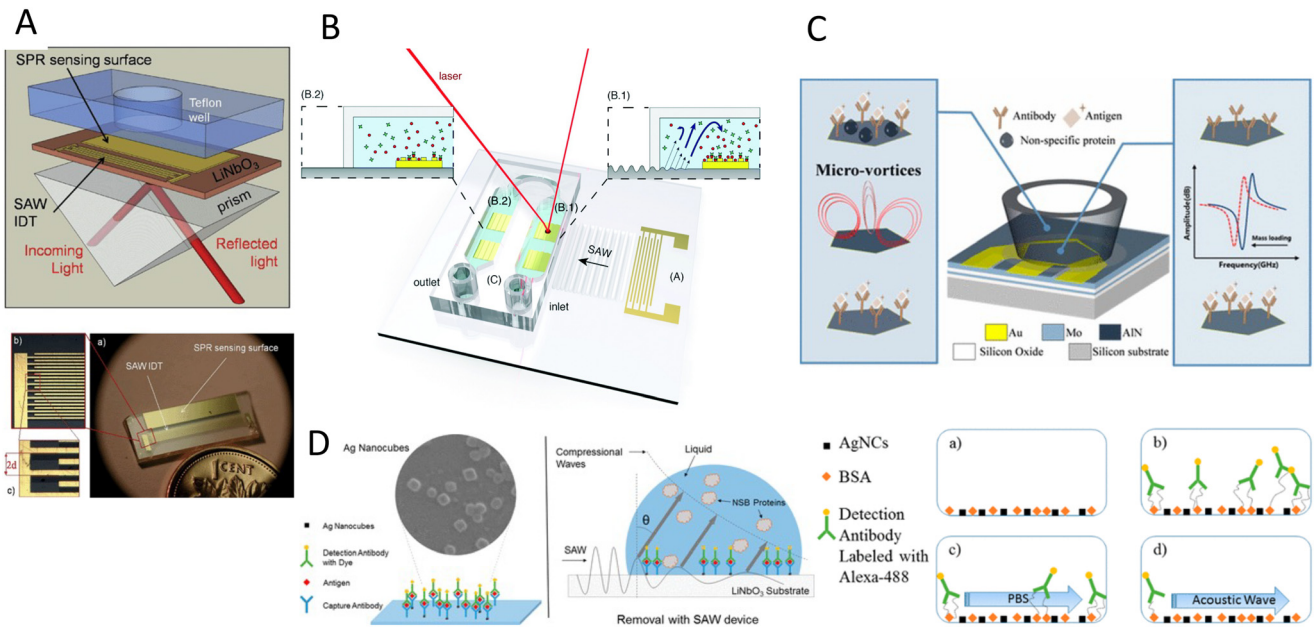

Fig. 12 Acoustic waves for improving sensitivity and limiting biofouling: A)[197] and B)[198] integration of SAW mixers with SPR sensing systems to enhance the binding kinetics. C) The hydrodynamic forces from acoustic microvortices are used to wash off the loosely surface-bound non-specific proteins.[200] D) SAW is used for both enhancing the mixing and removing non-specific protein bindings, showing significantly better performance over chemical rinsing.[202] Reprinted with permission.

nonspecific protein adsorption using SAW was significantly more effective compared to the technique of chemical rinsing, thus leading to an overall stronger fluorescence signal (Fig. 12D).[202]

Merging both SAW-based sensing and biofouling alleviation mechanisms can be a very promising and efficient biosensing strategy. However, one should cautiously consider the difference in wave modes and the piezoelectric substrate used in each application. As mentioned earlier, the wave mode suitable for biosensing is SH-SAW and Love, which limit the damping of the wave in the liquid medium. However, for biofouling removal, the leakage of the waves is necessary to induce vortices, and therefore, substrates that support Rayleigh-SAWs are required.

To overcome this obstacle, substrates like $LiTaO_3$ and LGS can be used to generate both wave modes by changing the direction of the wave propagation. A set of IDTs can be embedded on these substrates in the direction in which shear vertical waves are generated to create microstreams for inducing mixing and cleaning the surface, while the IDTs in the direction that activate shear horizontal waves can be used for the biosensing.[203,204] Given this efficient integrability, there is an increasing interest for SAW-based sensors to combine these two features to increase the biosensing specificity and detection limits.

7 Acoustofluidics for particle separation, sorting, and enrichment

The label-free and biocompatible nature of acoustic forces render them as one of the most powerful tools for the separation, enrichment, and sorting of bioparticles. These systems, also called acoustic tweezers, can manipulate bioparticles without disrupting the surrounding fluid and separate them based on the size or acoustic contrast factor. One of the unique features of the acoustic tweezers is the ability to tailor the size sensitivity of the system by different acoustic phenomena. Acoustofluidics offers various force relations by producing hydrodynamic acoustic streaming ($F \propto R$), standing fields ($F \propto R^3$), traveling fields ($F \propto R^6$), or the combination of these forces on a single particle.

7.1 Acoustofluidic particle separation

ARF in standing waves stands out for particle separation due to their high controllability, relatively large magnitude, and its third power relationship with the particle's radius (R^3), in which a small increase in the particle size leads to significantly stronger ARFs. Stronger ARFs in larger particles can overcome the fluid resistance due to drag force. Therefore, bigger particles can travel faster and longer distances towards low acoustic pressure nodes, while the movement of smaller particles is dominated by drag forces of background streamlines. This difference in the reposing site of particles, based on their size, has been extensively used in both BAW and SAW modes for particle separation (Fig. 13).[51]

The use of standing BAWs (SBAWs) have been reported for separating MCF-7 cancer cells from red blood cells (RBC),[205] prostate cancer cells from white blood cells with flow rates up to 100 μl min^{-1},[206] and platelets from undiluted whole blood with over 85% platelet recovery, and flow rates of 10 mL min^{-1}.[207] SBAW were also used to separate different sized polystyrene particles (2, 5, 8, 10 μm) by increasing the source input power from ~0.5 to ~2.0 W.[208] In a similar manner, standing SAWs (SSAWs) can separate particles by creating a single pressure node in the channel center, and relocate particles based on their size (Fig. 13A).[209] This approach was used for the separation of platelets from whole blood with a purity of 98%,[210] water in oil droplets with a sorting rate of 222 droplets per second,[211] and extracellular microvesicles and 200 nm nanoparticles.[212]

Despite the great potential in applications, the isolation and enrichment of target nanosized organisms with this method is challenging. The difference in scaling order in the nanoparticles (ARF $\propto R^3$, $F_d \propto R$) results in the dominance of Drag forces in the nano realm. Therefore, for the ARFs to dominate the manipulation of particles, the frequency of acoustic waves should be in the high MHz-to-GHz range, a feature typically exclusive to SAWs. SSAWs were successfully used to separate 500 nm from 100 nm particles,[213] and exosomes (<300 nm) from a mixture of extracellular vesicles with >90% separation yields.[212,214]

The maximum travel distance of particles in standing waves is the spatial distance between pressure nodes and antinodes ($\lambda/4$). This distance in SAW devices which usually have a high frequency of operation can be very short, limiting their sensitivity and efficiency of separation.[42] Hence, by tilting the SSAW direction, such that the pressure nodal lines stand at an angle to the flow direction (optimally 15°), the normal displacement of the particles can be increased by ~10 times, while the trajectory of smaller particles is still dominated by the flow field (Fig. 13B).[215] This mechanism was adopted by various groups to separate breast cancer cells from leukocytes with a purity of 84% and throughput of 2 μL min^{-1},[215] and for the isolation of low concentrations of cancer cells (~100 cells per mL) from white blood cells with an 83% recovery.[216]

In addition to the size, the acoustic contrast factor (Φ), associated with the compressibility and density of a particle and its contrast to the surrounding medium, can also be used to separate particles by standing acoustic waves.[217] A particle with a higher density mismatch has a larger Φ value, and thus experiences a larger ARF. This concept can be particularly used when mixed particles are indistinguishable by their size. Furthermore, the acoustic contrast factor can have a negative value when the density of the particle is below that of the medium. As such, the density of the medium can be modulated, such that it divides the relative contrast factor of particles into negative ($-\Phi$) and positive ($+\Phi$), where in the presence of ARFs, two particles can move in opposite directions from one another, *i.e.*, antinodes ($-\Phi$) and nodes ($+\Phi$) (Fig. 13C). To exploit

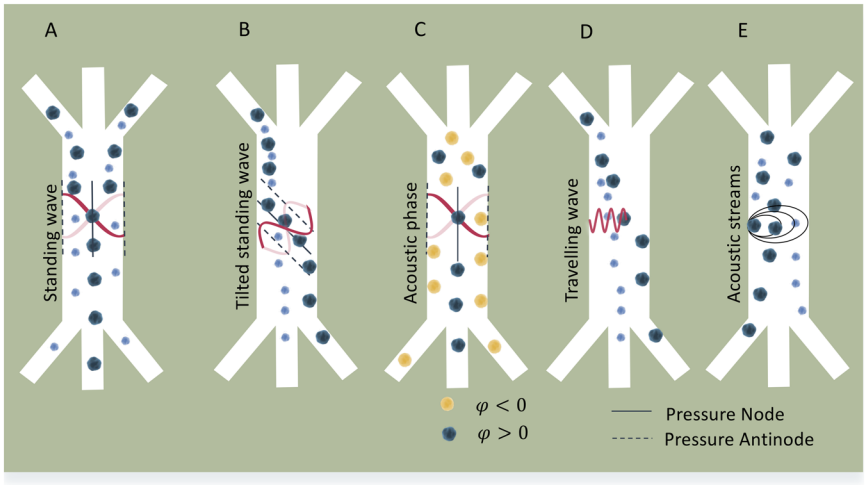

Fig. 13 Acoustophoretic mechanisms for particle separation. A) Bigger particles experience stronger ARF in standing waves and can move faster to the pressure nodes. B) Tilted standing waves increase the separation path of bigger particles. C) Separation by acoustic phase contrast. Particles with positive acoustic contrast move to pressure nodes while particles with negative acoustic contrast move to pressure antinodes. D) Traveling acoustic waves separate bigger particles in the direction of wave propagation. E) Acoustic streams trap or deflect the path of bigger particles closer to the vortex source while smaller particle can pass with less deflection.

this method, cesium chloride was added to the working media to reach a density of 1.16 g cm^{-3} and separate 3 μm polystyrene particles (1.05 g cm^{-3}) from PMMA particles (1.22 g cm^{-3}) of the same size.[208] Similarly, a high acoustic impedance-to-viscosity ratio medium (OptiPrep™ density gradient medium) was used to increase the acoustic impedance of the medium. Cells were injected in normal media near the sidewalls where the pressure antinode was located, and high-contrast media was infused in the central channel where the pressure node sits. This allowed to effectively quantify the acoustic impedance of various cell types, including monocytes, lymphocytes, neutrophils, and cancer cells.[218] In another study, RBCs were sorted in a BAW device by guiding RBCs ($+\Phi$) towards the pressure nodes while lipid microemboli ($-\Phi$) were located at the anti-pressure nodes, with a 100% efficiency.[219]

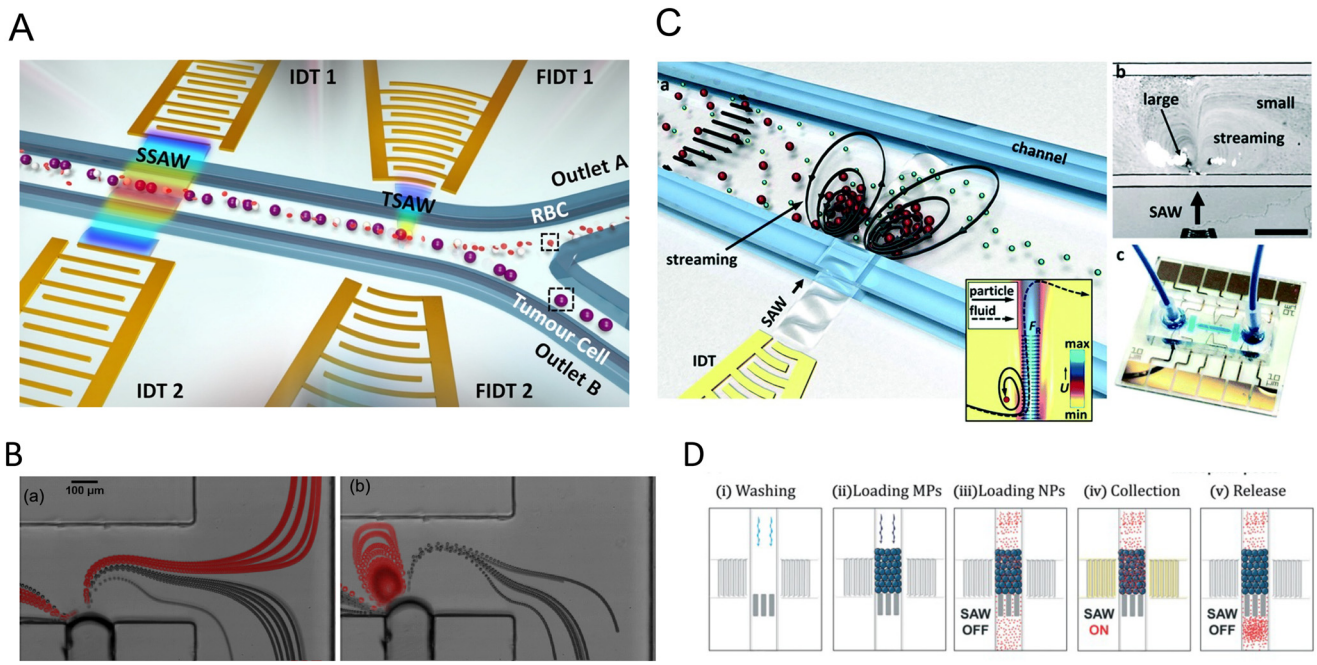

Fig. 14 Acoustophoresis mechanisms for separation, isolation, and enrichment of particles. A) Double stage acoustic system using SSAW for alignment and TSAW for separation,[224] B) particle separation by microstreams from oscillatory bubbles,[227] C) particle separation by microstreams from focused TSAW.[225] D) Exosome enrichment by Bjerknes forces.[238] Reprinted with permission.

Table 5 Acoustophoresis for particle manipulation

Acoustic mode	Acoustic parameters	Particles/cells	Throughput/efficiency
SBAW (primary ARF)	2 MHz, 0.5–2.0 W; 0.36, 0.13, 0.04 mL min^{-1}	PS particles (2, 5, 8, 10 μm), RBC[208]	~96% PS recovery, ~92% RBC recovery
	4.91 MHz and 10 V (pre-alignment); 1.99 MHz and 0–12 V (actuation); 100 μL min^{-1}	PS particles (5, 7 μm), MCF-7, RBC, DU-145, WBC[205]	99.3 ± 0.3% PS, 91.8 ± 1.0% MCF-7, 84.1 ± 2.1% DU145 recovery
	10 V_{pp}, 0.3 ml min^{-1}	Lipid particles (5 μm), RBC[219]	100% separation efficiency, 70% recover (RBC) >80% of lipid particles removed
SSAW (primary ARF)	12.6 MHz, (30-160 mW), 2 μL min^{-1}	Fluorescent PS beads (4.17 μm and 0.87 μm)[209]	90% recovery (4.17 μm) and 80% (0.87 μm)
	13.0168 MHz, 23.8–26.7 dBm, 0.8 μL min^{-1} (particles), 0.5 μL min^{-1} (cells)	Fluorescent PS particles (2 μm and 5.86 μm); *E. Coli*, PBMCs[239]	95.65% purity (*E. coli*/PBMCs)
	410–463 mW, 0.25–5.0 μL min^{-1}	RBC, platelets, whole blood[210]	99% RBC clearance ratio, 98% purity of platelets, 2.7 × 10^4 cells per s
	10.02, 10.20, 10.35, 10.46, 10.60 MHz, 48 V_{pp}, 0.2–8.0 μL min^{-1}	Picoliter water-in-oil droplets[211]	222 droplets per s
	38.5 MHz, 0.5 W, 2.8 mm s^{-1} (particles), 1.5 W, 2 mm s^{-1} (eMVs)	PS beads (190 nm and 1000 nm), microvesicles (<200 nm)[212]	>90% recovery rate particles, >80% for exosomes, >90% for larger MVs
taSSAW (primary ARF)	19.40 to 19.60 MHz (15°-tilted), 20–40 V_{pp}, 1–5 μl min^{-1}	PS beads (9.77 μm and 0.87 μm), MCF-7, WBC[215]	>98% recovery (9.77/0.87 μm) >97% purity (WBC/MCF-7)
	39.4 MHz, 45 V_{pp}, 4–8 μL min^{-1}	PS particles (110 nm, 5 μm), exosomes, MV (50–600 nm) from whole blood[214]	99% recovery rate 98.4% purity (EVs) with 99.999% blood cell removal rate
Acoustic streaming	381 MHz, 68–200 mW, 0.5–8 μL min^{-1}	Particles (1 μm and 2 μm), MDA-MB-231, RBC[225]	>98% capture efficiency at ν^* = 112 2 um particles
	32 kHz, 20–27 V_{pp}, 3 μL min^{-1}	K562, PS beads (10 μm)[228]	800 cells per s, 99% sorted cells, 94.5 ± 4.7 cell viability
	15–50 kHz, 70 V_{rms}, 1.33 mm s^{-1}	PS particles (radius, 1, 2.5, 5 μm)[226]	1 μm resolution
	49.8 KHz, 2.75–6.5 V_{pp}, 27.5 μL min^{-1}	PS particles (7.32, 25 μm), DU-145, WBCs, RBCs, monocytes[231]	>50 × 10^6 min^{-1}, 90% efficiency, 77 × enrichment, 91.7% purity (DU-145)
	2.5–5.0 V_{pp}, 25 μL min^{-1}	Platelets, RBCs and WBCs, MCF-7, SKBR-3[229]	100% trapping efficiency, MCF7, 200× enrichment ratio
SAW (Bjerknes)	48.8 MHz (λ = 80 μm), 18.3 V (0.12 W mm^{-2}), 12.2 μL min^{-1}	PS particles (100, 300 nm)[240]	86.3% separation efficiency
	663 MHz, 251 mW, 0.45 μL min^{-1}	PS particles (300, 500 and 100 nm)[233]	84 ± 9% capture of 300 nm
	55–85 MHz, 12 dBm power, 1 μL h^{-1} flow rate	Particles (100 nm, 190 nm, 500 nm)[238]	97% collection efficiency (500 nm)
BAW (Bjerknes)	4 MHz, 17 V_{pp}, 10 μL min^{-1}	PS particles (110 nm, 490 nm), *E. coli*[236]	95 ± 3% capture efficiency
	4 MHz, 10 V_{pp}, 15 μL min^{-1}	PS particles (0.1–1 μm), EVs (30–500 nm)[241]	81.7% trapping efficiency (1 μm), 9.3% CV

The other acoustophoretic method is traveling surface acoustic waves (TSAW), which can be a double-edged sword for particle separation. On one hand, its R^6 relation results in smaller magnitudes of ARF compared to that of SSAW, on the other hand, the R^6 relation renders it more sensitive to the size of particles. Another interesting feature of TSAW is the migration distance of particles, which unlike SSAWs, is not limited to the node-antinode distance. Instead, TSAW applies a unidirectional force on particles, continuously pushing them away from the source (IDT). Therefore, particles travel longer lateral distances allowing them to be sorted more efficiently (Fig. 13D). Straight TSAWs have been used to guide the direction of water droplets in oil and polyacrylamide particles,[220] and slanted TSAW were used to sort human keratinocytes, mice fibroblasts, and melanoma cells.[221] TSAW has also been used in combination with functionalized microparticles to separate target-protein complexes which have bigger diameter unbound particles.[222] To compensate for the lower force magnitude, the acoustic field in TSAW is usually limited to a small, focused domain by using focused-IDTs (FIDT), used for the continuous separation of 3 μm and 10 μm particles with a 100% efficiency.[223] SSAW and TSAW can also be combined in a multi-module platform to enhance separation (Fig. 14A).[224]

Another efficient separation method is the use of acoustic streaming. Acoustically-induced microvortices are advantageous due to their high controllability, rapid formation, facile tuning, precise location, and the ability to scale up for high-throughput applications.[225] When particles approach the acoustic field, microstreaming can deflect the trajectory of the particles based on their size. Larger particles move to the center of rotation, being trapped in closed streamlines, while smaller particles can pass through the vortex (Fig. 13E). By using oscillating microbubbles, the selective capturing and release of different sized particles was attained with a resolution of 1 μm.[226] Bubbles can be used at the neck of bifurcated channels to deflect the trajectory of particles from the streamline and thus be collected at the outlets (Fig. 14B).[227,228] Lateral cavity acoustic transducers (LCATs) with oscillatory bubbles at the sides of a channel,

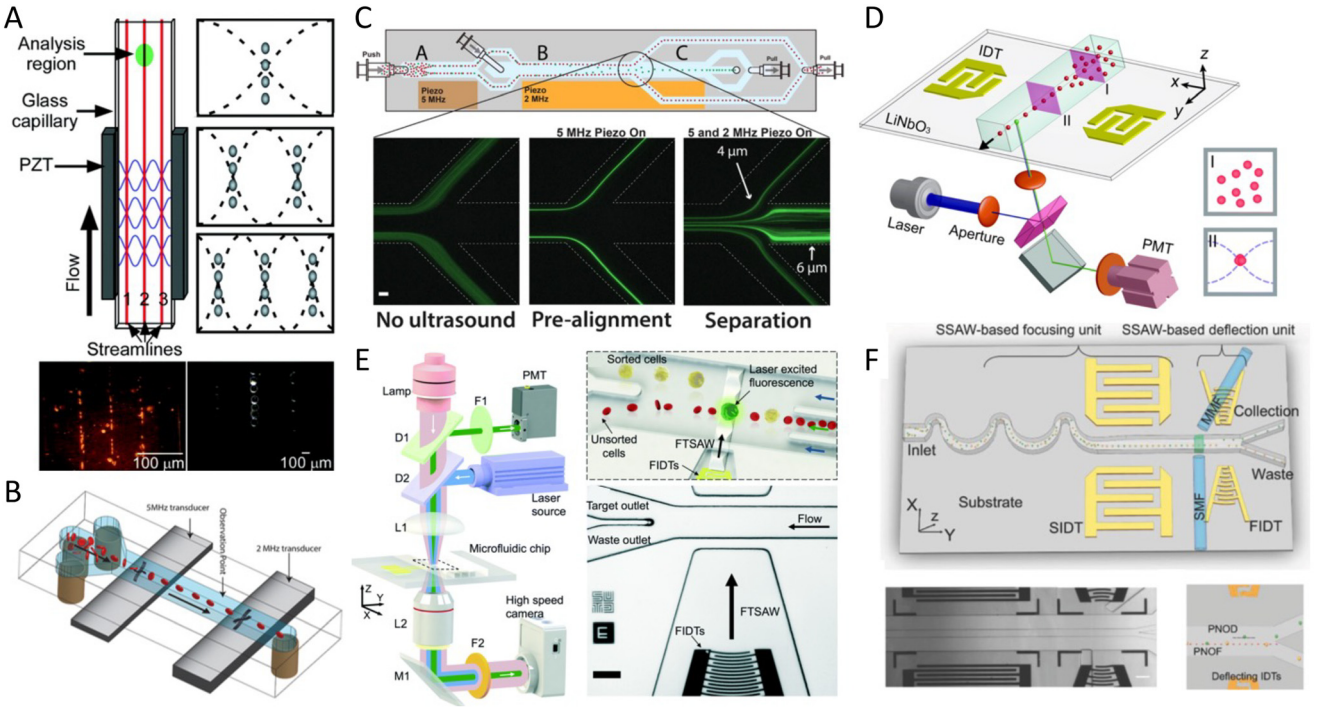

Fig. 15 Acoustic cell sorting mechanisms including cell focusing (pre-alignment) and cell separation (deflection). A) BAW-based multi-node acoustic focusing in a rectangular glass capillary showing the location of pressure nodes ($\lambda/2$, λ, and $3/2$ λ, respectively) (top) and optical micrographs showing two sizes of PS particles focused into 3 nodes (scale bar = 100 μm).[247] B) Schematic illustration of BAW-based 2D-rotation cell focusing by the activation of two different frequency transducers of 5 MHz and 2 MHz for focusing and orientation, respectively.[254] C) Schematic image of BAW-based acoustic chip for separation showing the laminated sample with no ultrasound (left), pre-aligned particles (center) with 5 MHz piezo ON, and separation of the pre-aligned 4 μm and 6 μm particles with 5 MHz and 2 MHz piezo elements (scale bar is 100 μm).[252] D) Schematic image of SSAW-based microfluidic cytometer with an integrated LIF detection system, before (I) and after (II) SSAW focusing.[253] E) Schematic image of SAW-based FACS platform showing optical set-up for fluorescence interrogation and high-speed imaging (left) and illustration of the FACS process in the sorting chip with focused interdigital transducer and micrograph of the acoustic sorting chip showing the focused and sorting regions (scale bar is 100 μm).[255] F) SSAW-based FACS chip schematic (top) with a microscopic image of focusing and deflection units (bottom left) and illustration of the path of pressure nodes of deflected (PNOD) particles and pressure nodes of focused (PNOF) particles (bottom right) (scale bar = 200 μm).[256] Reprinted with permission.

could efficiently separate platelets, red, and white blood cells from undiluted whole blood,[229,230] with high throughput (50×10^6 cells per min).[231] Moreover, acoustic streaming can be coupled to ARFs in SAW platforms. As an example, an acoustic beam was employed as a virtual filter membrane to separate 8 μm from 5 μm particles,[232] 2 μm from 1 μm particles, and MDA-MB-231 cancer cell lines from a mixture with red blood cells (Fig. 14C).[225]

The dominance of drag forces in sub-micron particles encourages the use of acoustic streaming-induced drag forces to separate and enrich nanoparticles. Using SAW-based acoustic streams, the enrichment of particles with sizes of 300 nm,[233] 87 nm,[234] and even 80 nm were shown.[235]

Another interesting nanoparticle enrichment approach is using Bjerknes forces. In the presence of acoustic waves, microparticles scatter acoustic energy and emanate secondary ARF (or Bjerknes force), which can attract nanoscale particles and vesicles near the microparticles for filtration and enrichment. This technique was explored in both SAW and BAW devices for trapping *E. coli* bacteria and 110 nm diameter polymeric nanoparticles with a 95% efficiency,[236] enriching extracellular vesicles (EVs) from cell culture media, urine, and blood plasma,[237] and the enrichment of 100 nm particles by increasing the input power (Fig. 14D).[238] The overview of acoustic modes, parameters, throughput, and efficiency of recent acoustophoretic systems for particle and cell manipulation is presented in Table 5.

7.2 Cell sorting

Sorting in definition differs from the separation process, as it involves the active detection of targeted particles or cells, usually through fluorescence-activated cell sorting (FACS).[1] Acoustic forces in particle sorting have been used in two roles: a) to pre-focus particles in lines to facilitate the detection of particles, and b) as the active pushing mechanism to move the particles that are signaled by the detection system.

Cell focusing. Acoustic cell/particle focusing can occur in 2D, in which particles and cells are horizontally or vertically focused at the center of a microchannel; and in 3D, where particles are focused in both planes. Cell-focusing is typically a pre-step in downstream processes, including detection, separation, and manipulation of labelled bioparticles.[242,243]

Cell pre-focusing is a crucial step for controlling the trajectory of cells for optical scanning regions used in FACS and flow cytometers.[244] ARFs in BAW platforms have shown their potential for flow cytometry, where CHO-K1 cells were successfully focused in 2D in a glass tube.[245] To increase the throughput of the optical interrogation region, a parallel acoustic focusing setup was used, showing a total of 39 pressure lines with a throughput of 50 000 s^{-1} (Fig. 15A),[246,247] and 100 000 s^{-1} with high flow rates of up to 10 mL min^{-1}.[248]

BAW-based focusing systems have also shown their applications for high throughput platforms such as the "Imaging FlowCytobot" with resolutions up to 1 μm.[249,250] Integrating a time-encoded pulsed laser to an embedded acoustic actuator was reported to move high acoustic contrast factor particles towards the center of the channel with flow rates up to 1000 μL h^{-1} and a throughput of 2000 cells per s.[251] Furthermore, by using two different frequency transducers, simultaneous separation and enrichment of cancer cells were attained for direct on-chip tumor cell identification and counting (Fig. 15C).[252] SSAW-based flow cytometry has also been shown in a simple design using one pair of IDTs, wherein particles were focused into pressure nodes and directed to an integrated laser-induced fluorescence (LIF) set up with less than 10% variation coefficient for 1000 beads per s (Fig. 15D).[253]

In addition to focusing cells on pressure lines, acoustic forces can also be used for locating cells in the camera's focus plane to enhance the quality of the focusing system as well as the imaging throughput. A BAW device was integrated with an imaging flow cytometer to manipulate particles in a single flat layer, allowing for low noise CMOS camera and high resolution with throughputs of 208 000 beads per s and 60 000 cells per s at 104 mm s^{-1}. This method can eliminate the error of not counting cells shadowed in vertical lines by another cell. Apart from cell focusing, acoustic waves can also control the 2D orientation of non-spherical particles. Two transducers with different excitation frequencies which correspond to the horizontal or vertical alignment of red blood cells were embedded in a single platform and could reorient 87.8 ± 3.8% and 98.7 ± 0.3% of red blood cells vertically and horizontally respectively (Fig. 15B).[254,257] Acoustofluidic systems can also rotate cells and particles and capture planar images at different angles of rotation. For instance, the actuation of air microbubbles trapped in sidewall microcavities allowed the gradual and controlled rotation of GFP-expressed *C. elegans* and L. longiflorum flowers reducing the problem of single plane overlapping even at high rotation speeds (300 rpms).[258,259] A SAW-based system was also used to produce a single acoustic vortex in millimeter scale for rapid rotation of model organisms such as multispectral imaging and 3D reconstruction of zebrafish larvae. The single vortex system could provide a more stable and controllable fluid motion for precise angular alignment of the zebrafish, leading to better visualization.[260]

Acoustics as the sorting force in FACS. The capability to focus the ARF to a confined domain, and lag-free on–off control have made the acoustic force an appealing sorting tool to redirect particles after detection in fluorescence activating cell sorting (FACS) systems. One example is the SBAW-based device that was integrated with the FACS capability for single-cell sorting. The sample stream is sheathed between flows with different densities, and after detection, a pulse of the ARF deflects the fluid stream of the targeted particle to the outlet of interest.[261] This platform was further improved by integrating a 2D acoustic pre-focusing module to guide particles in narrow regions with the same flow velocity, ensuring maximum ARF.[262] Using SSAW, a "microfluidic drifting" technique was implemented to focus particles and cells in 3D and control the flow of single streams of particles/cells as they pass through a region exposed with a laser, followed by short (150 μs) burst pulses to sort particles/cells with a high throughput of 1200 events per s, a purity of 92.3 ± 3.39%, and post-sorting cell viability of 99.18%.[263] Similarly, a SAW-based pumped lense microfluidic imaging system was shown for cell detection and counting with a low statistical error (6.53%).[264] SSAW platforms also facilitate the integrability of various modes of action, such as a cell deflection unit, a 3D cell-focusing unit, and an in-plane fluorescent detection unit on a single chip (Fig. 15F).[256]

In addition to SSAWs, TSAWs have also been proposed to drive cells into desired channels for fluorescent cell analysis. One application of TSAW emerged from its marriage with a fluorescence interrogation system and a high-speed imaging camera for FACS, where the width of acoustic beams was reduced to ~50 μm to sort fluorescent MCF-7 cells from diluted blood with a 86% purity (Fig. 15E).[255] Another clever mechanism combined TSAW with a multilayer feature consisting of a flow-focusing nozzle and a slanted groove to improve the sorting efficiency by a vertical component of the refracted acoustic wave with a purity rate up to 92%.[265]

8 Summary

To summarize, we compare the performance and potentials of the most widely used acoustic mechanisms for tissue engineering, therapeutics development and delivery, biosensing, cell separation, sorting, and enrichment. Moreover, to better distinguish the performance of direct BAW and SAW radiation forces from the secondary phenomena such as Bjerknes forces and streaming, they are categorized separately, although Bjerknes forces and streaming can occur in these systems too.

Tissue engineering

Acoustofluidics offers biocompatible and rapid methods to pattern cells for tissue engineering purposes with a diverse range of resolution and complexity. To help with adopting the best-suited strategy, we ranked the capacity of each acoustic technique in tissue engineering based on a) cost and

facility of fabrication, b) resolution, c) ability to pattern complex structures, d) the size of printing domain, and e) the integrability with other tissue engineering modules such as 3D printers (Fig. 16). To obtain complex geometries, acoustic holography is the leading choice, and it also offers a large patterning domain. However, their poor resolution and complicated fabrication processes should be considered. Moreover, the integrability of the platform with tissue engineering systems necessitates dynamic holograms, which require sophisticated systems to locally block sound waves with bubbles. SAW systems have the highest resolution, enabling the pattern at the single-cell level, but they offer limited-size domains and architectures. Nevertheless, the controllable SAW systems, particularly systems with variable frequencies, have enormous potential to be integrated with stereolithography-based printers to pattern complex and precise tissue geometries. Acoustic streaming systems are easily integrable with other tissue engineering systems such as 3D printers and their resolution can easily be tuned, however, the geometries they produce are mostly restricted to spheroids and ring shapes. So far, BAW systems are a more established technique for tissue engineering applications and offer a sizable patterning domain, satisfactory resolution in most applications, a dynamic frequency for producing various geometries, and easy integration with tissue engineering systems.

Therapeutics development and delivery

Acoustic synthesis of therapeutic agents and nanoparticles is mostly done with two methods of acoustic microstreaming and nebulization. Both of these methods show remarkable levels of compatibility with biological components and versatility for the production of a diverse range of therapeutics. Acoustic streaming methods generally show higher throughput and easier retrieval of the output products while nebulization lays the groundwork for novel reactions and processes during formation such as layer-by-layer coating. Moreover, nebulization proved to be an efficient mechanism for drug delivery through the respiratory system.

For transfection and drug delivery to cells by sonoporation, the performance of different techniques are compared based on a) throughput of cells that can be treated b) biocompatibility to both cells and the bioagents c) delivery efficiency, d) rapidity of sonoporation, and e) controllability and uniformity of forces on each cell (Fig. 16). Cavitation-based techniques are fast approach with high delivery efficiency while their spontaneous nature renders them uncontrollable and harmful to cells. SAW and BAW systems offer a more controllable force field, but their delivery efficiency needs to be further improved. BAW systems can handle outstanding throughputs while high-frequency SAW systems offer excellent biocompatibility. Continuous

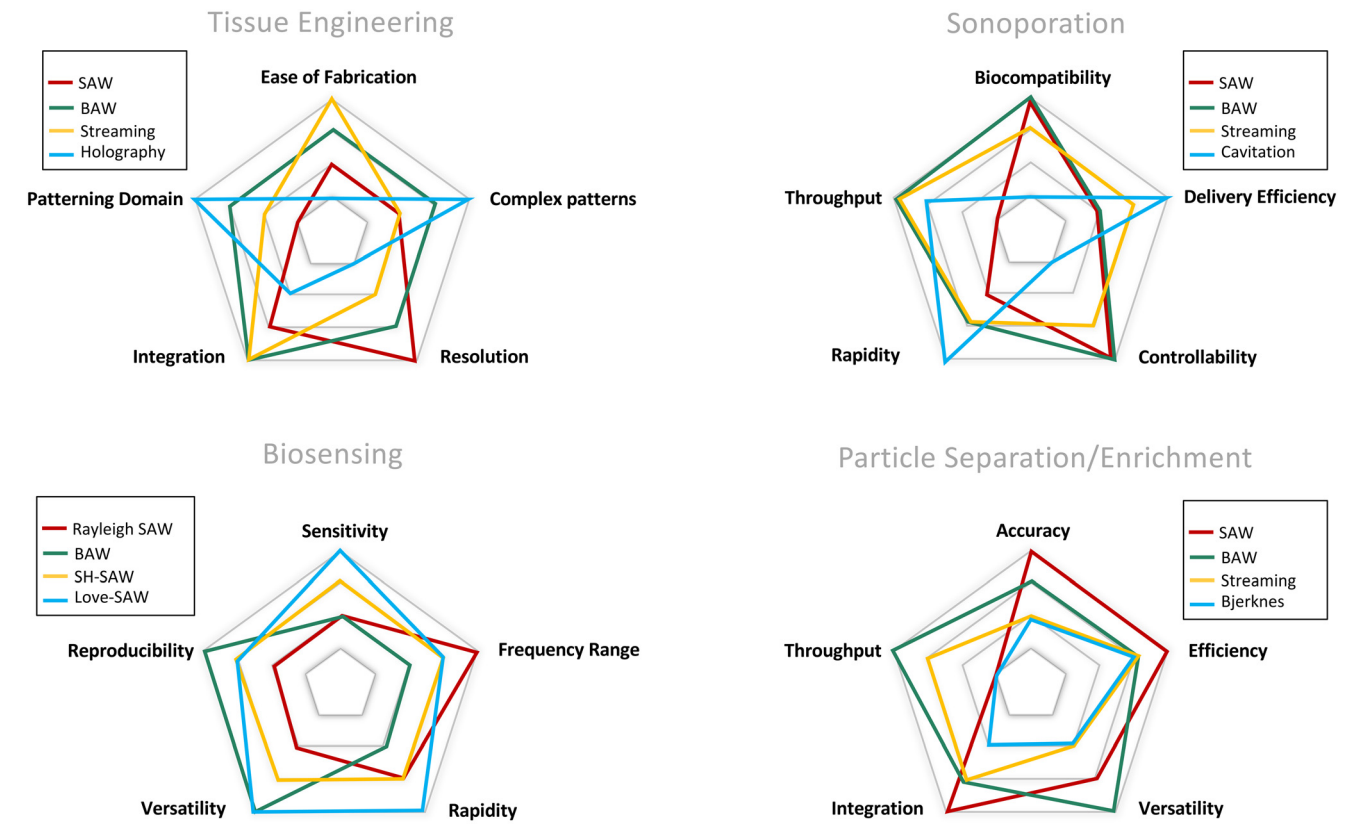

Fig. 16 Schematic sketches comparing the performance of acoustofluidic strategies in different applications. Each system is ranked based on 5 criteria, with the outer level showing the highest score. The comparisons are relative and based on the commonly reported performances, therefore, may not be conclusive for individual cases.

microstreams are reported to have high delivery efficiency while maintaining cell viability and offering high throughput. The controllable shear forces, present in acoustic microstream, are one of the main mechanisms of membrane rupture. In fact, even some of the SAW and BAW systems acknowledge the presence of the coexisting microstreams as the root cause of sonoporation.[38] Moreover, the integrability of microstreams with other methods such as electroporation can ensure uniform exposure to forces and enhanced efficiency.[135]

Acoustically induced phenotypes in biological organisms

The overview of studies shows that both SAW and BAW systems can enhance the growth and proliferation of cells without harming cell viability. Moreover, acoustic waves are shown to trigger and direct differentiation in stem cells and modulate the ion flux in numerous cell types including neurons. The performance comparison of the SAW and BAW for each effect cannot be conclusive due to the cell-type dependency and also variation of the dominant acoustic phenomena even in similar platforms. For instance, in many of the reviewed papers, the accompanying streaming was suggested as a primary effect. This indicates that apart from frequency and wave mode, other parameters that can influence the balance of various acoustic phenomena should be standardized before concluding the effects of acoustic waves.[266] Time of exposure, the amplitude of the driving voltage, and the chamber setting and geometry can also influence the dominant acoustic phenomenon and should be carefully considered. Moreover, the property of media such as viscosity and density are other important factors in determining acoustic radiation forces, dissipation of waves, and microstreaming.

Biosensing

The criteria chosen for comparison of acoustic biosensors are a) sensitivity b) reproducibility of data c) range of available frequencies for each method d) rapidity of sensing, and e) versatility of each strategy in sensing biological components in liquids, gases, and complex or corrosive buffers (Fig. 16). The BAW methods such as QCM-D are reported with generally high reproducibility of data and the versatility for detection of various biological samples and suspended bioparticles in liquids due to their more established technology, but have lower sensitivity compared to many SAW systems. Rayleigh waves have a wide range of frequencies and are excellent for integration with fouling removal mechanisms and preparation steps, however, their leaky nature leads to low reproducibility and energy loss in liquids. SH-SAW and Love waves both offer a similarly wide range of frequency, rapid detection, and facile integrability. The waveguide layer in Love waves allows for better sensitivity and also the versatility to operate in corrosive materials. However, to ensure the reproducibility of the data, adverse interference effects should be carefully monitored and further measures for removing the interference might be necessary.

Particle separation/enrichment

The performance of acoustic tweezers for particle separation, sorting, and enrichment are discussed based on a) the accuracy and resolution of differentiation b) efficiency, c) throughput, d) the ability for integration to downstream or upstream modules, and e) the versatility for distinguishing particles based on physical characteristics (Fig. 16). The BAW method is appropriate for high-throughput requirements and offers excellent versatility by offering separation based on both size and acoustic contrast factor and compatibility with complex biological buffers. For applications requiring higher resolution and smaller thresholds, SAW systems are the superior choice, however, it should be noted that they usually operate in lower throughputs. Both SAW and BAW offer high separation efficiency and are integratable as upstream modules in micro total analysis systems, but their functionality diminishes in the nano realm, particularly in BAW systems. Therefore, in applications focusing on nanoscale particle separation and sorting, Bjerknes' strategies can be a very promising alternative. Acoustic streaming offers continuous flow and high throughput separation, easily integratable into multimodule systems. The streaming-based separation is however less size sensitive compared to the ARF-based system, due to the linear relationship of the drag forces with size. However, since this linear relationship leads to the dominance of drag forces in the nanoscale, acoustic streaming can be a promising choice for the enrichment and separation of nanoparticles.

9 Future trend and outlook

In this review, we have provided an overview of the most frequently studied acoustofluidic concepts and forces in both SAW and BAW-based devices, their resulting acoustic phenomena for sensing and manipulation of bioparticles and biofluids, as well as their application in biomedical sciences. The most recent advances of acoustofluidics in biological settings as actuators, sensors, or both, were presented and discussed, including cell patterning for tissue engineering, therapeutic synthesis and delivery, acoustofluidics as a functional force, bioparticle separation and enrichment, and biosensing applications.

The miniaturization of acoustofluidics platforms opens a new venue for studying the physiological and physicochemical effects of acoustic waves in biological samples within a confined microscale domain with a uniform, precise, and controllable exposure to acoustic pressure. Moreover, acoustofluidics offer a wide frequency range, various waveforms, acoustic wave transmission settings, and a variety of acoustic forces and phenomena that can be tailored for miscellaneous experiment requirements, from cell separation, bioparticle isolation, and patterning to acoustic sensing. The unique features of miniatured acoustic

systems open myriads of new applications with higher versatility in biotechnology applications compared to conventional ultrasound systems. Miniaturized systems can also potentially offer favorable and well-established functionalities of conventional ultrasound systems while increasing their usability by having enhanced and localized energy delivery, a controlled environment, low amplitude, and continuous wave exposure.

It would be particularly remarkable to investigate the capabilities of acoustofluidic in recreating the conventional ultrasound effects for inducing cytoskeletal vibration and reorganization of the cell structure,[267,268] altering cell body morphology and contractility,[269,270] studying the change in adhesion and migration, enhancing the degradation of cell scaffolds in tissues,[271] enhancing drug delivery by ECM loosening in tumors,[272] opening of the blood–brain barrier,[273] and preventing toxin protein aggregation in neurodegenerative diseases.[274] Hence, a great body of work is remained to be done both to translate the classic ultrasound effects at a microscale level as well as to investigate the change in the aforementioned effects when they are being translated to MEMS settings as well as their implications.

One of the most anticipated directions of acoustofluidics is in the emerging field of tissue engineering where acoustic devices have shown enormous compatibility and potential to be integrated with 3D bioprinters. The continuous and rapid formation of tissue structures such as cellular spheroids, linearly aligned cells within hydrogel fibers, and novel holographic patterning lays the groundwork for recapitulating complex tissue architectures to advance regenerative medicine.[93,103,275]

Another possibility that MEMS-based acoustic devices offer, owing to the biocompatible and flexible materials, is to either be implanted inside the body or as wearable devices to deliver continuous, low-amplitude, localized and high-frequency acoustic waves with minimal energy decay. The integration of MEMS devices with electronic devices is also another potential area for acoustic devices where the implanted devices can be combined with wireless activation, charging, sensing, and continuous monitoring.[276,277]

New trends advocate for the integration of low-cost and portable imaging systems, such as smartphones, with acoustic micro-imaging techniques to revolutionize the field of PoC sensing.[278] As an example, smartphones can be integrated to acoustofluidics platforms for point of care testing,[279] where the digital input and output of acoustic biosensors facilitate both the activation and the electronic readout. Moreover, the integration of acoustic biosensing and biofouling reduction mechanisms is one of the unique and promising potentials of acoustofluidics to develop rapid and precise biosensing strategies.

As observed, there is a wide range of opportunities in the field for both the manipulation and sensing of bioparticles using acoustofluidics. To transfer the acoustic devices to clinical applications, one challenge is the numerous parameters and boundary-conditions that influence the performance of the acoustofluidic devices. The miscellaneous working conditions can significantly compromise data reproducibility. Therefore, the standardization of devices and simplification of design is required to ensure robust, yet experimentally economical platforms.[266] By cleverly selecting the wave mode, acoustic excitation method, chamber design, and materials, biomedical researchers can exploit a myriad of applications and benefit from the versatility of these platforms for single-cell analysis, development of therapeutic mechanisms, replicating tissue architectures, and the detection and quantification of small particles such as viruses, exosomes, proteins, and DNA. All these potentials prove that this field can contribute significantly to fundamental biological studies, tissue engineering, clinical sample handling, drug development, biosensing, as well as point of care devices.

Author contributions

The manuscript was written through contributions of all authors.

Conflicts of interest

There are no conflicts to declare.

Acknowledgements

The authors would like to acknowledge Natural Science and Engineering Council of Canada for their financial support through Discovery Grant and CREATE in Continuous Flow Synthesis.

References

1 A. Lenshof, C. Johannesson, M. Evander, J. Nilsson and T. Laurell, *Acoustic Cell Manipulation, in Microsystems and Nanosystems*, 2017, pp. 129–173, DOI: **10.1007/978-3-319-44139-9_5**.
2 G. Destgeer and H. J. Sung, Recent advances in microfluidic actuation and micro-object manipulation via surface acoustic waves, *Lab Chip*, 2015, **15**, 2722–2738.
3 R. Pethig, Dielectrophoresis: Using Inhomogeneous AC Electrical Fields to Separate and Manipulate Cells, *Crit. Rev. Biotechnol.*, 1996, **16**, 331–348.
4 M. P. MacDonald, G. C. Spalding and K. Dholakia, Microfluidic sorting in an optical lattice, *Nature*, 2003, **426**(6965), 421–424.
5 A. Ozcelik, *et al.* Acoustic tweezers for the life sciences, *Nat. Methods*, 2018, **15**, 1021–1028.
6 Y. Xie, H. Bachman and T. J. Huang, Acoustofluidic methods in cell analysis, *TrAC, Trends Anal. Chem.*, 2019, **117**, 280–290.
7 Y. Gao, A. K. Fajrial, T. Yang and X. Ding, Emerging on-chip surface acoustic wave technology for small biomaterials manipulation and characterization, *Biomater. Sci.*, 2021, **9**, 1574–1582.

8 A. L. Bernassau, F. Gesellchen, P. G. A. MacPherson, M. Riehle and D. R. S. Cumming, Direct patterning of mammalian cells in an ultrasonic heptagon stencil, *Biomed. Microdevices*, 2012, **14**, 559–564.
9 F. Gesellchen, A. L. Bernassau, T. Déjardin, D. R. S. Cumming and M. O. Riehle, Cell patterning with a heptagon acoustic tweezer-application in neurite guidance, *Lab Chip*, 2014, **14**, 2266–2275.
10 X. Tao, *et al.* 3D patterning/manipulating microparticles and yeast cells using ZnO/Si thin film surface acoustic waves, *Sens. Actuators, B*, 2019, **299**, 126991.
11 Z. Tian, Z. Wang, P. Zhang, T. D. Naquin, J. Mai, Y. Wu, S. Yang, Y. Gu, H. Bachman, Y. Liang and Z. Yu, Generating multifunctional acoustic tweezers in Petri dishes for contactless, precise manipulation of bioparticles, *Sci. Adv.*, 2020, **6**(37), eabb0494.
12 X. Ding, *et al.* Surface acoustic wave microfluidics, *Lab Chip*, 2013, **13**, 3626.
13 B. Kang, *et al.* High-resolution acoustophoretic 3D cell patterning to construct functional collateral cylindroids for ischemia therapy, *Nat. Commun.*, 2018, **9**, 5402.
14 S. M. Naseer, *et al.* Surface acoustic waves induced micropatterning of cells in gelatin methacryloyl (GelMA) hydrogels, *Biofabrication*, 2017, **9**, 015020.
15 B. Chen, *et al.* High-throughput acoustofluidic fabrication of tumor spheroids, *Lab Chip*, 2019, **19**, 1755–1763.
16 L. Alhasan, *et al.* Rapid Enhancement of Cellular Spheroid Assembly by Acoustically Driven Microcentrifugation, *ACS Biomater. Sci. Eng.*, 2016, **2**, 1013–1022.
17 J. P. Lata, *et al.* Surface Acoustic Waves Grant Superior Spatial Control of Cells Embedded in Hydrogel Fibers, *Adv. Mater.*, 2016, **28**, 8632–8638.
18 J. Zhang, L. Meng, F. Cai, H. Zheng and C. R. P. Courtney, Multi-scale patterning of microparticles using a combination of surface acoustic waves and ultrasonic bulk waves, *Appl. Phys. Lett.*, 2014, **104**, 224103.
19 S. Cohen, *et al.* Large-scale acoustic-driven neuronal patterning and directed outgrowth, *Sci. Rep.*, 2020, **10**, 1–11.
20 C. Imashiro, *et al.* Cell Patterning Method on a Clinically Ubiquitous Culture Dish Using Acoustic Pressure Generated from Resonance Vibration of a Disk-Shaped Ultrasonic Transducer, *IEEE Trans. Biomed. Eng.*, 2019, **66**, 111–118.
21 W. T. Coakley, *et al.* Cell-cell contact and membrane spreading in an ultrasound trap, *Colloids Surf., B*, 2004, **34**, 221–230.
22 D. Bazou, G. A. Foster, J. R. Ralphs and W. T. Coakley, Molecular adhesion development in a neural cell monolayer forming in an ultrasound trap, *Mol. Membr. Biol.*, 2005, **22**, 229–240.
23 K. Olofsson, *et al.* Acoustic formation of multicellular tumor spheroids enabling on-chip functional and structural imaging, *Lab Chip*, 2018, **18**, 2466–2476.
24 K. A. Garvin, D. Dalecki and D. C. Hocking, Vascularization of Three-Dimensional Collagen Hydrogels Using Ultrasound Standing Wave Fields, *Ultrasound Med. Biol.*, 2011, **37**, 1853–1864.
25 Y. Sriphutkiat, S. Kasetsirikul, D. Ketpun and Y. Zhou, Cell alignment and accumulation using acoustic nozzle for bioprinting, *Sci. Rep.*, 2019, **9**, 1–12.
26 H. Cai, *et al.* Acoustofluidic assembly of 3D neurospheroids to model Alzheimer's disease, *Analyst*, 2020, **145**, 6243–6253.
27 S. Li, *et al.* Standing Surface Acoustic Wave Based Cell Coculture, *Anal. Chem.*, 2014, **86**, 9853–9859.
28 J. Baca, V. Severns, D. Lovato, D. Branch and R. Larson, Rapid Detection of Ebola Virus with a Reagent-Free, Point-of-Care Biosensor, *Sensors*, 2015, **15**, 8605–8614.
29 Y. Jiang, *et al.* SAW sensor for Influenza A virus detection enabled with efficient surface functionalization, *Sens. Actuators, B*, 2015, **209**, 78–84.
30 E. R. Gray, *et al.* Ultra-rapid, sensitive and specific digital diagnosis of HIV with a dual-channel SAW biosensor in a pilot clinical study, *NPJ Digit. Med.*, 2018, **1**, 35.
31 V. Turbé, *et al.* Towards an ultra-rapid smartphone-connected test for infectious diseases, *Sci. Rep.*, 2017, **7**, 11971.
32 V. Turbé, *et al.* Towards an ultra-rapid smartphone- connected test for infectious diseases, *Sci. Rep.*, 2017, **7**, 11971.
33 S. I. Zida, Y. Lin and Y. L. Khung, Current Trends on Surface Acoustic Wave Biosensors, *Adv. Mater. Technol.*, 2021, **6**, 2001018.
34 M. R. Rasouli and M. Tabrizian, An ultra-rapid acoustic micromixer for synthesis of organic nanoparticles, *Lab Chip*, 2019, **19**, 3316–3325.
35 A. Rajapaksa, A. Qi, L. Y. Yeo, R. Coppel and J. R. Friend, Enabling practical surface acoustic wave nebulizer drug delivery via amplitude modulation, *Lab Chip*, 2014, **14**, 1858–1865.
36 A. E. Rajapaksa, *et al.* Effective pulmonary delivery of an aerosolized plasmid DNA vaccine via surface acoustic wave nebulization, *Respir. Res.*, 2014, **15**, 60.
37 A. R. Rezk, H. Ahmed, S. Ramesan and L. Y. Yeo, High Frequency Sonoprocessing: A New Field of Cavitation-Free Acoustic Materials Synthesis, Processing, and Manipulation, *Adv. Sci.*, 2021, **8**, 2001983.
38 S. Ramesan, *et al.* Acoustofection: High-Frequency Vibrational Membrane Permeabilization for Intracellular siRNA Delivery into Nonadherent Cells, *ACS Appl. Bio Mater.*, 2021, **4**, 2781–2789.
39 M. E. Stamp, M. S. Brugger, A. Wixforth and C. Westerhausen, Acoustotaxis – in vitro stimulation in a wound healing assay employing surface acoustic waves, *Biomater. Sci.*, 2016, **4**(7), 1092–1099.
40 J. I. Rosenblum, M. I. Gazes and N. Greenberg, Surface acoustic wave patch therapy affects tissue oxygenation in ischemic feet, *Wounds*, 2014, **26**, 301–305.
41 M. Miansari, *et al.* Inducing Mild Traumatic Brain Injury in C. elegans via Cavitation-Free Surface Acoustic Wave-Driven Ultrasonic Irradiation, *Sci. Rep.*, 2019, **9**, 1–11.
42 P. Li and T. J. Huang, Applications of Acoustofluidics in Bioanalytical Chemistry, *Anal. Chem.*, 2019, **91**, 757–767.

43 M. Wu, *et al.* Acoustofluidic separation of cells and particles, *Microsyst. Nanoeng.*, 2019, **5**, 32.
44 S. Mohanty, I. S. M. Khalil and S. Misra, Contactless acoustic micro/nano manipulation: a paradigm for next generation applications in life sciences, *Proc. R. Soc. A*, 2020, **476**, 20200621.
45 A. Hashmi, G. Yu, M. Reilly-Collette, G. Heiman and J. Xu, Oscillating bubbles: a versatile tool for lab on a chip applications, *Lab Chip*, 2012, **12**, 4216.
46 J. Rufo, P. Zhang, R. Zhong, L. P. Lee and T. J. Huang, A sound approach to advancing healthcare systems: the future of biomedical acoustics, *Nat. Commun.*, 2022, **131**(13), 1–8.
47 L. Y. Yeo and J. R. Friend, Surface Acoustic Wave Microfluidics, *Annu. Rev. Fluid Mech.*, 2014, **46**, 379–406.
48 J. Pons, *Emerging Actuator Technologies. Emerging Actuator Technologies: A Micromechatronic Approach*, John Wiley & Sons, Ltd, 2005, DOI: **10.1002/0470091991**.
49 L. Y. Yeo and J. R. Friend, Surface acoustic wave microfluidics, *Annu. Rev. Fluid Mech.*, 2014, **46**(1), 379–406.
50 H. Ahmed, S. Ramesan, L. Lee, A. R. Rezk and L. Y. Yeo, On-Chip Generation of Vortical Flows for Microfluidic Centrifugation, *Small*, 2020, **16**, 1903605.
51 L. Meng, *et al.* Acoustic tweezers, *J. Phys. D: Appl. Phys.*, 2019, **52**, 273001.
52 J. Zhang, Q. Wu, X. Zhang, H. Wan and P. Wang, *Acoustic Transducer and Its Applications in Biosensors, in Handbook of Cell Biosensors*, Springer International Publishing, 2021, pp. 1–19, DOI: **10.1007/978-3-319-47405-2_65-1**.
53 D. B. B. Go, M. Z. Z. Atashbar, Z. Ramshani, H.-C. Chang and P. D. Degree, Surface acoustic wave devices for chemical sensing and microfluidics: a review and perspective, *Anal. Methods*, 2017, **9**, 4112–4134.
54 J. Friend and L. Y. Yeo, Microscale acoustofluidics: Microfluidics driven via acoustics and ultrasonics, *Rev. Mod. Phys.*, 2011, **83**, 647–704.
55 H. Bruus, Acoustofluidics 10: Scaling laws in acoustophoresis, *Lab Chip*, 2012, **12**, 1578–1586.
56 C. Eckart, Vortices and Streams Caused by Sound Waves, *Phys. Rev.*, 1948, **73**, 68–76.
57 M. Wiklund, R. Green and M. Ohlin, Acoustofluidics 14: Applications of acoustic streaming in microfluidic devices, *Lab Chip*, 2012, **12**(14), 2438–2451.
58 W. L. Nyborg, Acoustic Streaming near a Boundary, *J. Acoust. Soc. Am.*, 1958, **30**, 329–339.
59 J. Lei, P. Glynne-Jones and M. Hill, Comparing methods for the modelling of boundary-driven streaming in acoustofluidic devices, *Microfluid. Nanofluid.*, 2017, **21**, 23.
60 I. Leibacher, P. Hahn and J. Dual, Acoustophoretic cell and particle trapping on microfluidic sharp edges, *Microfluid. Nanofluid.*, 2015, **19**, 923–933.
61 R. Manasseh, *Acoustic Bubbles, Acoustic Streaming, and Cavitation Microstreaming, in Handbook of Ultrasonics and Sonochemistry*, Springer, Singapore, 2016, pp. 33–68, DOI: **10.1007/978-981-287-278-4_5**.
62 B. W. Drinkwater, Dynamic-field devices for the ultrasonic manipulation of microparticles, *Lab Chip*, 2014, **16**(13), 2360–2375.
63 R. Mettin, I. Akhatov, U. Parlitz, C. Ohl and W. Lauterborn, Bjerknes forces between small cavitation bubbles in a strong acoustic field, *Phys. Rev. E: Stat. Phys., Plasmas, Fluids, Relat. Interdiscip. Top.*, 1997, **56**, 2924–2931.
64 R. Habibi, V. He, S. Ghavamian, A. de Marco, T.-H. Lee and M.-I. Aguilar, *et al.* Exosometrapping and enrichment using a sound wave activated nano-sieve (SWANS), *Lab Chip*, 2020, **20**(19), 3633–3643.
65 D. J. Collins, *et al.* Self-Aligned Acoustofluidic Particle Focusing and Patterning in Microfluidic Channels from Channel-Based Acoustic Waveguides, *Phys. Rev. Lett.*, 2018, **120**, 074502.
66 A. G. Guex, N. Di Marzio, D. Eglin, M. Alini and T. Serra, The waves that make the pattern: a review on acoustic manipulation in biomedical research, *Mater. Today Bio*, 2021, **10**, 100110.
67 J. P. K. Armstrong and M. M. Stevens, Using Remote Fields for Complex Tissue Engineering, *Trends Biotechnol.*, 2020, **38**, 254–263.
68 D. Dalecki and D. C. Hocking, *Advancing Ultrasound Technologies for Tissue Engineering, in Handbook of Ultrasonics and Sonochemistry*, Springer, Singapore, 2015, pp. 1–26, DOI: **10.1007/978-981-287-470-2_28-1**.
69 Z. Wang, *et al.* Single-cell patterning technology for biological applications, *Biomicrofluidics*, 2019, **13**, 061502.
70 J. P. K. Armstrong, *et al.* Engineering Anisotropic Muscle Tissue using Acoustic Cell Patterning, *Adv. Mater.*, 2018, **30**, 1802649.
71 K. Olofsson, B. Hammarström and M. Wiklund, Ultrasonic Based Tissue Modelling and Engineering, *Micromachines*, 2018, **9**, 594.
72 J. W. Buikema, P. Van Der Meer, J. P. G. Sluijter and I. J. Domian, Engineering Myocardial Tissue: The Convergence of Stem Cells Biology and Tissue Engineering Technology, *Stem Cells*, 2013, **31**, 2587.
73 R. L. Mauck, *et al.* Engineering on the Straight and Narrow: The Mechanics of Nanofibrous Assemblies for Fiber-Reinforced Tissue Regeneration, *Tissue Eng., Part B*, 2009, **15**, 171.
74 J. Shi, *et al.* Acoustic tweezers: patterning cells and microparticles using standing surface acoustic waves (SSAW), *Lab Chip*, 2009, **9**, 2890.
75 F. Guo, *et al.* Controlling cell–cell interactions using surface acoustic waves, *Proc. Natl. Acad. Sci. U. S. A.*, 2015, **112**, 43–48.
76 S. Li, *et al.* Standing Surface Acoustic Wave Based Cell Coculture, *Anal. Chem.*, 2014, **86**, 9853–9859.
77 E. S. Comeau, D. C. Hocking and D. Dalecki, Ultrasound patterning technologies for studying vascular morphogenesis in 3D, *J. Cell Sci.*, 2017, **130**, 232–242.
78 P. Chansoria, L. K. Narayanan, K. Schuchard and R. Shirwaiker, Ultrasound-assisted biofabrication and bioprinting of preferentially aligned three-dimensional cellular constructs, *Biofabrication*, 2019, **11**, 035015.

79 A. L. Bernassau, P. G. A. MacPherson, J. Beeley, B. W. Drinkwater and D. R. S. Cumming, Patterning of microspheres and microbubbles in an acoustic tweezers, *Biomed. Microdevices*, 2013, **15**, 289–297.
80 A. Gladkov, *et al.* Design of Cultured Neuron Networks in vitro with Predefined Connectivity Using Asymmetric Microfluidic Channels, *Sci. Rep.*, 2017, **7**, 1–14.
81 C. Bouyer, *et al.* A Bio-Acoustic Levitational (BAL) Assembly Method for Engineering of Multilayered, 3D Brain-Like Constructs, Using Human Embryonic Stem Cell Derived Neuro-Progenitors, *Adv. Mater.*, 2016, **28**, 161–167.
82 A. Tait, *et al.* Engineering multi-layered tissue constructs using acoustic levitation, *Sci. Rep.*, 2019, **9**, 9789.
83 X. Ding, *et al.* Tunable patterning of microparticles and cells using standing surface acoustic waves, *Lab Chip*, 2012, **12**, 2491–2497.
84 P. Kang, *et al.* Acoustic tweezers based on circular, slanted-finger interdigital transducers for dynamic manipulation of micro-objects, *Lab Chip*, 2020, **20**, 987–994.
85 Y. Bian, *et al.* Acoustofluidic waveguides for localized control of acoustic wavefront in microfluidics, *Microfluid. Nanofluid.*, 2017, **21**, 132.
86 P. Chen and J. Viñals, Amplitude equation and pattern selection in Faraday waves, *Phys. Rev. E: Stat. Phys., Plasmas, Fluids, Relat. Interdiscip. Top.*, 1999, **60**, 559–570.
87 P. Chen, S. Güven, O. B. Usta, M. L. Yarmush and U. Demirci, Biotunable Acoustic Node Assembly of Organoids, *Adv. Healthcare Mater.*, 2015, **4**, 1937–1943.
88 D. Petta, *et al.* Sound-induced morphogenesis of multicellular systems for rapid orchestration of vascular networks, *Biofabrication*, 2020, **13**, 15004.
89 T. Ren, P. Chen, L. Gu, M. G. Ogut and U. Demirci, Soft Ring-Shaped Cellu-Robots with Simultaneous Locomotion in Batches, *Adv. Mater.*, 2020, **32**, 1905713.
90 P. Chen, *et al.* Bioacoustic-enabled patterning of human iPSC-derived cardiomyocytes into 3D cardiac tissue, *Biomaterials*, 2017, **131**, 47–57.
91 J. Wang, *et al.* Acoustic Fabrication of Living Cardiomyocyte-based Hybrid Biorobots, *ACS Nano*, 2022, **16**, 10219–10230.
92 K. Melde, A. G. Mark, T. Qiu and P. Fischer, Holograms for acoustics, *Nature*, 2016, **537**, 518–522.
93 Z. Ma, *et al.* Acoustic Holographic Cell Patterning in a Biocompatible Hydrogel, *Adv. Mater.*, 2020, **32**, 1904181.
94 D. Bazou, W. T. Coakley, A. J. Hayes and S. K. Jackson, Long-term viability and proliferation of alginate-encapsulated 3-D HepG2 aggregates formed in an ultrasound trap, *Toxicol. In Vitro*, 2008, **22**, 1321–1331.
95 L. A. Kuznetsova, D. Bazou, G. O. Edwards and W. T. Coakley, Multiple three-dimensional mammalian cell aggregates formed away from solid substrata in ultrasound standing waves, *Biotechnol. Prog.*, 2009, **25**, 834–841.
96 J. Liu, *et al.* Functional three-dimensional HepG2 aggregate cultures generated from an ultrasound trap: Comparison with HepG2 spheroids, *J. Cell. Biochem.*, 2007, **102**, 1180–1189.
97 K. Olofsson, V. Carannante, M. Takai, B. Önfelt and M. Wiklund, Ultrasound-Based Scaffold-Free Core-Shell Multicellular Tumor Spheroid Formation, *Micromachines*, 2021, **12**, 329.
98 K. Chen, *et al.* Rapid formation of size-controllable multicellular spheroids via 3D acoustic tweezers, *Lab Chip*, 2016, **16**, 2636–2643.
99 X. Hu, *et al.* On-chip hydrogel arrays individually encapsulating acoustic formed multicellular aggregates for high throughput drug testing, *Lab Chip*, 2020, **20**, 2228–2236.
100 Y. Wu, *et al.* Acoustic assembly of cell spheroids in disposable capillaries, *Nanotechnology*, 2018, **29**, 504006.
101 F. Guo, *et al.* Precise Manipulation and Patterning of Protein Crystals for Macromolecular Crystallography Using Surface Acoustic Waves, *Small*, 2015, **11**, 2733–2737.
102 Y. Kurashina, K. Takemura and J. Friend, Cell agglomeration in the wells of a 24-well plate using acoustic streaming, *Lab Chip*, 2017, **17**, 876–886.
103 R. Rasouli and M. Tabrizian, Rapid Formation of Multicellular Spheroids in Boundary-Driven Acoustic Microstreams, *Small*, 2021, **17**, 2101931.
104 T. D. Nguyen, *et al.* Large-Scale Fabrication of 3D Scaffold-Based Patterns of Microparticles and Breast Cancer Cells using Reusable Acoustofluidic Device, *Adv. Eng. Mater.*, 2021, **23**, 2001377.
105 Z. Tian, S. Yang, P. H. Huang, Z. Wang, P. Zhang, Y. Gu, H. Bachman, C. Chen, M. Wu, Y. Xie and T. J. Huang, Wave number–spiral acoustic tweezers for dynamic and reconfigurable manipulation of particles and cells, *Sci. Adv.*, 2019, **5**(5), eaau6062.
106 E. Blanco, H. Shen and M. Ferrari, Principles of nanoparticle design for overcoming biological barriers to drug delivery, *Nat. Biotechnol.*, 2015, **33**, 941–951.
107 P. Huang, *et al.* Acoustofluidic Synthesis of Particulate Nanomaterials, *Adv. Sci.*, 2019, **6**, 1900913.
108 N. H. A. Le, *et al.* Acoustically enhanced microfluidic mixer to synthesize highly uniform nanodrugs without the addition of stabilizers, *Int. J. Nanomed.*, 2018, **13**, 1353–1359.
109 N. H. Le, H. Deng, C. Devendran, N. Akhtar, X. Ma, C. Pouton, H. K. Chan, A. Neild and T. Alan, Ultrafast star-shaped acoustic micromixer for high throughput nanoparticle synthesis, *Lab Chip*, 2020, **20**(3), 582–591.
110 A. Pourabed, *et al.* High throughput acoustic microfluidic mixer controls self-assembly of protein nanoparticles with tuneable sizes, *J. Colloid Interface Sci.*, 2021, **585**, 229–236.
111 M. Kurosawa, T. Watanabe, A. Futami and T. Higuchi, Surface acoustic wave atomizer, *Sens. Actuators, A*, 1995, **50**, 69–74.
112 A. Qi, *et al.* Template-free Synthesis and Encapsulation Technique for Layer-by-Layer Polymer Nanocarrier Fabrication, *ACS Nano*, 2011, **5**, 9583–9591.
113 M. Alvarez, J. Friend and L. Y. Yeo, Rapid generation of protein aerosols and nanoparticles via surface acoustic wave atomization, *Nanotechnology*, 2008, **19**, 455103.
114 A. Qi, J. R. Friend and L. Y. Yeo, *Investigation of SAW atomization, in Proceedings - IEEE Ultrasonics Symposium*,

IEEE, 2009, pp. 787–790, DOI: 10.1109/ULTSYM.2009.5441556.
115 D. Van Assche, *et al.* Gradient acoustic focusing of sub-micron particles for separation of bacteria from blood lysate, *Sci. Rep.*, 2020, **10**, 1–13.
116 A. Winkler, S. M. M. Harazim, S. B. B. Menzel and H. Schmidt, SAW-based fluid atomization using mass-producible chip devices, *Lab Chip*, 2015, **15**, 3793–3799.
117 A. Qi, *et al.* Miniature inhalation therapy platform using surface acoustic wave microfluidic atomization, *Lab Chip*, 2009, **9**, 2184.
118 D. B. Go, M. Z. Atashbar, Z. Ramshani and H. C. Chang, Surface acoustic wave devices for chemical sensing and microfluidics: a review and perspective, *Anal. Methods*, 2017, **9**(28), 4112–4134.
119 M. Steinacher, H. Du, D. Gilbert and E. Amstad, Production of Additive-Free Amorphous Nanoparticles with a SAW-Based Microfluidic Spray-Dryer, *Adv. Mater. Technol.*, 2019, **4**, 1800665.
120 P. Barnes, New treatments for chronic obstructive pulmonary disease, *Curr. Opin. Pharmacol.*, 2001, **1**, 217–222.
121 Y. Wang, A. R. Rezk, J. S. Khara, L. Y. Yeo and P. L. R. Ee, Stability and efficacy of synthetic cationic antimicrobial peptides nebulized using high frequency acoustic waves, *Biomicrofluidics*, 2016, **10**, 034115.
122 K. S. Wong, W. T. Lim, C. W. Ooi, L. Y. Yeo and M. K. Tan, In situ generation of plasma-activated aerosols via surface acoustic wave nebulization for portable spray-based surface bacterial inactivation, *Lab Chip*, 2020, **20**(10), 1856–1868.
123 S. Marqus, *et al.* High frequency acoustic nebulization for pulmonary delivery of antibiotic alternatives against Staphylococcus aureus, *Eur. J. Pharm. Biopharm.*, 2020, **151**, 181–188.
124 L. Alhasan, A. Qi, A. R. Rezk, L. Y. Yeo and P. P. Y. Chan, Integrative Biology Assessment of the potential of a high frequency acoustomicrofluidic nebulisation platform for inhaled stem cell therapy †, This J. is Cite this, *Integr. Biol.*, 2016, **8**, 12.
125 S. Ramesan, A. R. Rezk and L. Y. Yeo, High frequency acoustic permeabilisation of drugs through tissue for localised mucosal delivery, *Lab Chip*, 2018, **18**, 3272–3284.
126 Y. Li, Z. Chen and S. Ge, Sonoporation: Underlying Mechanisms and Applications in Cellular Regulation, *BIO Integr.*, 2021, **2**, 29–36.
127 M. P. Stewart, R. Langer and K. F. Jensen, Intracellular delivery by membrane disruption: Mechanisms, strategies, and concepts, *Chem. Rev.*, 2018, **118**, 7409–7531.
128 M. Tomizawa, *et al.* Sonoporation: Gene transfer using ultrasound, *World J. Methodol.*, 2013, **3**, 39–44.
129 Y. Qiu, C. Zhang, J. Tu and D. Zhang, Microbubble-induced sonoporation involved in ultrasound-mediated DNA transfection in vitro at low acoustic pressures, *J. Biomech.*, 2012, **45**, 1339–1345.
130 M. A. Hassan, *et al.* Modulation control over ultrasound-mediated gene delivery: Evaluating the importance of standing waves, *J. Controlled Release*, 2010, **141**, 70–76.
131 D. Morshedi Rad, *et al.* A Comprehensive Review on Intracellular Delivery, *Adv. Mater.*, 2021, **33**, 2005363.
132 A. van Wamel, *et al.* Vibrating microbubbles poking individual cells: Drug transfer into cells via sonoporation, *J. Controlled Release*, 2006, **112**, 149–155.
133 Z. Fan, R. E. Kumon and C. X. Deng, Mechanisms of microbubble-facilitated sonoporation for drug and gene delivery, *Ther. Delivery*, 2014, **5**, 467–486.
134 L. Meng, *et al.* Sonoporation of Cells by a Parallel Stable Cavitation Microbubble Array, *Adv. Sci.*, 2019, **6**, 1900557.
135 M. Aghaamoo, *et al.* High-Throughput and Dosage-Controlled Intracellular Delivery of Large Cargos by an Acoustic-Electric Micro-Vortices Platform, *Adv. Sci.*, 2022, **9**, 2102021.
136 D. Carugo, *et al.* Contrast agent-free sonoporation: The use of an ultrasonic standing wave microfluidic system for the delivery of pharmaceutical agents, *Biomicrofluidics*, 2011, **5**, 044108.
137 J. N. Belling, *et al.* Acoustofluidic sonoporation for gene delivery to human hematopoietic stem and progenitor cells, *Proc. Natl. Acad. Sci. U. S. A.*, 2020, **117**, 10976–10982.
138 Z. Zhang, *et al.* Hypersonic Poration: A New Versatile Cell Poration Method to Enhance Cellular Uptake Using a Piezoelectric Nano-Electromechanical Device, *Small*, 2017, **13**, 1602962.
139 T. Reusch, *et al.* Collective lipid bilayer dynamics excited by surface acoustic waves, *Phys. Rev. Lett.*, 2014, **113**, 118102.
140 S. Ramesan, A. R. Rezk, C. Dekiwadia, C. Cortez-Jugo and L. Y. Yeo, Acoustically-mediated intracellular delivery †, *Nanoscale*, 2018, **10**, 13165.
141 D. Peng, *et al.* Mechanisms and Applications of Neuromodulation Using Surface Acoustic Waves—A Mini-Review, *Front. Neurosci.*, 2021, **15**, 27.
142 K. Martinez Villegas, R. Rasouli and M. Tabrizian, Enhancing metabolic activity and differentiation potential in adipose mesenchymal stem cells via high-resolution surface-acoustic-wave contactless patterning, *Microsyst. Nanoeng.*, 2022, **8**, 79.
143 C. Devendran, J. Carthew, J. E. Frith and A. Neild, Cell Adhesion, Morphology, and Metabolism Variation via Acoustic Exposure within Microfluidic Cell Handling Systems, *Adv. Sci.*, 2019, **6**, 1902326.
144 G. Greco, *et al.* Surface-Acoustic-Wave (SAW)-Driven Device for Dynamic Cell Cultures, *Anal. Chem.*, 2018, **90**, 7450–7457.
145 M. S. Brugger, *et al.* Orchestrating cells on a chip: Employing surface acoustic waves towards the formation of neural networks, *Phys. Rev. E*, 2018, **98**, 012411.
146 N. Doan, P. Reher, S. Meghji and M. Harris, In vitro effects of therapeutic ultrasound on cell proliferation, protein synthesis, and cytokine production by human fibroblasts, osteoblasts, and monocytes, *Kouqiang Hemian Waike Zazhi*, 1999, **57**, 409–419.
147 M. S. Brugger, *et al.* Vibration enhanced cell growth induced by surface acoustic waves as in vitro wound-

healing model, *Proc. Natl. Acad. Sci. U. S. A.*, 2020, **117**, 31603–31613.
148 I.-C. Lee, H.-J. Wu and H.-L. Liu, Dual-Frequency Ultrasound Induces Neural Stem/Progenitor Cell Differentiation and Growth Factor Utilization by Enhancing Stable Cavitation, *ACS Chem. Neurosci.*, 2019, **10**, 1452–1461.
149 Y. S. Lee, *et al.* An ultra-effective method of generating extramultipotent cells from human fibroblasts by ultrasound, *Biomaterials*, 2017, **143**, 65–78.
150 U. S. Jonnalagadda, *et al.* Acoustically modulated biomechanical stimulation for human cartilage tissue engineering, *Lab Chip*, 2018, **18**, 473–485.
151 L. A. Ambattu, *et al.* High frequency acoustic cell stimulation promotes exosome generation regulated by a calcium-dependent mechanism, *Commun. Biol.*, 2020, **3**, 1–9.
152 S. S. Ranade, R. Syeda and A. Patapoutian, Mechanically Activated Ion Channels, *Neuron*, 2015, **87**, 1162–1179.
153 P. Kumar, D. Kumar, S. K. Jha, N. K. Jha and R. K. Ambasta, *Ion Channels in Neurological Disorders. in Advances in Protein Chemistry and Structural Biology*, Academic Press Inc., 2016, vol. 103, pp. 97–136.
154 J. Ye, *et al.* Ultrasonic Control of Neural Activity through Activation of the Mechanosensitive Channel MscL, *Nano Lett.*, 2018, **18**, 4148–4155.
155 Z. Lin, *et al.* On-Chip Ultrasound Modulation of Pyramidal Neuronal Activity in Hippocampal Slices, *Adv. Biosyst.*, 2018, **2**, 1800041.
156 Z. Lin, X. Huang, W. Zhou, W. Zhang, Y. Liu, T. Bian, L. Niu, L. Meng and Y. Guo, Ultrasound stimulation modulates voltage-gated potassium currents associated with action potential shape in hippocampal CA1 pyramidal neurons, *Front. Pharmacol.*, 2019, **10**, 544.
157 Y. Pan, *et al.* Mechanogenetics for the remote and noninvasive control of cancer immunotherapy, *Proc. Natl. Acad. Sci. U. S. A.*, 2018, **115**, 992–997.
158 W. Zhou, J. Wang, K. Wang, B. Huang, L. Niu, F. Li, F. Cai, Y. Chen, X. Liu, X. Zhang and H. Chen, Ultrasound neuromodulation chip: activation of sensory neurons in Caenorhabditis elegans by surface acoustic waves, *Lab Chip*, 2017, **17**(10), 1725–1731.
159 M. A. Hilliard, *et al.* Cellular response and adaptation to chemical repellents, In vivo imaging of C. elegans ASH neurons, *EMBO J.*, 2005, **24**, 63–72.
160 E. Gourgou and N. Chronis, Chemically induced oxidative stress affects ASH neuronal function and behavior in C. elegans, *Sci. Rep.*, 2016, **6**, 38147.
161 Z. Lin, *et al.* Non-invasive ultrasonic neuromodulation of neuronal excitability for treatment of epilepsy, *Theranostics*, 2020, **10**, 5514–5526.
162 A. Adamo, *et al.* Microfluidics-based assessment of cell deformability, *Anal. Chem.*, 2012, **84**, 6438–6443.
163 W. H. Grover, *et al.* Measuring single-cell density, *Proc. Natl. Acad. Sci. U. S. A.*, 2011, **108**, 10992–10996.
164 S. E. Cross, Y. S. Jin, J. Rao and J. K. Gimzewski, Nanomechanical analysis of cells from cancer patients, *Nat. Nanotechnol.*, 2007, **2**, 780–783.
165 S. Suresh, Biomechanics and biophysics of cancer cells, *Acta Biomater.*, 2007, **3**, 413–438.
166 G. Y. H. Lee and C. T. Lim, Biomechanics approaches to studying human diseases, *Trends Biotechnol.*, 2007, **25**, 111–118.
167 Y. Xie, *et al.* Probing Cell Deformability via Acoustically Actuated Bubbles, *Small*, 2016, **12**, 902–910.
168 N. F. Läubli, *et al.* 3D mechanical characterization of single cells and small organisms using acoustic manipulation and force microscopy, *Nat. Commun.*, 2021, **12**, 1–11.
169 D. Hartono, Y. Liu, P. L. Tan, X. Y. Then, L. Y. Yung and K. M. Lim, On-chip measurements of cell compressibility via acoustic radiation, *Lab Chip*, 2011, **11**(23), 4072–4080.
170 H. Wang, *et al.* A continuous-flow acoustofluidic cytometer for single-cell mechanotyping, *Lab Chip*, 2019, **19**, 387–393.
171 C. Grenvall, C. Antfolk, C. Z. Bisgaard and T. Laurell, Two-dimensional acoustic particle focusing enables sheathless chip Coulter counter with planar electrode configuration, *Lab Chip*, 2014, **14**, 4629–4637.
172 C. Grenvall, C. Magnusson, H. Lilja and T. Laurell, Concurrent Isolation of Lymphocytes and Granulocytes Using Prefocused Free Flow Acoustophoresis, *Anal. Chem.*, 2015, **87**, 5596–5604.
173 D. Kamsma, *et al.* Single-Cell Acoustic Force Spectroscopy: Resolving Kinetics and Strength of T Cell Adhesion to Fibronectin, *Cell Rep.*, 2018, **24**, 3008–3016.
174 D. Kamsma, R. Creyghton, G. Sitters, G. J. L. Wuite and E. J. G. Peterman, Tuning the Music: Acoustic Force Spectroscopy (AFS) 2.0, *Methods*, 2016, **105**, 26–33.
175 G. Sitters, *et al.* Acoustic force spectroscopy, *Nat. Methods*, 2014, **12**, 47–50.
176 R. Sorkin, *et al.* Probing cellular mechanics with acoustic force spectroscopy, *Mol. Biol. Cell*, 2018, **29**, 2005–2011.
177 S. Yang, *et al.* Harmonic acoustics for dynamic and selective particle manipulation, *Nat. Mater.*, 2022, **215**(21), 540–546.
178 J. K. Luo, Y. Q. Fu and W. I. Milne, Acoustic wave based microfluidic and lab-on-chip, *Modeling and Measurement Methods for Acoustic Waves and for Acoustic Microdevices*, IntechOpen, 2013.
179 M.-I. Rocha-Gaso, C. March-Iborra, Á. Montoya-Baides and A. Arnau-Vives, Surface Generated Acoustic Wave Biosensors for the Detection of Pathogens: A Review, *Sensors*, 2009, **9**, 5740–5769.
180 K. Chang, *et al.* Label-free and high-sensitive detection of human breast cancer cells by aptamer-based leaky surface acoustic wave biosensor array, *Biosens. Bioelectron.*, 2014, **60**, 318–324.
181 T. Wang, *et al.* Surface Acoustic Waves (SAW)-Based Biosensing for Quantification of Cell Growth in 2D and 3D Cultures, *Sensors*, 2015, **15**, 32045–32055.
182 H. L. H.-L. Cai, *et al.* A third-order mode high frequency biosensor with atomic resolution, *Biosens. Bioelectron.*, 2015, **71**, 261–268.

183 J. Zhang, *et al.* Recent advances in acoustic wave biosensors for the detection of disease-related biomarkers: A review, *Anal. Chim. Acta*, 2021, **1164**, 338321.
184 X. Wei, J. Zhang, L. Zhuang, H. Wan and P. Wang, A Novel Surface Acoustic Wave Biosensor for Real-Time Monitoring of Cell Contractile Properties, *ECS Meeting Abstracts*, 2020, **MA2020-01**, 1970.
185 S. U. Senveli, *et al.* A surface acoustic wave biosensor for interrogation of single tumour cells in microcavities, *Lab Chip*, 2016, **16**, 163–171.
186 L. Lamanna, F. Rizzi, V. R. Bhethanabotla and M. De Vittorio, Conformable surface acoustic wave biosensor for E-coli fabricated on PEN plastic film, *Biosens. Bioelectron.*, 2020, **163**, 112164.
187 S. T. Ten, *et al.* Highly sensitive Escherichia coli shear horizontal surface acoustic wave biosensor with silicon dioxide nanostructures, *Biosens. Bioelectron.*, 2017, **93**, 146–154.
188 A. Kordas, *et al.* Rapid Salmonella detection using an acoustic wave device combined with the RCA isothermal DNA amplification method, *Sens. Bio-Sens. Res.*, 2016, **11**, 121–127.
189 K. Tsougeni, *et al.* Lab-on-Chip platform and protocol for rapid foodborne pathogen detection comprising on-chip cell capture, lysis, DNA amplification and surface-acoustic-wave detection, *Sens. Actuators, B*, 2020, **320**, 128345.
190 X. Liu, J.-Y. Wang, X.-B. Mao, Y. Ning and G.-J. Zhang, Single-Shot Analytical Assay Based on Graphene-Oxide-Modified Surface Acoustic Wave Biosensor for Detection of Single-Nucleotide Polymorphisms, *Anal. Chem.*, 2015, **87**, 9352–9359.
191 Y. Zhang, F. Yang, Z. Sun, Y. T. Li and G. J. Zhang, A surface acoustic wave biosensor synergizing DNA-mediated: In situ silver nanoparticle growth for a highly specific and signal-amplified nucleic acid assay, *Analyst*, 2017, **142**, 3468–3476.
192 D. Matatagui, *et al.* Comparison of two types of acoustic biosensors to detect immunoreactions: Love-wave sensor working in dynamic mode and QCM working in static mode, *Sens. Actuators, B*, 2013, **189**, 123–129.
193 Y.-S. Choi, J. Lee, Y. Lee, J. Kwak and S. Suk Lee, Increase in detection sensitivity of surface acoustic wave biosensor using triple transit echo wave, *Appl. Phys. Lett.*, 2018, **113**, 083702.
194 A. Tretjakov, V. Syritski, J. Reut, R. Boroznjak and A. Öpik, Molecularly imprinted polymer film interfaced with Surface Acoustic Wave technology as a sensing platform for label-free protein detection, *Anal. Chim. Acta*, 2016, **902**, 182–188.
195 C. C. Wang, *et al.* AuNP-Amplified Surface Acoustic Wave Sensor for the Quantification of Exosomes, *ACS Sens.*, 2020, **5**, 362–369.
196 Y. Huang, P. K. Das and V. R. Bhethanabotla, Surface acoustic waves in biosensing applications, *Sensors and Actuators Reports*, 2021, **3**, 100041.
197 A. Renaudin, V. Chabot, E. Grondin, V. Aimez and P. G. Charette, Integrated active mixing and biosensing using surface acoustic waves (SAW) and surface plasmon resonance (SPR) on a common substrate, *Lab Chip*, 2010, **10**, 111–115.
198 A. Sonato, M. Agostini, G. Ruffato, E. Gazzola, D. Liuni, G. Greco, M. Travagliati, M. Cecchini and F. Romanato, A surface acoustic wave (SAW)-enhanced grating-coupling phase-interrogation surface plasmon resonance (SPR) microfluidic biosensor, *Lab Chip*, 2016, **16**(7), 1224–1233.
199 G. D. G. D. Meyer, *et al.* Nonspecific binding removal from protein microarrays using thickness shear mode resonators, *IEEE Sens. J.*, 2006, **6**, 254–261.
200 S. Pan, *et al.* Biofouling Removal and Protein Detection Using a Hypersonic Resonator, *ACS Sens.*, 2017, **2**, 1175–1183.
201 S. Cular, D. W. Branch, V. R. Bhethanabotla, G. D. Meyer and H. G. Craighead, Removal of Nonspecifically Bound Proteins on Microarrays Using Surface Acoustic Waves, *IEEE Sens. J.*, 2008, **8**, 314–320.
202 J. Liu, S. Li and V. R. Bhethanabotla, Integrating Metal-Enhanced Fluorescence and Surface Acoustic Waves for Sensitive and Rapid Quantification of Cancer Biomarkers from Real Matrices, *ACS Sens.*, 2018, **3**, 222–229.
203 S. Cular, V. R. Bhethanabotla and D. W. Branch, *Simultaneous surface manipulation and sensing in a biosensor using a hexagonal saw device. in AIChE Annual Meeting, Conference Proceedings*, 2006.
204 R. Singh, S. K. R. S. Sankaranarayanan and V. R. Bhethanabotla, Cite as, *Appl. Phys. Lett.*, 2009, **94**, 263503.
205 M. Antfolk, C. Magnusson, P. Augustsson, H. Lilja and T. Laurell, Acoustofluidic, Label-Free Separation and Simultaneous Concentration of Rare Tumor Cells from White Blood Cells, *Anal. Chem.*, 2015, **87**, 9322–9328.
206 M. Antfolk, C. Antfolk, H. Lilja, T. Laurell and P. Augustsson, A single inlet two-stage acoustophoresis chip enabling tumor cell enrichment from white blood cells, *Lab Chip*, 2015, **15**, 2102–2109.
207 Y. Chen, *et al.* High-throughput acoustic separation of platelets from whole blood, *Lab Chip*, 2016, **16**, 3466–3472.
208 F. Petersson, L. Åberg, A.-M. Swärd-Nilsson and T. Laurell, Free Flow Acoustophoresis: Microfluidic-Based Mode of Particle and Cell Separation, *Anal. Chem.*, 2007, **79**, 5117–5123.
209 J. Shi, H. Huang, Z. Stratton, Y. Huang and T. J. Huang, Continuous particle separation in a microfluidic channel via standing surface acoustic waves (SSAW), *Lab Chip*, 2009, **9**, 3354.
210 J. Nam, H. Lim, D. Kim and S. Shin, Separation of platelets from whole blood using standing surface acoustic waves in a microchannel, *Lab Chip*, 2011, **11**, 3361.
211 S. Li, *et al.* An On-Chip, Multichannel Droplet Sorter Using Standing Surface Acoustic Waves, *Anal. Chem.*, 2013, **85**, 5468–5474.
212 K. Lee, *et al.* Acoustic Purification of Extracellular Microvesicles, *ACS Nano*, 2015, **9**, 2321–2327.
213 M. Wu, *et al.* Acoustic Separation of Nanoparticles in Continuous Flow, *Adv. Funct. Mater.*, 2017, **27**, 1606039.

214 M. Wu, *et al.* Isolation of exosomes from whole blood by integrating acoustics and microfluidics, *Proc. Natl. Acad. Sci. U. S. A.*, 2017, **114**, 10584–10589.
215 X. Ding, *et al.* Cell separation using tilted-angle standing surface acoustic waves, *Proc. Natl. Acad. Sci. U. S. A.*, 2014, **111**, 12992–12997.
216 P. Li, *et al.* Acoustic separation of circulating tumor cells, *Proc. Natl. Acad. Sci. U. S. A.*, 2015, **112**, 4970–4975.
217 H. Bruus, Acoustofluidics 7: The acoustic radiation force on small particles, *Lab Chip*, 2012, **12**, 1014.
218 P. Augustsson, J. T. Karlsen, H.-W. Su, H. Bruus and J. Voldman, Iso-acoustic focusing of cells for size-insensitive acousto-mechanical phenotyping, *Nat. Commun.*, 2016, **7**, 11556.
219 F. Petersson, A. Nilsson, C. Holm, H. Jönsson and T. Laurell, Continuous separation of lipid particles from erythrocytes by means of laminar flow and acoustic standing wave forces, *Lab Chip*, 2005, **5**, 20–22.
220 T. Franke, A. R. Abate, D. A. Weitz and A. Wixforth, Surface acoustic wave (SAW) directed droplet flow in microfluidics for PDMS devices, *Lab Chip*, 2009, **9**, 2625.
221 T. Franke, S. Braunmüller, L. Schmid, A. Wixforth and D. A. Weitz, Surface acoustic wave actuated cell sorting (SAWACS), *Lab Chip*, 2010, **10**, 789.
222 R. Ahmad, *et al.* Acoustic Wave-Driven Functionalized Particles for Aptamer-Based Target Biomolecule Separation, *Anal. Chem.*, 2017, **89**, 13313–13319.
223 G. Destgeer, B. H. Ha, J. H. Jung and H. J. Sung, Submicron separation of microspheres via travelling surface acoustic waves, *Lab Chip*, 2014, **14**, 4665–4672.
224 K. Wang, *et al.* Sorting of tumour cells in a microfluidic device by multi-stage surface acoustic waves, *Sens. Actuators, B*, 2018, **258**, 1174–1183.
225 D. J. J. Collins, *et al.* Selective particle and cell capture in a continuous flow using micro-vortex acoustic streaming, *Lab Chip*, 2017, **17**, 1769–1777.
226 C. Wang, S. V. Jalikop and S. Hilgenfeldt, Efficient manipulation of microparticles in bubble streaming flows, *Biomicrofluidics*, 2012, **6**, 012801.
227 R. Thameem, B. Rallabandi and S. Hilgenfeldt, Particle migration and sorting in microbubble streaming flows, *Biomicrofluidics*, 2016, **10**, 014124.
228 M. V. Patel, A. R. Tovar and A. P. Lee, Lateral cavity acoustic transducer as an on-chip cell/particle microfluidic switch, *Lab Chip*, 2012, **12**, 139–145.
229 N. Garg, *et al.* Whole-blood sorting, enrichment and in situ immunolabeling of cellular subsets using acoustic microstreaming, *Microsyst. Nanoeng.*, 2018, **4**, 17085.
230 M. V. Patel, I. A. Nanayakkara, M. G. Simon and A. P. Lee, Cavity-induced microstreaming for simultaneous on-chip pumping and size-based separation of cells and particles, *Lab Chip*, 2014, **14**, 3860.
231 N. Nivedita, N. Garg, A. P. Lee and I. Papautsky, A high throughput microfluidic platform for size-selective enrichment of cell populations in tissue and blood samples, *Analyst*, 2017, **142**(14), 2558–2569.
232 A. Fakhfouri, C. Devendran, D. J. J. Collins, Y. Ai and A. Neild, Virtual membrane for filtration of particles using surface acoustic waves (SAW), *Lab Chip*, 2016, **16**, 3515–3523.
233 D. J. Collins, Z. Ma, J. Han and Y. Ai, Continuous micro-vortex-based nanoparticle manipulation via focused surface acoustic waves, *Lab Chip*, 2017, **17**, 91–103.
234 W. Cui, L. Mu, X. Duan, W. Pang and M. A. Reed, A polarized nonlinear optical response in a topological insulator Bi 2 Se 3-Au nanoantenna hybrid-structure for all-optical switching Trapping of sub-100 nm nanoparticles using gigahertz acoustofluidic tweezers for biosensing applications†, *Nanoscale*, 2019, **11**, 14625.
235 Z. Mao, *et al.* Enriching Nanoparticles via Acoustofluidics, *ACS Nano*, 2017, **11**, 603–612.
236 B. Hammarström, T. Laurell and J. Nilsson, Seed particle-enabled acoustic trapping of bacteria and nanoparticles in continuous flow systems, *Lab Chip*, 2012, **12**, 4296.
237 A. Ku, *et al.* Acoustic Enrichment of Extracellular Vesicles from Biological Fluids, *Anal. Chem.*, 2018, **90**, 8011–8019.
238 R. Habibi and A. Neild, Sound wave activated nano-sieve (SWANS) for enrichment of nanoparticles, *Lab Chip*, 2019, **19**, 3032–3044.
239 Y. Ai, C. K. Sanders and B. L. Marrone, Separation of Escherichia coli Bacteria from Peripheral Blood Mononuclear Cells Using Standing Surface Acoustic Waves, *Anal. Chem.*, 2013, **85**, 9126–9134.
240 P. Sehgal and B. J. Kirby, Separation of 300 and 100 nm Particles in Fabry–Perot Acoustofluidic Resonators, *Anal. Chem.*, 2017, **89**, 12192–12200.
241 A. Ku, *et al.* Acoustic Enrichment of Extracellular Vesicles from Biological Fluids, *Anal. Chem.*, 2018, **90**, 8011–8019.
242 J. Shi, *et al.* Three-dimensional continuous particle focusing in a microfluidic channel via standing surface acoustic waves (SSAW), *Lab Chip*, 2011, **11**, 2319–2324.
243 X. Xuan, J. Zhu and C. Church, Particle focusing in microfluidic devices, *Microfluid. Nanofluid.*, 2010, **9**, 1–16.
244 T. Zhang, Z. Y. Hong, S. Y. Tang, W. Li, D. W. Inglis, Y. Hosokawa, Y. Yalikun and M. Li, Focusing of sub-micrometer particles in microfluidic devices, *Lab Chip*, 2020, **20**(1), 35–53.
245 G. Goddard, J. C. Martin, S. W. Graves and G. Kaduchak, Ultrasonic particle-concentration for sheathless focusing of particles for analysis in a flow cytometer, *Cytometry, Part A*, 2006, **69**, 66–74.
246 P. P. A. Suthanthiraraj, *et al.* One-dimensional acoustic standing waves in rectangular channels for flow cytometry, *Methods*, 2012, **57**, 259–271.
247 M. E. Piyasena, *et al.* Multinode Acoustic Focusing for Parallel Flow Cytometry, *Anal. Chem.*, 2012, **84**, 1831–1839.
248 D. M. Kalb, *et al.* Line-Focused Optical Excitation of Parallel Acoustic Focused Sample Streams for High Volumetric and Analytical Rate Flow Cytometry, *Anal. Chem.*, 2017, **89**, 9967–9975.
249 R. J. Olson, A. Shalapyonok, D. J. Kalb, S. W. Graves and H. M. Sosik, Imaging FlowCytobot modified for high

throughput by in-line acoustic focusing of sample particles, *Limnol. Oceanogr.: Methods*, 2017, **15**, 867–874.
250 B. S. Lambert, R. J. Olson and H. M. Sosik, A fluorescence-activated cell sorting subsystem for the imaging flowcytobot, *Limnol. Oceanogr.: Methods*, 2017, **15**, 94–102.
251 W. Zhao, *et al.* A high-throughput label-free time-stretch acoustofluidic imaging cytometer for single-cell mechanotyping, *Microfluid. Nanofluid.*, 2020, **24**, 88.
252 M. Antfolk, S. H. Kim, S. Koizumi, T. Fujii and T. Laurell, Label-free single-cell separation and imaging of cancer cells using an integrated microfluidic system, *Sci. Rep.*, 2017, **7**, 1–12.
253 Y. Chen, A. A. Nawaz, Y. Zhao, P. H. Huang, J. P. McCoy, S. J. Levine, L. Wang and T. J. Huang, Standing surface acoustic wave (SSAW)-based microfluidic cytometer, *Lab Chip*, 2014, **14**(5), 916–923.
254 O. Jakobsson, M. Antfolk and T. Laurell, Continuous Flow Two-Dimensional Acoustic Orientation of Nonspherical Cells, *Anal. Chem.*, 2014, **86**, 6111–6114.
255 Z. Ma, Y. Zhou, D. J. Collins and Y. Ai, Fluorescence activated cell sorting via a focused traveling surface acoustic beam, *Lab Chip*, 2017, **17**(18), 3176–3185.
256 L. Ren, *et al.* Standing Surface Acoustic Wave (SSAW)-Based Fluorescence-Activated Cell Sorter, *Small*, 2018, **14**, 1801996.
257 R. Zmijan, *et al.* High throughput imaging cytometer with acoustic focussing, *RSC Adv.*, 2015, **5**, 83206–83216.
258 D. Ahmed, A. Ozcelik, N. Bojanala, N. Nama, A. Upadhyay, Y. Chen, W. Hanna-Rose and T. J. Huang, Rotational manipulation of single cells and organisms using acoustic waves, *Nat. Commun.*, 2016, **7**(1), 1.
259 N. F. Läubli, *et al.* 3D Manipulation and Imaging of Plant Cells using Acoustically Activated Microbubbles, *Small Methods*, 2019, **3**, 1800527.
260 C. Chen, *et al.* Acoustofluidic rotational tweezing enables high-speed contactless morphological phenotyping of zebrafish larvae, *Nat. Commun.*, 2021, **121**(12), 1–13.
261 L. Johansson, F. Nikolajeff, S. Johansson and S. Thorslund, On-Chip Fluorescence-Activated Cell Sorting by an Integrated Miniaturized Ultrasonic Transducer, *Anal. Chem.*, 2009, **81**, 5188–5196.
262 O. Jakobsson, C. Grenvall, M. Nordin, M. Evander and T. Laurell, Acoustic actuated fluorescence activated sorting of microparticles, *Lab Chip*, 2014, **14**(11), 1943–1950.
263 A. A. Nawaz, *et al.* Acoustofluidic Fluorescence Activated Cell Sorter, *Anal. Chem.*, 2015, **87**, 12051–12058.
264 X. Huang, *et al.* A Surface Acoustic Wave Pumped Lensless Microfluidic Imaging System for Flowing Cell Detection and Counting, *IEEE Trans. Biomed. Circuits Syst.*, 2017, **11**, 1478–1487.
265 W. L. Ung, K. Mutafopulos, P. Spink, R. W. Rambach, T. Franke and D. A. Weitz, Enhanced surface acoustic wave cell sorting by 3D microfluidic-chip design, *Lab Chip*, 2017, **17**(23), 4059–4069.
266 J. Rufo, F. Cai, J. Friend, M. Wiklund and T. J. Huang, Acoustofluidics for biomedical applications, *Nat. Rev. Methods Primers*, 2022, **21**(2), 1–21.
267 S. Hameroff, *et al.* Transcranial ultrasound (TUS) effects on mental states: A pilot study, *Brain Stimul.*, 2013, **6**, 409–415.
268 M. Samandari, K. Abrinia, M. Mokhtari-Dizaji and A. Tamayol, Ultrasound induced strain cytoskeleton rearrangement: An experimental and simulation study, *J. Biomech.*, 2017, **60**, 39–47.
269 Y. Hu, W. Zhong, J. M. F. Wan and A. C. H. Yu, Ultrasound can Modulate Neuronal Development: Impact on Neurite Growth and Cell Body Morphology, *Ultrasound Med. Biol.*, 2013, **39**, 915–925.
270 Z. Fan, *et al.* Acoustic tweezing cytometry for live-cell subcellular modulation of intracellular cytoskeleton contractility, *Sci. Rep.*, 2013, **3**, 2176.
271 M. K. DeBari, *et al.* Therapeutic Ultrasound Triggered Silk Fibroin Scaffold Degradation, *Adv. Healthcare Mater.*, 2021, **10**, 2100048.
272 S. Lee, *et al.* Extracellular matrix remodeling in vivo for enhancing tumor-targeting efficiency of nanoparticle drug carriers using the pulsed high intensity focused ultrasound, *J. Controlled Release*, 2017, **263**, 68–78.
273 T. Mainprize, *et al.* Blood-Brain Barrier Opening in Primary Brain Tumors with Non-invasive MR-Guided Focused Ultrasound: A Clinical Safety and Feasibility Study, *Sci. Rep.*, 2019, **9**, 321.
274 G. Leinenga, C. Langton, R. Nisbet and J. Götz, Ultrasound treatment of neurological diseases-current and emerging applications, *Nat. Rev. Neurol.*, 2016, **12**, 161–174.
275 D. V. Deshmukh, *et al.* Continuous Production of Acoustically Patterned Cells Within Hydrogel Fibers for Musculoskeletal Tissue Engineering, *Adv. Funct. Mater.*, 2022, **32**, 2113038.
276 L. Zou, C. McLeod and M. R. Bahmanyar, Wireless Interrogation of Implantable SAW Sensors, *IEEE Trans. Biomed. Eng.*, 2020, **67**, 1409–1417.
277 O. H. Murphy, *et al.* Continuous in vivo blood pressure measurements using a fully implantable wireless SAW sensor, *Biomed. Microdevices*, 2013, **15**, 737–749.
278 A. Ozcan, Mobile phones democratize and cultivate next-generation imaging, diagnostics and measurement tools, *Lab Chip*, 2014, **14**, 3187–3194.
279 L. Zhang, Z. Tian, H. Bachman, P. Zhang and T. J. Huang, A Cell-Phone-Based Acoustofluidic Platform for Quantitative Point-of-Care Testing, *ACS Nano*, 2020, **14**, 3159–3169.
280 D. Baresch, J.-L. Thomas and R. Marchiano, Observation of a Single-Beam Gradient Force Acoustical Trap for Elastic Particles: Acoustical Tweezers, *Phys. Rev. Lett.*, 2016, **116**, 024301.

